A design of a marine radar mast system for minimum vibration

Suey-Yueh Hu
University of Northern Iowa

A DESIGN OF A MARINE RADAR MAST SYSTEM FOR MINIMUM VIBRATION

A Dissertation

Submitted

In Partial Fulfillment

Of the Requirement for the Degree

Doctor of Industrial Technology

Approved by:

John T. Fecik

Dr. John T. Fecik, Chair

Charles D. Johnson

Dr. Charles D. Johnson, Co-Chair

Rex W. Pershing

Dr. Rex W. Pershing

C. W. Hol

Dr. Charles W. Holcombe

Taifa Yu

Dr. Taifa Yu

Andrew R. Gilpin

Dr. Andrew R. Gilpin

Suey-Yueh Hu

University of Northern Iowa

May 1997

UMI Number: 9728884

UMI
300 North Zeeb Road
Ann Arbor, MI 48103

ACKNOWLEDGMENTS

The author would like to acknowledge the guidance and encouragement of Dr. John T. Fecik, advisor, Dr. Charles D. Johnson, co-advisor, and all the advisory committee members Dr. Rex. W. Pershing, Dr. Charles D. Holcombe, Dr. Taifa Yu and Dr. Andrew W. Gilpin. Without their continuous advice and assistance for this research, this study would have been impossible.

Special thanks would be given to Dr. Jin Guang, Dr. Betty Chang, Dr. Kirk J.K. Wu and David J.T. Kao who spent a lot of time and gave me assistance during this research.

This research was made possible by the life long teaching of my father, chei-kee Hu, my mother, and show-jen Hen. A Doctoral degree was one of the goals they set for me. If not for them, I might not have been able to gather myself for this struggle. The author especially thanks Taishine Ho, and his children wen- chen, wen-hwar for their love, patience, and support during the entire six years that author was absent from home to go abroad to pursue academic achievement. I would like to thank again to Dr. Fecik for giving me support thoughout the entire ordeal.

If the doctor degree is an honor, it is for all classmate of class 1971 of Chinese Naval Academy.

TABLE OF CONTENTS

LIST OF TABLES

LIST OF FIGURES

Figure | Page

Figure | Page

A DESIGN OF A MARINE RADAR MAST SYSTEM FOR MINIMUM VIBRATION

An Abstract of a Dissertation

Submitted

In Partial Fulfillment

of the Requirement for the Degree

Doctor of Industrial Technology

Approved by:

John T. Fecik

Dr. John T. Fecik, Committee Chair

John W. Somervill

Dr. John W. Somervill

Dean of the Graduate College

Suey-Yueh Hu

University of Northern Iowa

May 1997

ABSTRACT

This experimental research focused on four areas: (a) the design of a new procedure for imitating the dynamic behavior of an electronic base plate on a radar mast system; (b) determination of a reasonable oscillation modal state; (c) avoidance of the destruction of the ability of the radar on the mast of a ship to receive and analyze incoming signals; and (d) design of a vibration absorber and vibration isolator based on an oscillation frequency. An adapted design for the vibration absorber and vibration isolator contributed to the prevention of excessive amplitude being produced by random forces acting upon a radar system equipped on the mast of a ship.

In this research, finite element analysis was used to analyze the natural frequency and the modal state of the ship's mast in order to establish the reasonable finite element analysis model. This technique became the basis for the design of the adapted vibration isolator and the vibration absorber. In designing the adapted dynamic vibration absorber and vibration isolator, the Lagrange's engineering mathematical equation was used to study the system movement equation under differing random forces. This system movement equation led to the converted function between the radar replacement alteration and the random

force. By use of a Lagrange's optimum value method, the researcher obtained the optimum frequency modulation ratio and the optimum damping ratio of the dynamic vibration absorber so that the radar displacement alteration reached the minimum value. The optimum mass ratio between the vibration absorber and the radar base plate was located by studying the radar displacement alteration under its optimum dynamic absorber. The optimum frequency modulation ratio and the optimum damp ratio were determined by studying the effect of the spring constants of the vibration isolator, the damp ratio, and the position of the random force. The radar oscillation before and after installing the optimum dynamic absorber were compared to illustrate the accuracy of the field test for sea travel.

CHAPTER I

INTRODUCTION

When a ship navigates on the sea, the electronic equipment is the eyes or ears of the ship. The radar system is the largest piece of the electronic equipment, and the radar antenna is located on top of the mast. The radar system is used to find the correct direction and locate external objects. The signals received by the radar system are transferred to the control room for analysis.

A mast system is composed mainly of supporting frames, a circular base plate, radar, and an antenna. The base plate is stiffened by six aluminum tubes that are fixed on the supporting frames. The supporting frames are fixed on the upper deck of the ship. The radar and antenna are fixed on top of the base plate. The weight of the radar and antenna is supported by the base plate. Sometimes, there is an antenna frame to hold the antenna. This frame is sitting between the base plate and the antenna. The searching radar and the antenna are responsible for searching signals, therefore, they should be in a higher position. The supporting frames, in general, are very tall.

Ship structure vibration is caused by external forces such as waves, wind, and the rotation of the main engines, therefore, the vibration amplitude of the antenna can be severed (Wang, Shao, 1992). The mast system can transfer vibration displacement and force to the radar base plate. This can influence the accuracy of the signals that the radar system receives and may produce wrong analysis results in the control room leading to incorrect radar searching, tracking, and navigation.

It is very important that the signal transmission is free from noise. Due to the fact that the radar system is mounted on a ship mast, the oscillation frequency of the mast and the displacement of the radar plate should be within certain ranges, so the signal received by the radar system will be free from interference. Since oscillation of the mast is unavoidable, reducing the oscillation displacement of the mast and the radar base plate is the best approach to maintaining the accuracy of the radar system.

There are two commonly used methods to decrease the mast system oscillation. The first one is to add an isolator inside the equipment or between the base plate and the equipment. The major function of an isolator is to decrease the oscillation from the base plate to the equipment, and decrease the force transferred from the main body of the ship to the base plate. The disadvantage of the isolator is that it can only reduce the oscillation in one direction.

There are two connecting methods for a traditional isolator. One is elastic-connection and the other is rigid-connection.

The second method for decreasing oscillation is to insert a dynamic absorber in addition to an isolator. The main function of an absorber is to damp out the oscillation energy of the equipment (hence, decrease the oscillation) and to compensate for the disadvantages of an isolator. The absorber surrounds and holds the mast bolts in place. There are two kinds of damping instruments; one is a sticky damp, which is a liquid chemical encased in a hard material such as rubber and the other damping instrument is a damping pad, which is a rubber pad with holes throughout (Wang, Haung, & Hu, 1990).

The characteristics of an isolator or absorber for a structure should be determined by the vibration characteristics of the structure (Racca, 1982). Therefore, a systematic way to analyze the structure of the mast of a ship and to determine the design characteristics for optimal vibration isolators and absorbers is needed.

Statement of the Problem

The major engineering problem to be addressed in this research was how to improve the design of the radar base plate and mast for radar on an ocean vessel. The radar on the improved design of the mast should have higher precision, and the radar signal interference created by ship oscillation should be within an acceptable range. The scope of this research includes imitating the dynamic behavior of the ship mast structure, determining oscillation modal states, and designing the optimal vibration absorber and vibration isolator.

Purpose of the Study

The purpose of this research was to improve the precision of the radar system by reducing the vibration amplitude of the base plate caused by unavoidable ship structural oscillation. The ship structural oscillation is produced by stormy waves, wind loads, and the motion of main engine components. However, the influence of oscillation can be reduced by adding isolators and absorbers. In this research, optimal vibration absorbers and vibration isolators were designed, based on the results of oscillation analysis of the mast system. Once the vibration absorbers and isolators were mounted in the radar mast structure, it was believed that the amplitude of the radar vibration would be reduced.

Research Questions

Research questions in this study included:

1. What is the reasonable finite element analysis model to analyze the dynamic behavior of the mast, including the natural oscillation frequencies and the oscillation states of the mast structure?

2. With the addition of a dynamic vibration absorber and isolator, will the vibration amplitude of the radar on the base plate be within the prescribed maximum of 0.2 milli-radians when the ship is subject to stormy waves and wind load?

Limitations

This research had the following limitations:

1. This investigation was applicable to gas-turbine driven ocean vessels with a length under 400 feet.

2. The mast system considered contained only a radar system, satellite antenna, electronic communication equipment, and flag shelf line.

3. The height of the mast system was a maximum of 35 feet or less.

4. The material of the mast structure component was aluminum-alloy.

5. An impact hammer was used to produce oscillation on the metal tubes.

Assumptions

The following assumptions were made the study:

1. The aluminum tubes of the mast system were welded and the mast material was homogeneous.

2. The vibration of a mast structure can be characterized and simulated by natural frequencies and oscillation activity.

3. The mast design was flexible and anti-vibrating.

4. In the aluminum mast system, the resistance of the isolator and spring can be fixed to minimize the longitudinal displacement of the radar.

5. In the aluminum mast system, the mass ratio between the isolator and the radar is a given constant ($k = 25$).

6. The mast was considered to be a static structure, which is made up of radar plates and hundreds of tubes.

Definition of Terms

The definitions of the following terms used in this document.

1. Mast: A long pole of steel or wood usually circular in section, one or more of which are located, in an upright position, on the center line of a ship. Or it is a slender vertical structure which is not self-supporting and is required to be held in position by guy-ropes or electronic equipment antenna.

2. Aluminum mast: A mast which is composed of aluminum alloy tubes whose diameter ranges from 5 inches to 3 inches. It is located on top of the main deck of a ship, and its height is under 25 feet.

3. Hammer: The hammer used in this research is an impact hammer for structural behavior testing and modal analysis. Max. Force: 5000N.

4. Intensity: Basically the sound power (or pressure level) per unit area.

5. Natural Frequency: The frequency of free oscillation of a system.

6. Beam Element: A long piece of heavy, often squared, timber suitable for use in construction (Vibration and shock in damped mechanical systems, 1986, p. 286).

7. SMAW: Shielded Metal Arc Welding (SMAW) is an arc welding process in which coalescence of metals is produced by heat from an electric arc that is maintained between the tip of a covered electrode and the surface of the base metal in the joint being welded (Welding handbook, 1978, p. 44).

8. Resonant Vibration: The frequency at which resonant response is produced.

9. Viscous Damping: A damping system with asymptotic characteristics, the damping force being proportional to the velocity and acting in a direction opposite to the velocity.

10. Wavelength: The spatial separation of successive compression and rarefaction in wave form.

11. Damping: The dissipation of energy with time or distance.

12. Damped Natural Frequency: The frequency of free vibration of a damped linear system.

13. Oscillation: The variation, usually with time, of the magnitude of a quantity with respect to a specified reference when the magnitude is alternately greater and smaller than the reference.

14. Isolators: Known as "machinery mounts" to differentiate this family of isolators from those which might be designed, as components, into the internal structure of machinery.

15. Absorbers: When a primary system is excited by a force or displacement that has a constant frequency, or in some cases by an exciting force that is a constant multiple of a rotational speed, then it is possible to modify the vibration pattern and to reduce its amplitude significantly by the use of an auxiliary mass on a spring tuned to the frequency of the excitation. Then the auxiliary mass system has as little damping as possible. This is called an absorber.

16. The finite element analysis: A recent approach that is commonly used. One begins the analysis by approximating the region of interest by subdividing it into a number of

non-uniform finite elements that are connected to associated nodes.

17. 2.5g accelerate loading: The inertial loads of 2.5g each were placed in the longitudinal, the transverse, the vertical directions, for analysis while the ship is in motion. The results were used to analyze the vibration and the displacement of the ship's mast.

Research Design

Laboratory tests and field tests were two major components of the research activities in this study. Their procedures are outlined below:

Laboratory Tests

1. Compare the differences in vibration characteristics between welded aluminum-alloy tubes and homogeneous aluminum-alloy tubes, to see if the influence of welding on dynamic behavior should be considered.

2. Establish a mast simulation model considering the basic vibration characteristics of aluminum-alloy tubes, in order to determine the free vibration and the natural frequencies.

3. Develop finite element models for the mast to analyze the free vibration and the natural frequencies.

4. Analyze the displacement of the radar base plate at the top of the mast by applying the following loading cases in the mast finite element analysis:

a. wind loads applied on the ship

b. sea state loads applied on the ship

c. inertial loads with magnitude 2.5 times of gravitational acceleration (2.5g).

5. Determine the optimal frequency modulation ratio for isolators and absorbers to keep the vibration amplitude of radar base plate less than 0.2 milli-radians displacement and 50 Hz natural frequency to maintain the accuracy of the radar signal.

Field Tests

Compare the radar oscillation for the cases with and without optimal absorbers and isolators in sea travel. The following conditions were used in the field tests:

1. Mast without isolator and absorber at general speed (15 knots).

2. Mast with isolator and absorber at general speed (15 knots).

3. Mast without isolator and absorber at critical speed (18 knots).

4. Field test with isolator and absorber at critical speed (18 knots).

5. Field test without isolator and absorber at economic speed (22 knots).

6. Field test with isolator and absorber at economic speed (22 knots).

7. Field test without isolator and absorber at high speed (30 knots).

8. Field test with isolator and absorber at high speed (30 knots).

Subsequent Chapters

This dissertation contains five chapters. Chapter two involves a review of the literature related to research methodology. The research procedures of this study are included in chapter three. Chapter four reports the data analysis and findings of the study. The summary, conclusions, and recommendations are contained in chapter five.

CHAPTER II

REVIEW OF THE LITERATURE

This review of literature focuses on the design and construction of a radar mast system. Specifically, information presented in this chapter concerns (a) a historical perspective of the ship mast, (b) research on ship mast characteristic and radar quality, (c) general studies on the ship mast, and (d) summary.

A Historical Perspective of the Ship Mast

In the beginning of the history of the development of the ship mast, the mast was a part of the main power source of early sailing ships. The Dictionary of Business and Industry (Schwartz, 1954) indicated that a mast is a long pole of steel or wood usually circular in composition, one or more of which is located, in an upright position, on the center line of a ship (p. 320). Another view was noted in Chambers Science and Technical Dictionary (Walker, 1988) which noted that a mast is a slender vertical structure which is not self-supporting and is required to be held in position by guy-ropes (p. 529).

In recent years, the mast power source, the sail, was displaced by the power engine. The mast then evolved into a radar mast system to get correct location and direction.

The mast system on a ship is a frame, fixed on the ship's bridge, which supports the weight of the tracking radar and the tracking radar antenna. The searching radar and the searching antenna are responsible for detecting for signals, therefore they should be mounted at a higher level. The ship's mast is fixed at the deck; the radar system receives outside signals and transfers them with a controlling circuit to the control room for analysis (Mayne, 1980).

In 1960, The United States Navy designed a four-legged mast, sometimes referred to as a quadruped or a lattice-type mast, which consists of four essentially vertical members, joined together by horizontal and diagonal bracing. The four trusses formed by these members provide fairly rigid support at each panel point. Such a structure is suitable for carrying radar antennas and other equipment which cannot be concentrated within a small area. The advantage of a four-legged mast over a pole mast or tripod is that the principal forces and moments, including torsion effects, are resisted by axial reactions of the members. Bending moments are substantially eliminated. But because stresses in most members are determined by the moments on the mast as a whole, the analysis is similar in some respects to that of an unseated pole mast (US Navy, 1985).

<u>Research on Ship Mast Characteristics and Radar Quality</u>

The development of the design of the traditional dynamic absorber began with Den Hartong (1956) who was the first to study a dynamic instrument with a free undamped primary system. Warburton (1981) applied the theory developed by Den Hartong to a two-freedom undamped primary system. Lewis (1980) then applied the theory of Den Hartong to the N-freedom system. Lee-Glauser, Juang, and Sulla (1995) studied the optimum frequency ratio and the optimum damp ratio of a dynamic absorber with the damp system on the main body. In some forced oscillation systems, the frequency of an outside force is not a fixed value. Therefore, in recent years, some people have used the dynamic absorber of a random oscillation system instead of a traditional dynamic absorber. A useful technique for the elimination of undesirable vibration in problems of structural dynamics and machinery dynamics has been the application of one or more dynamic vibration absorbers. The first application of such a device was the application of a previously tuned u-shaped column of water to arrest the rolling motions of ships (Den Hartog, 1956). Another recent application was to damp wind induced oscillations in electronic transmission lines (Stefanides, 1984).

Optimum absorber parameters are determined numerically for cylindrical shells and compared with results for beams in flexure and single degree-of-freedom systems. The exciting force has a constant spectral density up to a cut-off frequency and the main system is hysterically damped. There is a close agreement between optimum parameters for single degree-of-freedom systems and beams, while those for shells diverge from the others. Thus the pattern of behavior for random and harmonic excitation is shown to be similar; that is, the single mode approach is adequate for structures with well-spaced natural frequencies.

Minimizing Structural Vibrations With Absorbers

Ayorinde and Warburton (1980) mentioned that for harmonic vibrations, the optimized parameters for a viscous damped tuned absorber, which is attached to a single degree-of-freedom system, apply also for an absorber attached to an elastic body, provided that it is permissible to represent the response of the body by a single mode. When optimization of the response in the vicinity of the fundamental resonance is specified, this is the fundamental mode of the body without attachments. The concept was an extension of an earlier work by Jacquot (1978) for an absorber which is attached to a beam; it depends upon the introduction of an effective mass for the elastic body. This mass, which had been used previously by Warburton (1981), was selected to give equality of kinetic energy for (a) the elastic body without attachments when vibrating in the relevant mode and (b) the lumped effective mass which is placed at the absorber attachment point and has the displacement of that point of the body in the same mode. Provided that an effective mass ratio, which is the ratio of the absorber mass to the effective mass of the body, is used, values of optimum absorber tuning and damping ratios from the classical absorber problem can be used directly for the elastic body problem. For a chosen absorber mass these ratios yield the optimum values of the absorber stiffness and damping for the elastic body problem. The optimized response of the elastic body can be generated simply from the optimized dynamic magnification factor for the classical absorber problem. This was achieved by Liu and Gorman (1993) when they introduced a response factor R, where the displacement at the point in the body for which optimization is required equals the triple product of the modal function evaluated at this point, the modal function evaluated at the point of application of the harmonic excitation force and the factor.

The validity of this approach was demonstrated by Ayorinde and Warburton (1980) presenting results for simply supported beams and quoting results from the literature for bars in extension, beams in flexure and rectangular and circular plates. In these comparative results the optimized absorber parameters and optimum response of the elastic body had been determined from either a closed form solution or a converged multi-mode expansion for the response. Some divergence of the true results from the standard curves of classical absorber theory was noted for (a) a rectangular plate of aspect ratio 1/3, for which the frequency ratio of the lowest neglected relevant mode to the fundamental mode was 1.8 and this ratio was lower than comparable values for the other elastic bodies considered, and (b) a cantilever beam when optimization was applied to the response at the third resonance. The main function of this optimum absorber design is to determine optimized absorber parameters for elastic bodies by appropriate changes of geometry. The frequency spacing can be changed. The relatively high modal density is typical of many practical structures, but an analytical solution is relatively simple. By using the format of Ayorinde and Warburton (1980) for the presentation of the results the increasing divergence of optimized absorber parameters from those of the classical problem, as frequency spacing is reduced, is demonstrated.

A cylindrical shell with closely spaced natural frequencies optimization, which is based on narrow and broad frequency bands, is likely to yield different results. In broad band optimization minimization is applied to all the resonant peaks within the frequency band. This topic is considered briefly by Ayorinde and Warburton (1980) who mentioned that optimum absorber parameters are determined for structures which are subjected to harmonic excitation. However, optimized parameters for other types of excitation, particularly random, are of practical importance. Studies of single and multi degree-of-freedom systems with attached absorbers exist (Jacquot & Hoppe, 1973; Luongo, 1995; Shi, Lee, & Mei, 1997).

Although the final optimum design of the mass structure radar system involves results for cylindrical shells under random excitation which complement those for harmonic excitation, the single degree-of-freedom system is considered initially. For ample noise excitation, explicit expressions for the random response of the main mass are given by Jacquot and Hoppe (1973) and by Luongo (1995). The researcher used these expressions to neglect damping in the main system and generate simple expressions for optimum absorber damping and tuning ratio response of the main system for the following cases: (a) force applied to the main mass and optimization with respect to the displacement response of that mass, (b) acceleration applied to the base or frame of the system and optimization with respect to the relative displacement response of the main mass, and (c) acceleration applied to the base and optimization with respect to the acceleration of the main mass. As expected from the form of the basic equations, cases (a) and (c) give identical expressions. These expressions are of similar form to those for the classical absorber problem with harmonic excitation.

Optimum Absorber Design for a Radar System

A vibration absorber could help to prevent excessive amplitude produced by random forces acting upon the mast of a ship equipped with a radar system. This system could contain damping. Although absorbers are likely to be added only to lightly damped systems, the effect of including damping in the main system on optimum absorber design is of importance and has been studied by several authors. Important contributions have been made recently by Lee-Glauser et al. (1995), who determined correction factors for the absorber parameters in terms of the main system damping, and by Sepulveda and Thomas (1995), who presented design charts for the optimum absorber parameters.

There has been considerable interest in the application of damped vibration absorbers to simple elastic mast structure radar systems, such as rods in extension, beams in flexure, plates and cylindrical shells, etc. In most of this work the concept of the invariant points of the classical problem has been used to determine optimum parameters for absorbers which are attached to elastic bodies. The effect of vibration absorbers upon the response of cylindrical shells showed the variation of the optimum turning ratio, i.e., the ratio of the absorber natural frequency to the fundamental natural frequency of the main system, against the effective mass ratio. The effective mass of the main system is determined by equating the kinetic energy of the main system in the mode of vibration under consideration to that of a lumped mass which is located at the point of attachment of the absorber and has the same direction constraints as the point of attachment. Expressions for effective masses of such bodies as beams in flexure are quite simple. With the introduction of the concept of the effective mass ratio it was shown that the curves of optimum turning ratio versus effective mass ratio for some elastic bodies were very similar. However, there were major departures from that latter curve when absorbers were applied to a cylindrical shell.

A major step in our understanding of the relations between the classical problem and that of the absorber attached to an elastic body was made in a paper by Jacquot (1978). He considered viscous, and also hysteretically, damped absorbers attached to an undamped beam, which is vibrating in flexure and subjected to a harmonic force. He showed that if the beam response was approximated by the fundamental mode, invariant points exist as in the classical problem and expressions for optimum turning ratio, optimum damping ratio and the corresponding maximum response of the beam were similar to those in the classical problem. The researcher obtained standard curves for optimum turning and damping ratios and optimum maximum response when plotted against the effective mass ratio.

An immediate result of the introduction of damping into the main radar system is the disappearance of the invariant points, whether the classical single degree-of-freedom system or an elastic body. It should be noted that the absorbers to be considered here consist of a mass, which is connected to the main system through a parallel spring and viscous damper. The importance of these results is that for specified damping in the main system they provide standard curves, which can be used with elastic bodies, provided Jacquot's assumption of a single mode shape is used. Specifically, standard curves are generated for the optimized response of a main radar system which has light hysteretic damping, as this facilitates comparison with hysteretically damped elastic bodies. Additionally, numerical results for main systems with viscous damping show very close agreement with the recently developed expressions for optimum parameters of Lee-Glauser et al. (1995).

General Studies On the Ship Mast

Design of structures to achieve static deflection and stress constraints are generally considered in terms of an optimal design. In such cases the objective of the design is to obtain the minimum mass structure, subject to limits on the displacements and stresses. In recent years the subject of optimal structural design has become fairly well defined as evidenced by several writers (Haug & Arora, 1979; Kirsch, 1981).

Approaches to solve the optimal structural design problem vary; however, they have been categorized as either direct or indirect methods (Schmit, 1984). Direct methods are based on mathematical programming, while indirect methods are based on optimal criteria.

Direct or mathematical programming methods solve the optimum structural design problem by numerical search techniques. Methods such as sequential unconstrained minimization techniques (Fiacco & McCormich, 1968) and sequential linear programming (Segalman, Dohrmann, & Slavin, 1996) are commonly used. Gradient projection methods, which require derivatives of structural response quantities with respect to design variables, are also used (Fletcher & Reeves, 1964; Rosen, 1961). Calculation of these derivatives can be performed using the state space method (Haug & Arora, 1979) or design space method (Fox, 1965; Schmit & Miura, 1976).

Indirect methods are those which are based on optimal criteria. In such methods, the criteria for the optimal design are obtained by applying the Kuhn-Tucher necessary condition to adapt to the baseline design. Typical criteria are the fully stressed design (Gallagher, 1973) and the uniform strain density design (Venkayya, 1971). A comprehensive discussion of optimal criteria methods can be found in Knot and Berke (1984).

Few authors have addressed the problem of an optimal design for an aluminum mast radar system. The optimal design arises after a baseline structure is analyzed and the resulting response characteristics are determined to be unacceptable. In such cases it is desirable to determine the mass structural system modifications required to achieve acceptable response characteristics of the radar control system. In many instances several candidate designs exist which meet the response objectives. These are considered to be optimal design problems concerning the mass radar system.

To solve the optimal design problem of mass radar control systems with deflection constraints, Spillers and Funaro (1975) developed an iterative procedure. For statistically determinate optimal designs their procedure modified the stiffness and joint load matrices in each redesign cycle. When statically indeterminate radar system structures were considered, the procedure required the allowable stress to be modified. Schmit (1984) proposed the use of design sensitivity analysis for the optimal design problem. Using design derivatives, changes in the mass radar system to meet the design objectives are determined.

Dynamic Design of a Mast Structure

The optimal mast design problem is not a new one. In 1946, Brack proposed a method to solve the problem of optimal design of mass radar systems with a wire stretched between two points to achieve a desired natural frequency (Brack 1946). Frequency-only problems were typically the first to be considered. More recently Taylor (1968) proposed a method where the free vibration equations were considered as equality constraints and handled using La-Grange multipliers. Bhat, Singh, and Mundkur (1993) solved the problem for an axially vibrating bar by minimizing the total energy of the system using Hamilton's principle. In an extension of his work, Taylor (1968) introduced inequality constraints on the cross-sectional area of the bar in addition to the total mass constraint. This new constraint was included in the problem by means of a continuous larger range multiplier. Sheu (1968) extended the work of Taylor to situations where the number of constant stiffness segments was specified, but the boundaries and specific stiffness values of the segments were design variables in the minimum bar weight problem. Sippel and Warner (1973) considered similar problems using a variation method to derive the minimum mass optimality criterion. Structural systems composed of N-element sandwich-type structures supporting non-structural mass were considered.

McCart (1970) used an iterative process to solve the minimum mass problem applied to portal frames. The boundary value nature of the free vibration equations was used in conjunction with a steepest descent method. Rubin (1970) used a two-step process in which he assumed the optimal design laid on a frequency constraint. The first step was a frequency modification mode where separate gradient equations were developed to achieve the natural frequency goal. In the second step, he used the method of steepest descent to find the minimum weight structure for the specified natural frequency. Armand (1971) developed the problem as an optimal control problem with distributed parameters. The method is powerful for simple structures and was demonstrated on a plate-like structure. For a more detailed review of many of these earlier methods the reader is referred to the survey by Pierson (1972).

In more recent work, Taylor (1977) investigated the frequency only constrained problem in terms of model correction. A procedure was developed to scale an existing structural model to meet experimentally measured natural frequencies. The modification scheme was based on the first order terms of a Taylor series expansion about the baseline model. Bellagamba and Yang (1981) employed an exterior penalty function technique based on the first derivatives of the violated constraints. Additional constraints are imposed on static displacements and element stresses. The combined natural frequency and mode shape constrained problem has lately received considerable attention in terms of perturbation based solution techniques. Stetson (1975) proposed a first order perturbation method based on the assumption that the new mode shapes could be expressed as admixtures of the baseline mode shapes. In subsequent works, the technique was cast in terms of finite elements and applied to several problems (Shi, Lee, & Mei 1997). Stetson's procedure, however, used a method of specifying mode shape constraints based on admixture coefficients which had no obvious physical interpretation. Sandstrom developed first order equations which are similar to Stetson's but provided a method for specifying mode shape constraints based on physical quantities (Sandstrom, 1979). Kim, Anderson and Sandstrom formulated the problem using complete nonlinear dynamic equilibrium perturbation equations. They employed a penalty function method where the objective function was a minimum weight or minimum mass condition and the penalty term was a set of residual force errors. Their method is theoretically exact, but may not achieve the desired solution since nonlinear numerical search techniques are employed during the equation solution. For large problems Kim and Anderson derived the method in terms of dynamic condensation since their original procedure was prohibitively expensive (Kim, Anderson, & Sandstrom 1983).

Summary

A review of literature germane to the research of the radar mast was discussed in this chapter. It is evident that methods of vibration control in a radar system may be grouped into three broad categories:

1. Reduction at the Source

a. Balancing of the Moving Mast: Where the vibration organizes in rotating or reciprocating members, the magnitude of a vibrator force frequently can be reduced or possibly eliminated by balancing or counterbalancing.

b. Balancing of Magnetic Forces: Vibrator forces arising in magnetic effects of electrical machinery sometimes can be reduced by modification of the magnetic path.

c. Control of Clearances: Vibration and shock frequently result from impact involved in the operation of machinery. In some instances, impact results from inferior design or manufacture.

2. Isolation

a. Isolation of Source: When a machine creates significant shock or vibration during its normal operation, it may be supported upon isolators to protect other machinery and personnel from shock and vibration.

b. Isolation of Sensitive Equipment: Equipment often is required to operate in an environment characterized by severe shock or vibration. The equipment may be protected from these environmental influences by mounting it on isolators.

3. Reduction of the Response

a. Alteration of Natural Frequency: If the natural frequency of the structure of a piece of equipment coincides with the frequency of the applied vibration, the vibration may be made much worse as a result of resonance. Under such circumstances, if the frequency of the excitation is substantially constant, it often is possible to alleviate the vibration by changing the natural frequency of the structure.

b. Energy Dissipation: If the vibration frequency is not constant or if the vibration involves a large number of frequencies, the desired reduction of vibration may not be attainable by altering the natural frequency of the responding system. It may be possible to achieve equivalent results by the dissipation of energy to eliminate the severe effects of resonance.

c. Auxiliary Mass: Another method of reducing the vibration of the responding system is to attach an auxiliary mass to the system by a spring; with proper tuning the mass vibrates and reduces the vibration of the system to which it is attached.

CHAPTER III

METHODOLOGY

The purpose of this research was to develop a methodology to analyze and design the vibration isolator and absorber of a ship's mast to reduce the signal error of the radar mounted on the mast. Two aspects of the research to be completed included (a) laboratory experiments to simulate the dynamic behavior of the aluminum tubes of a ship's mast and to design an optimum vibration absorber and isolator and (b) to compare the responses of the mast with and without the optimal vibration absorber and isolator in field tests at sea.

This chapter describes the methodology and contains the following five sections: (a) the overall design of the research; (b) the determination of the analysis model of mast tubes; (c) the design of the mast to obtain oscillation states, sea state loads, and wind loads; (d) the design of the experiment for an optimal isolator and the absorber; and (e) field tests to compare the difference in mast vibration due to the isolator and absorber.

The Overall Design of This Research

In this research, finite element analysis (Pegg, 1985) has been used to analyze the natural frequency and vibration displacements of a ship's mast. If the radar base plate displacements are greater than the acceptable range, the vibration must be reduced by adding vibration isolators and absorbers.

An optimization program was used to design the optimal vibration isolator and absorber. In the optimal design of the vibration isolator and absorber, the following factors were considered: the effect of the spring constant of the isolator, the damping ratio of the absorber, the position of the applied external force, the optimal frequency modulation ratio, and the optimal damping ratio of the radar mast. When minimizing the radar displacement, the optimal frequency modulation ratio and resistance ratio of the dynamic isolator can be obtained. At the same time, the optimal mass ratio between the absorber and the radar can be determined.

In the field test, radar vibration before and after the installation of the optimal dynamic absorber were compared to illustrate the accuracy of the radar signal improved by the methodology developed in this research.

Analysis Model of Mast Tubes

A mast structure is a complicated spatial beam that is composed of many aluminum-alloy tubes welded together. Before applying traditional beam theory (Haug & Arora, 1979), the influences or errors that can be caused by two features of an aluminum-tube mast are analyzed. First, the aluminum tubes are hollow which is different than a solid beam. Second, these aluminum-alloy tubes are welded together. The heat treatment on the original material and the added welding material may make the mast different than a structure made by homogeneous aluminum tubes.

Hence, it is necessary to analyze the influences of these welding constants on the behavior of the structures. To determine the difference in structural behavior between a tube and a solid beam element, the finite element analysis method was used to analyze the oscillation state. To clarify the influence of welding on the mechanical properties of aluminum alloys, aluminum alloy tubes were separated into two groups: original and welded tubes. The natural frequency of these two groups was analyzed by the finite element method and compared.

The Design of the Experiment of Pipe Elements

In the experiment conducted in this research, three aluminum alloy tubes (6061-T6) were used. The length of the longer tube was twice that of the other two tubes. The two shorter tubes were welded together according to the welding method of shielded metal arc welding. Hence, the longer tube and the welded one had the same length, as shown in Figure 1.

The mast was made of aluminum alloy 6061-T6. The mechanical property of this type of material was as follows:

E = 10×10^6 lb/in^2 (Young Modules)

υ = 0.35 (Poisson ratio)

σ_r = 40 lb/in^2 (bending stress)

σ = 45 lb/in^2 (broken stress)

ρ = 2.70 g/cm^3 (density)

Prior to initiating the experiment, the following were decided: (a) the locations and the directions of the measurement, (b) the installation method of the tested components, (c) the method to produce oscillation and (d) the equipment for the experiment. Redarding the location and the direction of the measurement, the positions of the measuring points needed to be fully based on the geometry characteristics of the structure to be measured. It was necessary to measure only the longitudinal oscillation because the tested components were axis-symmetrical, and the focus of this experiment was to find the wind oscillation.

The installation method of the tested components was determined. First, the aluminum tubes were clamped with a three-foot clamp, as shown in Figure 2. With the tube base clamped, the tube was considered a cantilever beam.

In most structural vibration experiments, oscillations are made by: (i) a shaker that produces Sine, Random, Pseudo Random, or Periodic impulses; and (ii) a hammer that produces impulses. Within the limitations of the available equipment in the laboratory, an impact hammer was used to produce oscillation, as shown in Figure 3. The advantages of this oscillation excitation method was simple equipment, ease of operation and efficiency.

The equipment for the experiment was as follows(Figure 4):

Computers and peripherals:

(i) HP (Hewelett-Packard) 9000/350C workstation.

(ii) HP2227B printing machine.

(iii) HP7475A drawing machine (A3 / A4 Size, 6-pen)

Frequency band analysis machine:

B & K (B & K Corporation) 2032 Dual Channel Signal Analyzer.

Induction machine:

(i) Electric accelerator B & K 4371 (0.1-12600 Hz).

(ii) The converter of dynamic B & K 8200 (0-5000N).

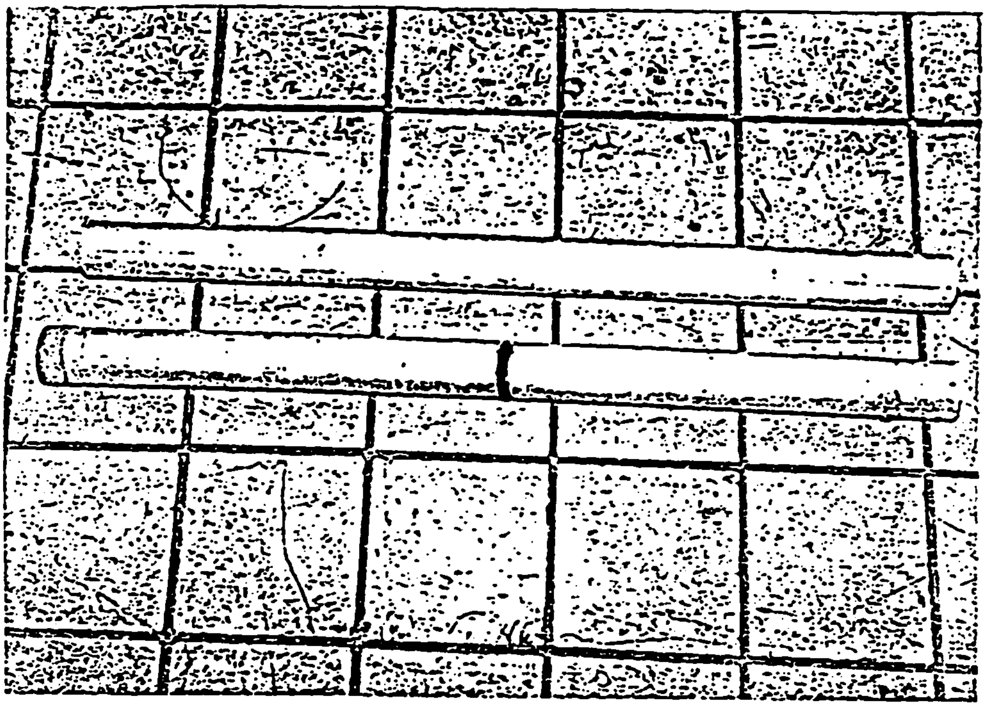

Figure 1. Welded and Non-Welded Tubes.

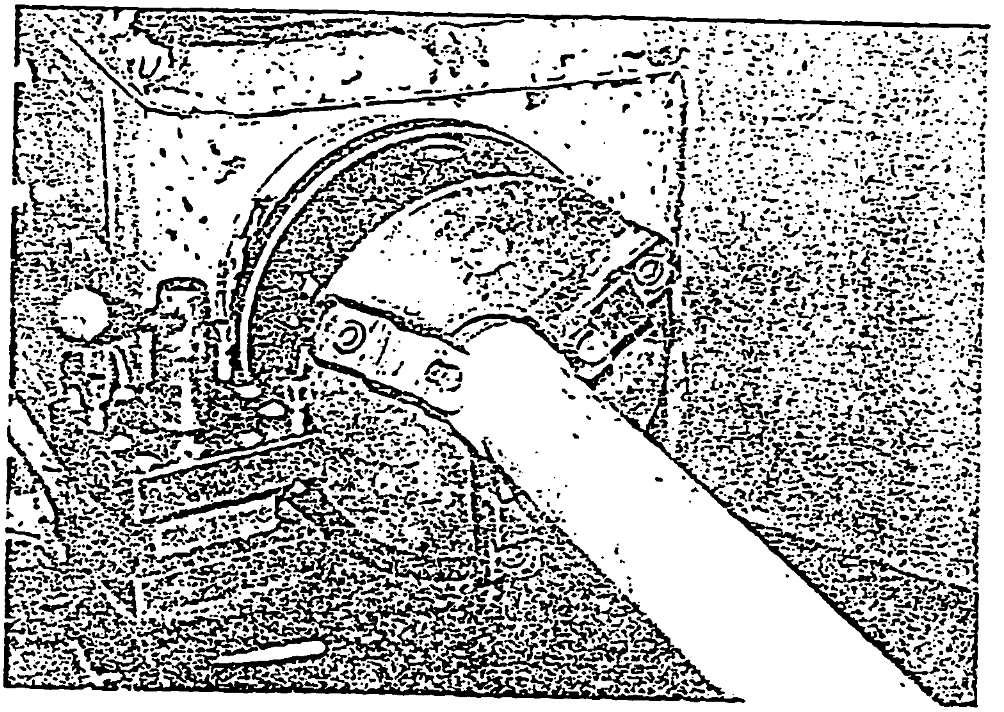

Figure 2. The situation of fixed tested parts.

Impulse hammer:

(i) Impact Hammer B & K 8202. The characteristics of the impact hammer are shown in Table 1.

The signal amplifiers:

(i) Amplifiers B & K 2635, 2644.

Table 1

Characteristics of Impact Hammer

Impact Hammer	Force Range (N)	Duration Range (ms)	Approx. Frequency Range (-10dB, Hz)
Rubber Tip	100-700	5-1.5	0-500
Plastic Tip	300-1000	1-0.5	0-2000
Steel Tip	500-5000	0.25-0.2	0-7000

The procedure of the experiment is illustrated in Figure 5:

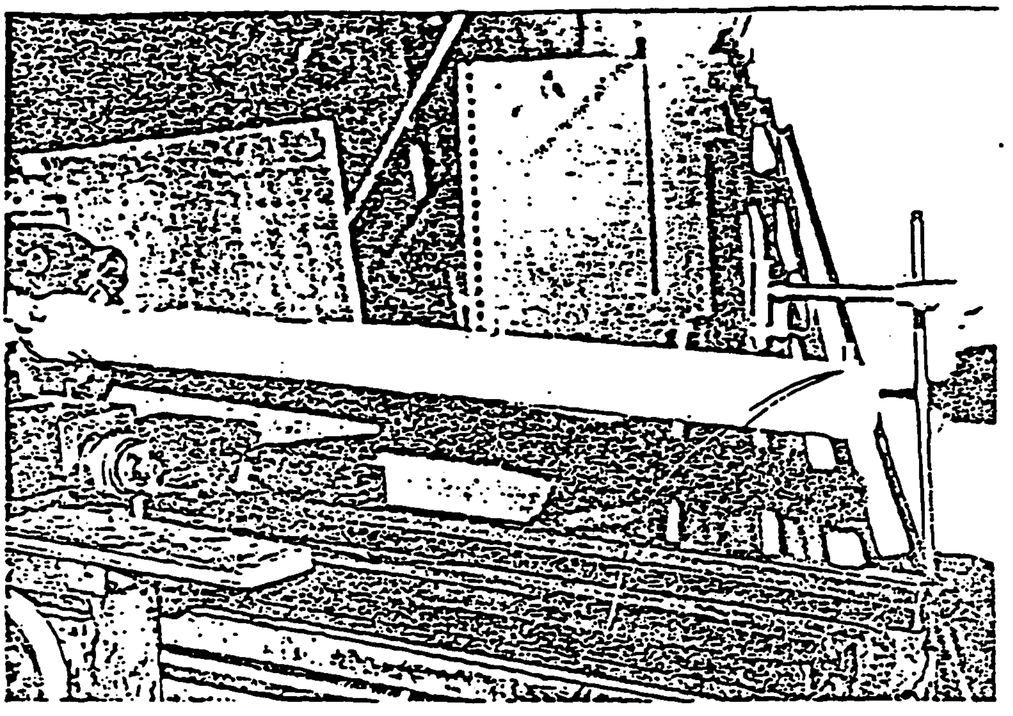

Figure 3. The shaking situation

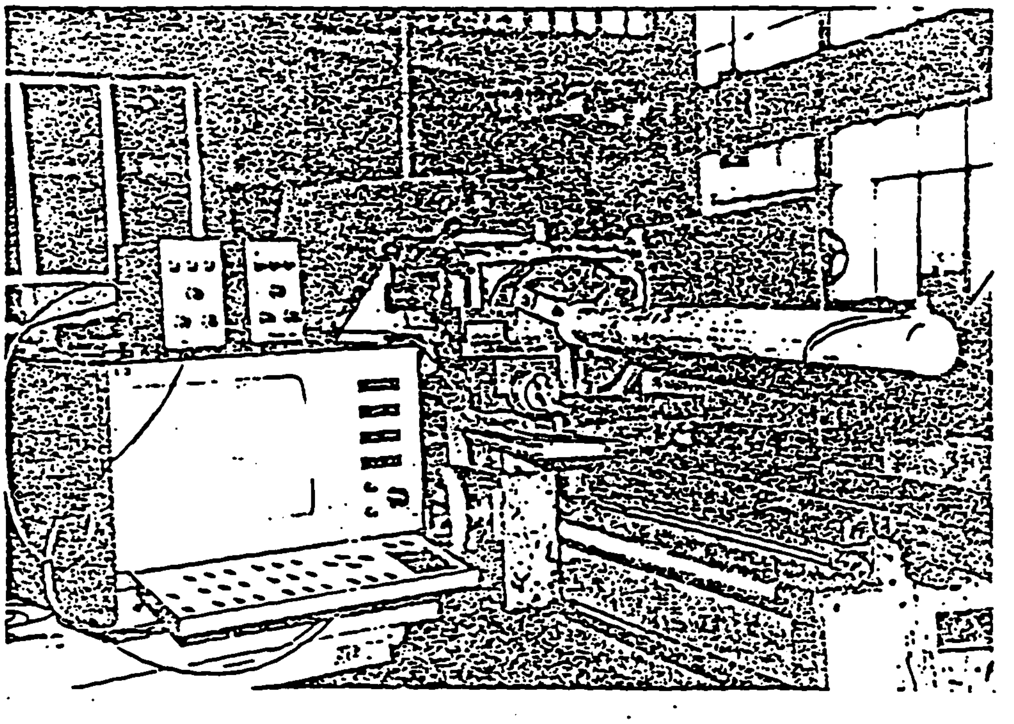

Figure 4. The layout of the experiment

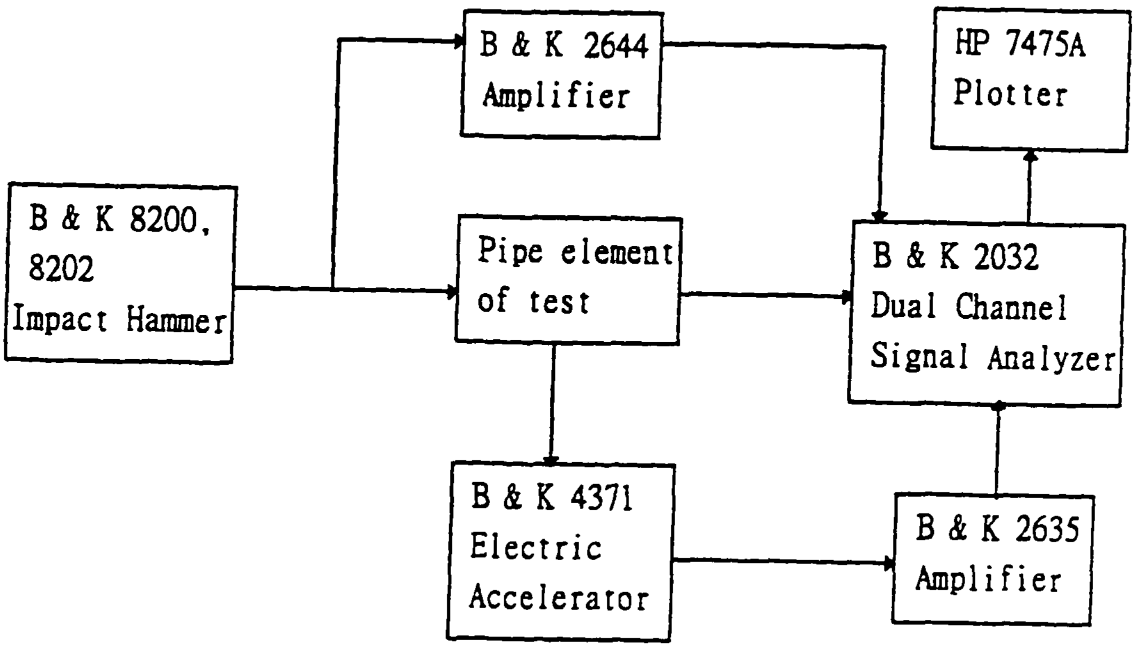

Figure 5. The layout figure of the equipment for the experiment.

The following steps was followed in testing the pipe elements:

Step 1. A 3.5 inch aluminum alloy tube was fixed with a three-foot clamp to simulate a fixed-end beam.

Step 2. The aluminum alloy tube was struck with the impact hammer. The following four kinds of oscillating signal were produced: (i) sine signal (ii) random signal (iii) pseudo random signal (iv) periodic impulse signal

Step 3. The oscillating signals were manipulated by the following two approaches: (i) The signals were amplified by a B & K 2644 amplifier. (ii) The signals were accelerated by a B & K 4371 electronic accelerator prior to being sent to B & K 2635 amplifier.

Step 4. The amplified signals were sent to a B & K 2032 dual channel signal analyzer separately to analyze and compare.

Step 5. The frequency responses were plotted by an HP 7475 plotter.

The Design of the Mast for Experimentation

Finite element analysis was used to design the model mast, and is shown in Figure 6. The mast structure was modeled by 110 structural elements and 40 nodal points. Among the 110 elements, there was a circular plate element at the top of the mast. The rest were space beam elements. The circular plate element has four nodal points, which are points 1 to 4.

Figure 7 shows the assembly of the radar and the base plate. The volumes and the masses of the searching radar and antenna were small (relative to the mast), therefore, these two masses were assumed to be concentrated on a mass center that is above the middle of the circular base plate. Figure 8 shows the finite element model plus the center

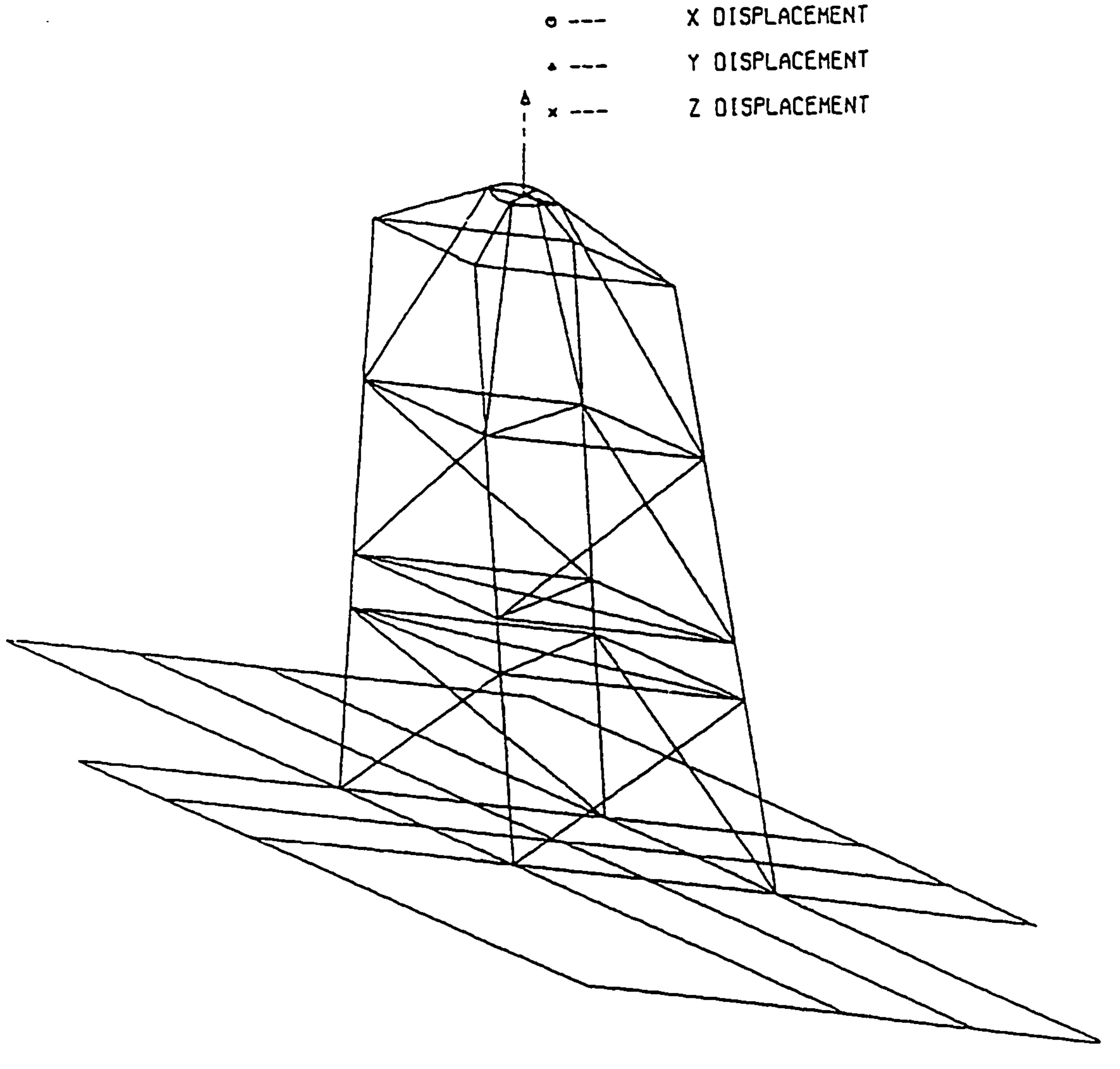

Figure 6. The finite element analysis model of mast.

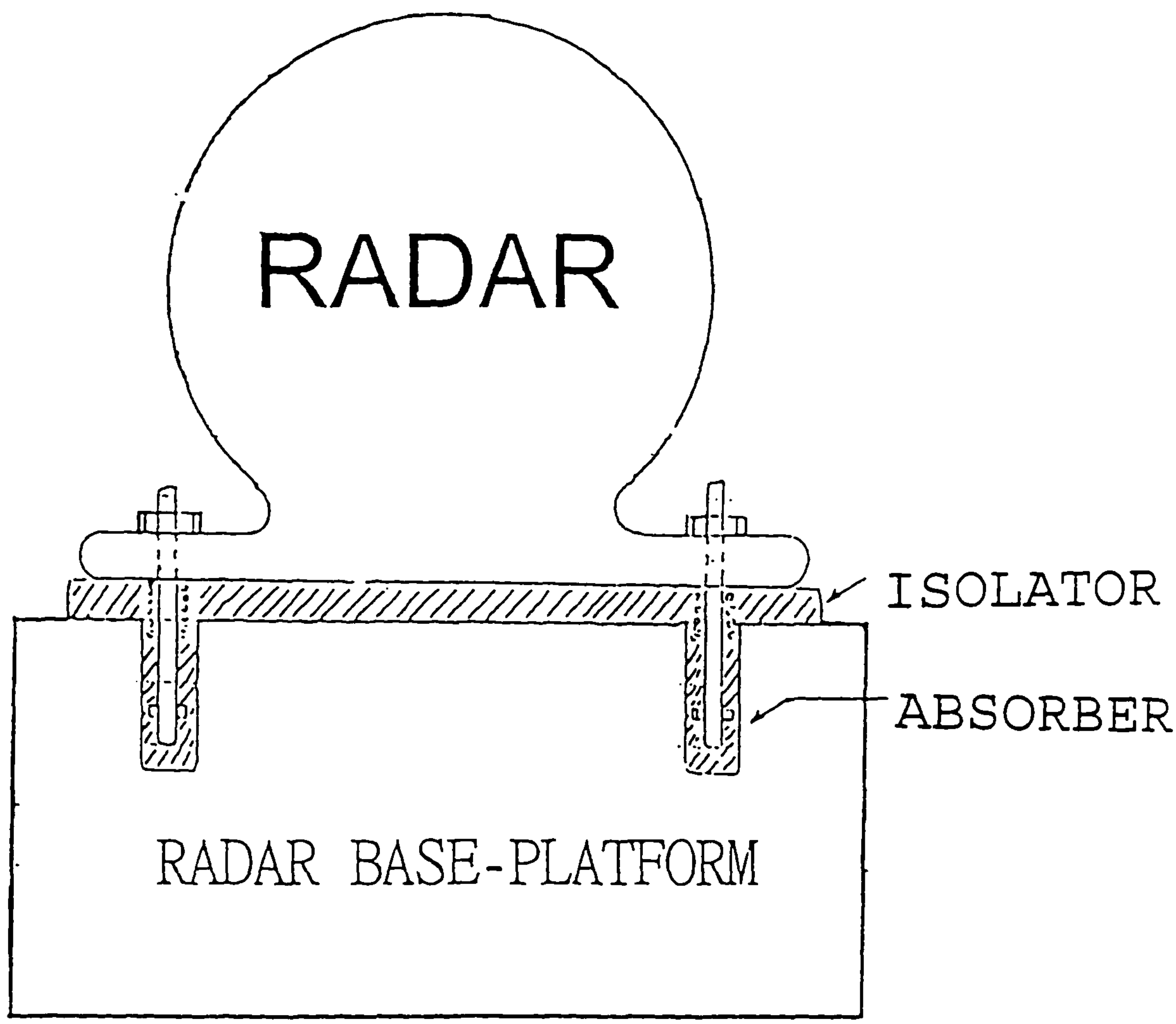

Figure 7. Radar and mast base plate.

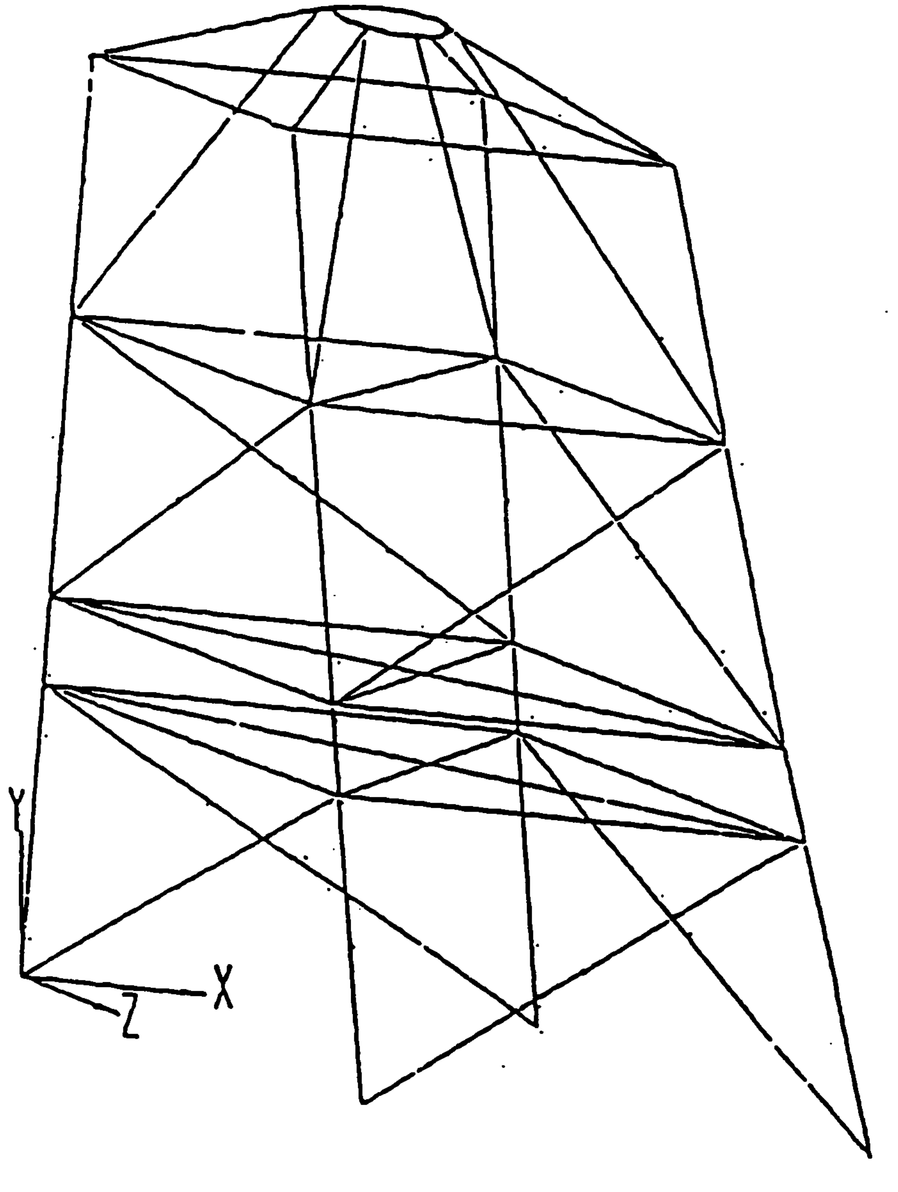

Figure 8. The finite element analysis model

point (point 5) of the radar base plate, the mass center of the radar (point 6), and the ship's deck.

A simulation of the loadings applied on real ships was used. These loadings included wind load, sea state load, as well as 2.5 g inertial loads in longitudinal, transverse, and vertical directions. The results were used to analyze the vibration and displacement of the ship's mast (see Appendix A). The experiment and design were as follows:

Wind Load

Typical wind loading was calculated considering the mast structure area, wind velocity, air density, and wind pressure. In this research, the wind load was estimated by an empirical formula, as follows:

$$Fw = Pw \times A = 1/2c\rho V^2$$

Fw = Wind loading

Pw = Wind pressure (lbs/ft)

A = Wind application area (ft^2)

ρ = Air density ($slug/ft^3$)

V = Wind speed (ft/sec)

C = Constant

In this experiment, the following data were used:

Front (longitudinal) wind speed = 70 mile/hr,

Side (transverse) wind speed = 50 mile/hr,

Air density = 0.00238 $slug/ft^2$,

Constant = 1.28.

Sea State Load

The sea state load is a dynamic loading factor for ship movement. Sea conditions directly influence the motion of a ship and determine the dynamic loading of ship mcvement (Roy and Craig, 1981). Dynamic loadings can be divided into longitudinal(X), transverse(Y), and vertical(Z) directions (Clough and Peuzien, 1975). According to ship motion and attitude (U.S. Navy 1985), the seventh sea state is an adverse sea condition, in which wave height can reach 19.7 to 29.5 feet as shown in Table 2. The load caused by sea states can be estimated by the following formula:

$$A_X = A_s + g * Sin\theta_p + \frac{4\pi^2}{T_p^2}\theta_p^2 X + \frac{4\pi^2}{T_p^2}\theta_p Z$$

$$A_y = g * Sin\theta_p + \frac{1}{2}\frac{4\pi^2}{T_p^2}\theta_p X + \frac{4\pi^2}{T_r^2}\theta_r 2Y + \frac{4\pi^2}{T_r^2}\theta_r Z$$

$$A_z = g \pm (A_h + \frac{4\pi^2}{T_p^2}\theta_p X + \frac{4\pi^2}{T_r^2}\theta_r Y)$$

In the formula to estimate the load in Z direction, the positive sign in Az is downward, the negative sign is upward.

g	=	Gravity Acceleration
θ_r	=	Maximum Roll Angle
θp	=	Maximum Pitch Angle
T_r	=	Rolling Period

T_p = Pitch Period

A_h = Heave Acceleration

A_s = Surge Acceleration

X = Distance between the Center of Gravity of the ship and the Longitudinal Axis (fore and aft) of the ship on the deck

Y = Distance between the Center of Gravity of the ship and the Horizontal Axis (port side and starboard side) of the ship on the deck

Z = Distance between the Center of Gravity of the ship and the vertical direction (top and bottom) of the ship on the deck

A_x = Sea state load in X Direction

A_y = Sea state load in Y Direction

A_z = Sea state load in Z Direction

Table 2 shows the wave heights of different sea states. The seventh stage of the sea state load was adopted in this research. The following parameter values for sea state load calculation were recorded on the ship under sea stage 7 and were used in this experiment:

θ_p = 0.0873 radian, T_p = 6.0 sec

θ_r = 0.49 radian, T_r = 8.0 sec

A_h = 0.3g, A_s = 0.15g

Table 2

Sea State

Sea State Number	Wave Height (ft.)
0-1	0.0-0.3
2	0.3-1.6
3	1.6-4.1
4	4.1-8.2
5	8.2-13.1
6	13.1-19.7
7	19.7-29.5
8	29.5-45.5
>8	>45.5

The Experimental Procedure for the Mast Base Plate

Displacement of the radar base plate was determined using the steps below:

1. Estimate the wind load magnitude. Load in the following situations was applied in the experiment:

   (a) front wind speed was 70 miles per hour.

   (b) side wind speed was 50 miles per hour.

2. Estimate the sea state load Ax, Ay, and Az.

3. Check if the displacement at each of the six points on the radar base plate was less than 0.2 milliradians under stage 7 sea load and wind loads.

4. Examine if the displacement at each of the six points on the radar base plate was less than 0.2 milliradians under stage 7 sea load, wind load and 2.5g acceleration loads in Ax, Ay, and Az directions.

The Mathematical Model of the Isolator and Absorber on the Radar Base Plate

The two commonly used approaches to reduce the vibration of ship radar systems are as follows:

1. Put an isolator between the radar and the base plate as shown in Figure 9. The main function of the isolator is to reduce the radar vibration that is transferred from the base plates. Additionally, the isolators can damp out the force which is transferred from the radar to the base plate.

2. Link a dynamic absorber with the radar as shown in Figure 10. The main purpose of the absorbers is to sponge the energy of vibration, to reduce the vibration of the radar and increase the isolation.

The equations of motion for the mast system with an isolator were as follows:

1. The equation for an isolator was:

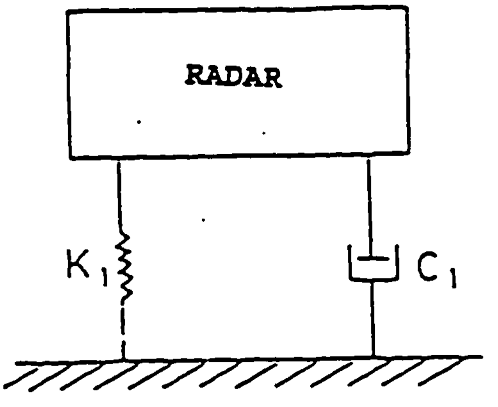

Figure 9. An isolator between the radar and the base plate.

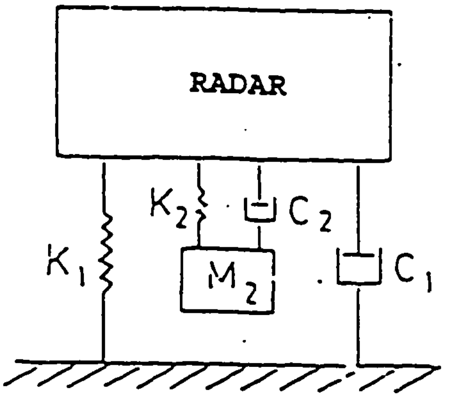

Figure 10. An added absorber with the isolator and the radar and base plate.

$$mx + c\dot{x} + k\ddot{x} = 0$$

2. The equation for the combination of an isolator and an absorber was:

$$k2/k1 = m1.m2/(m1+m2)^2$$

k1	Constant for isolator.
k2	Constant for absorber.
m, m1	Mass of radar.
m2	Mass of absorber.
c	Constant for isolator.
x	Amplitude at middle of the radar base plate of the isolator.
$\dot{x}$	Velocity at middle of the radar base plate.
$\ddot{x}$	Acceleration at middle of the radar base plate.

The optimum design of the radar was obtained when the above two equations were used in the finite element analysis. The constraints used in the optimization were (1) the displacement at the middle of the base plate is less than 0.2 milliradian and (2) the frequency is less than 50 Hz.

The major purpose of this experiment was to determine the optimum frequency modulation ratio (K2/K1 in equation 2) of a combined absorber and isolator and the optimum resistance ratio (k in equation 1) of the absorber when the radar displacement was minimized. The goal was to increase the stability and accuracy of the radar.

Field Test (on a Ship at the Sea)

The main purpose of the field test was to verify the effect of the isolator and the absorber in reducing radar vibration. The following conditions were used in the field tests on a ship at sea.

1. Mast without isolator and absorber at general speed (15 knots).

2. Mast with isolator and absorber at general speed (15 knots).

3. Mast without isolator and absorber at critical speed (18 knots).

4. Field test with isolator and absorber at critical speed (18 knots).

5. Field test without isolator and absorber at economic speed (22 knots).

6. Field test with isolator and absorber at economic speed (22 knots).

7. Field test without isolator and absorber at high speed (30 knots).

8. Field test with isolator and absorber at high speed (30 knots).

Critical speed for a ship is the speed at which resonance vibrations occurs. Economic speed is also called normal speed during which noise and vibration are smallest. High speed is one at which the engine rotational speed is very close to its upper limits.

CHAPTER IV

PRESENTATION AND DATA ANALYSIS

The results of the data analysis and experiment described in the previous chapter are presented in this chapter. The purpose of the data analysis and experiment was to determine the reasonable oscillation model state to design the optimum vibration absorber and vibration isolator.

Data Analysis

Research question one: What is the reasonable finite element analysis model to analyze the dynamic behavior of the mast, including the natural oscillation frequencies and the oscillation states of the mast structure?

A series of laboratory experiments were conducted in order to answer research question one. These experiments included an aluminum alloy tube experiment, a pipe element experiment, and a finite element analysis experiment. In addition, to make the experiments complete, a mast structure simulation of an oscillation state was conducted and the natural frequency was measured. The data in Figures 11 and 12 show the two free vibration models of aluminum alloy tubes. The results shown in these figures were needed for

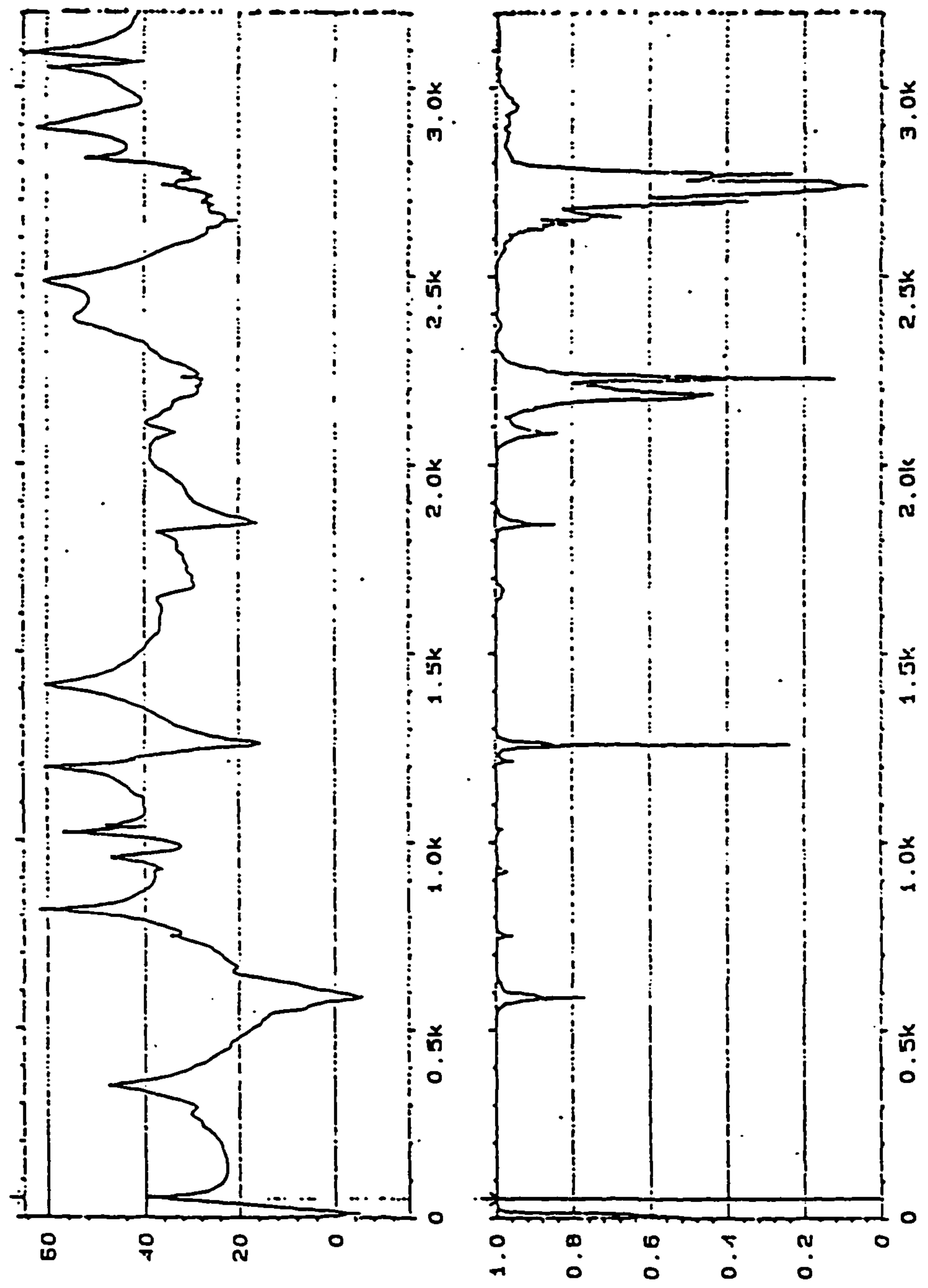

Figure 11. The result of the experiment of the non-welding conduit model state.

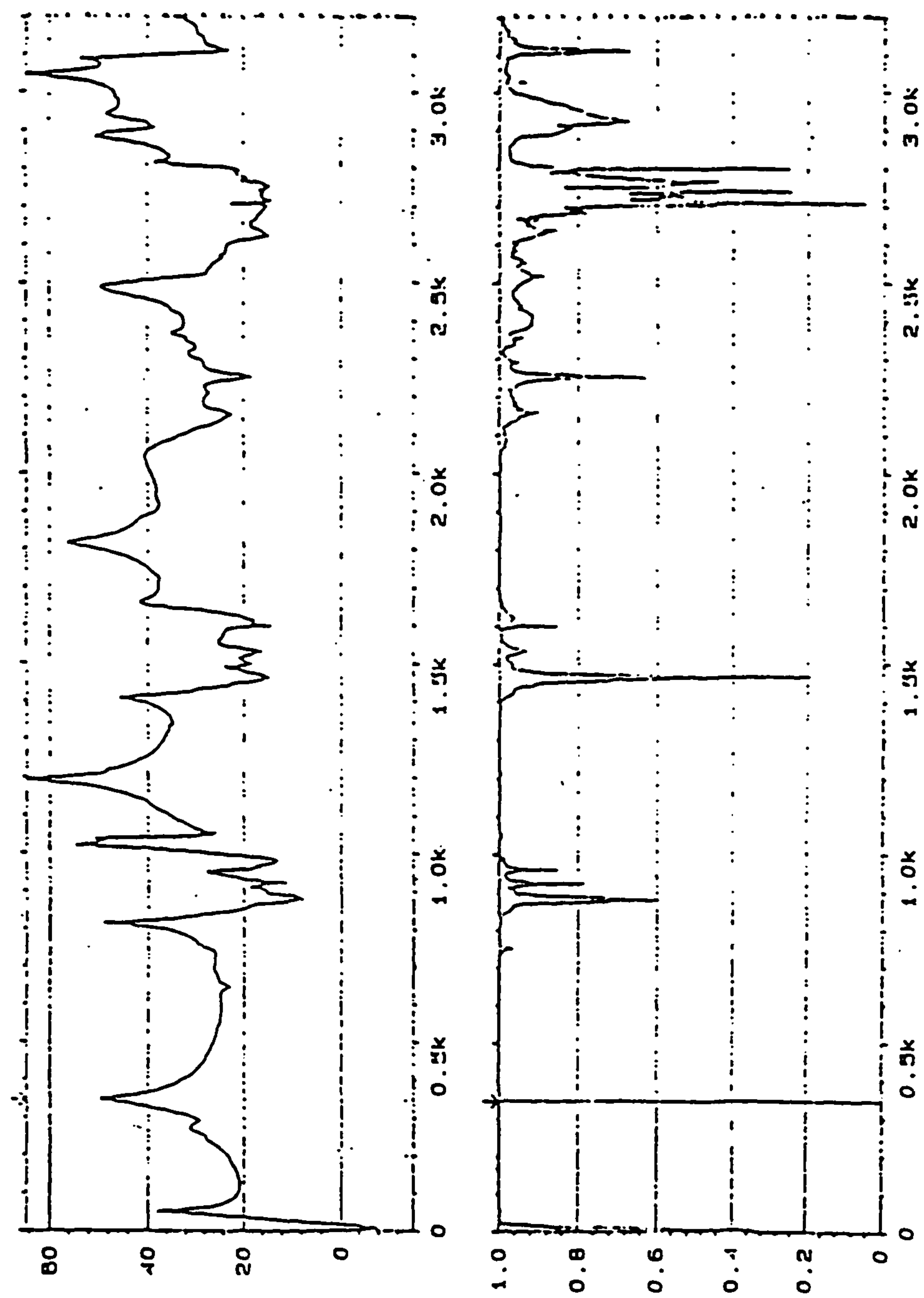

Figure 12. The result of the experiment of the welding conduit model state.

selecting pipe elements for data analysis, for determining pipe elements for analysis, and for design of the pipe elements. The data in Figure 11 illustrates the frequency responses of an aluminum tube. Figure 12 shows the frequency responses of a welded aluminum tube. The frequencies of an aluminum alloy tube obtained from the experiments are shown in Table 3. There were no significant differences in natural frequencies between welded tubes and continuous tubes. In other words, the difference in mechanical properties of welded aluminum tubes and continuous aluminum tubes were very limited.

Table 3

Table of Natural Frequencies

Item Number	Tubes	Welded Tubes
1	48	52
2	324	332
3	808	844
4	920	924
5	1032	1028
6	1144	1180
7	1384	1396
8	1648	1664

The following observations were derived from the previous results:

1. Welding had no obvious influence on the mechanical properties of mast structure.

2. The aluminum alloy tubes welded with good quality (6061-T6) can be considered as rigidly fixed. The welded aluminum alloy tube structure can be considered as a beam structure. Each beam element i.e., an aluminum alloy tube, could sustain external forces and displacements of six degrees of freedom in X, Y, and Z directions.

3. The vibration modes of aluminum alloy tubes (6061-T6) were the same as that of a beam element.

The Analysis Element of a Tube

According to the sizes of the tested components, the investigator set up a finite element analysis model by the use of shell and beam elements. The integrated software SUPERTAB and SAP6 were adapted to analyze oscillation. SUPERTAB was used to build an analysis model and displace the analysis results. SAP6 was used to construct a system of equations and solve the equations. The results are shown in Tables 4 and 5. Figure 13 to Figure 17 are graphs of each oscillation type. For the bending and longitudinal oscillation types, there was no difference in using either a shell element or a beam element for analysis. The shell element model, however, was more effective for detecting wrist and radial oscillation (Figures 18 and 19).
In other words, the beam element model does not have this function.

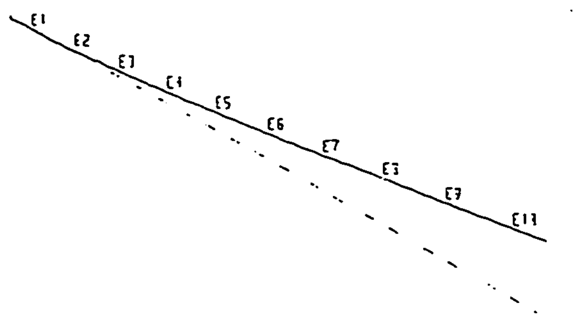

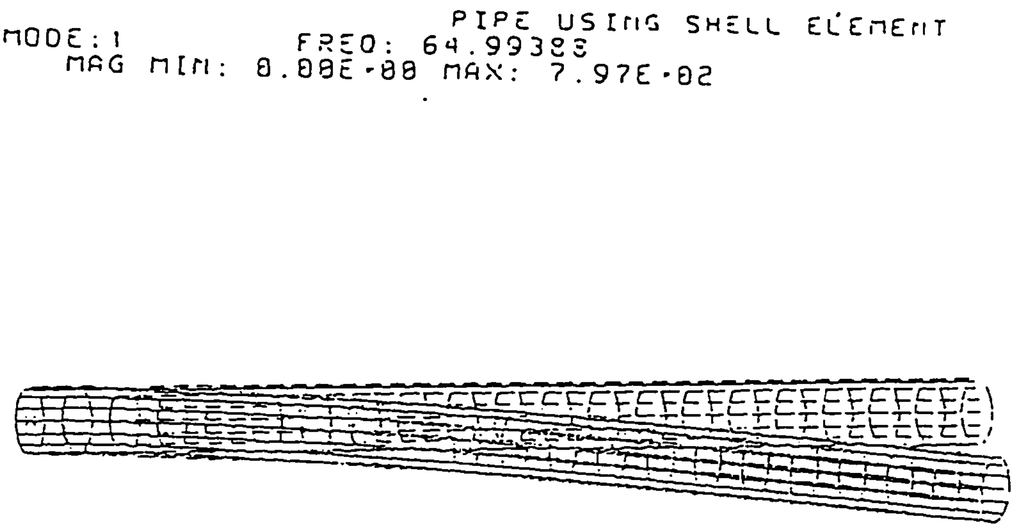

Figure 13. The first bending oscillation (a) beam element (b) shell element.

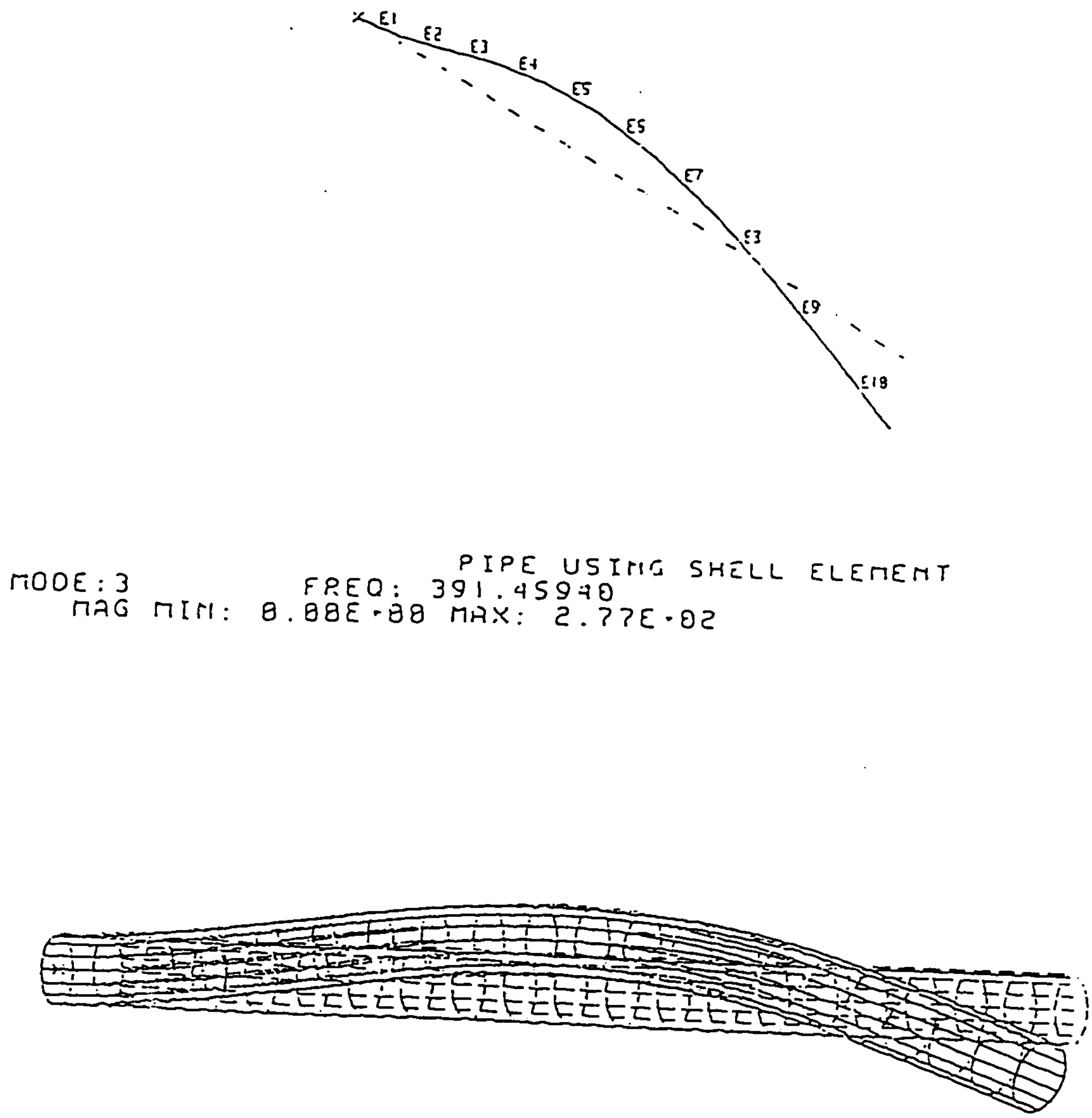

Figure 14. The second bending oscillation (a) beam element (b) shell element.

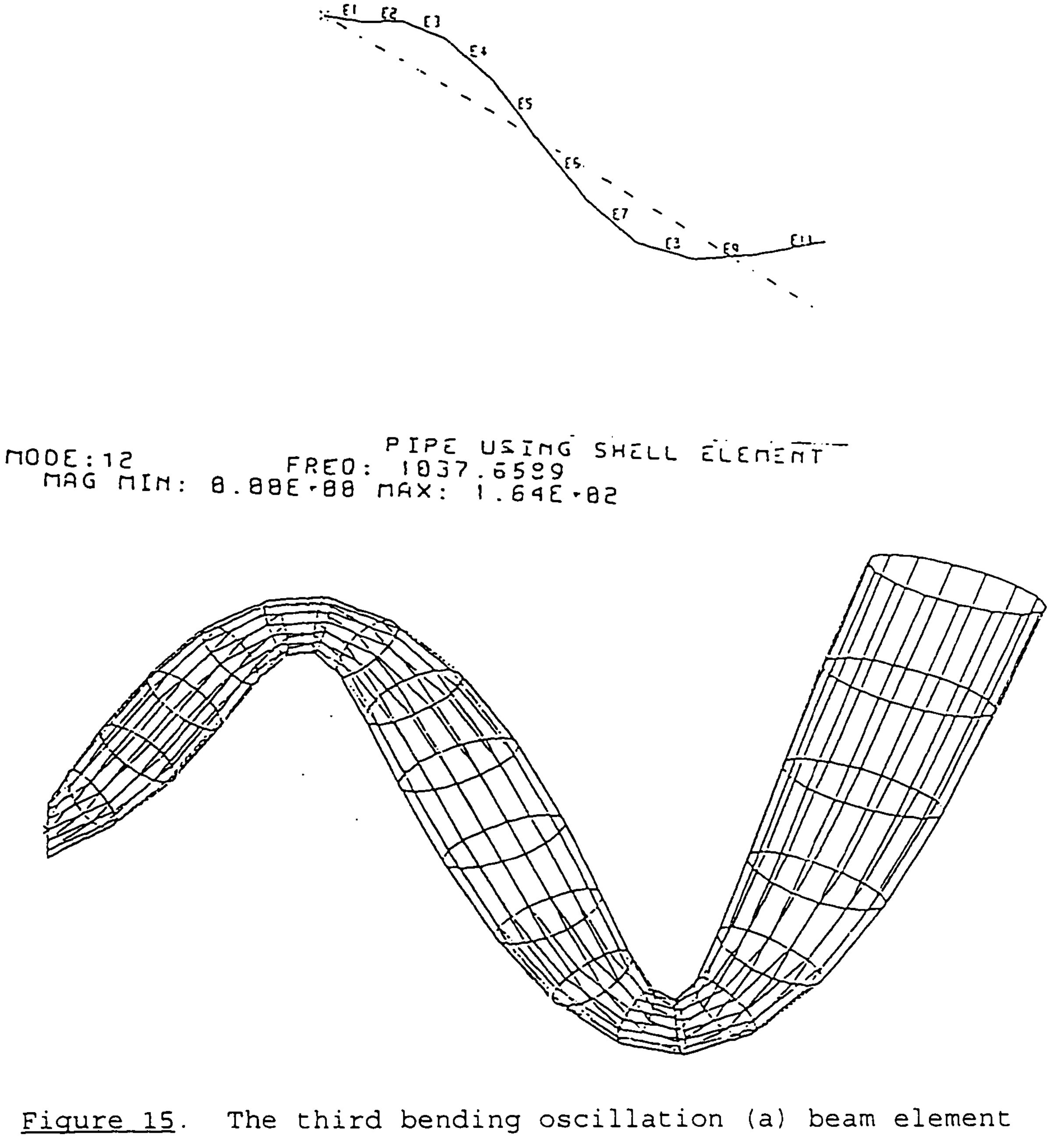

Figure 15. The third bending oscillation (a) beam element (b) shell element.

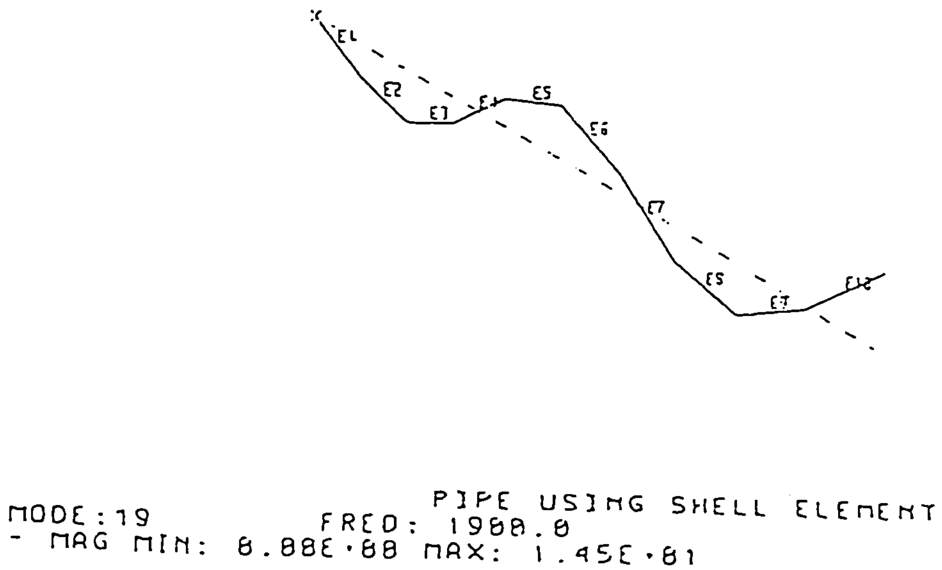

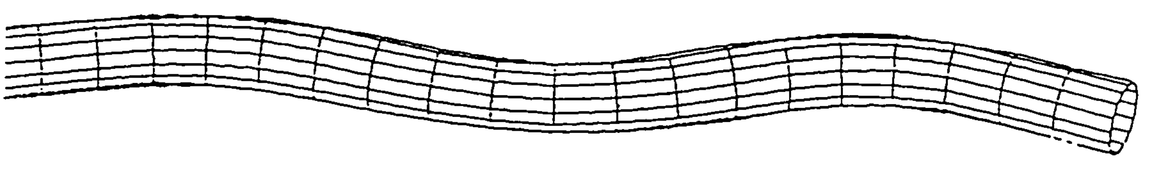

Figure 16. The fourth bending oscillation (a) beam element (b) shell element.

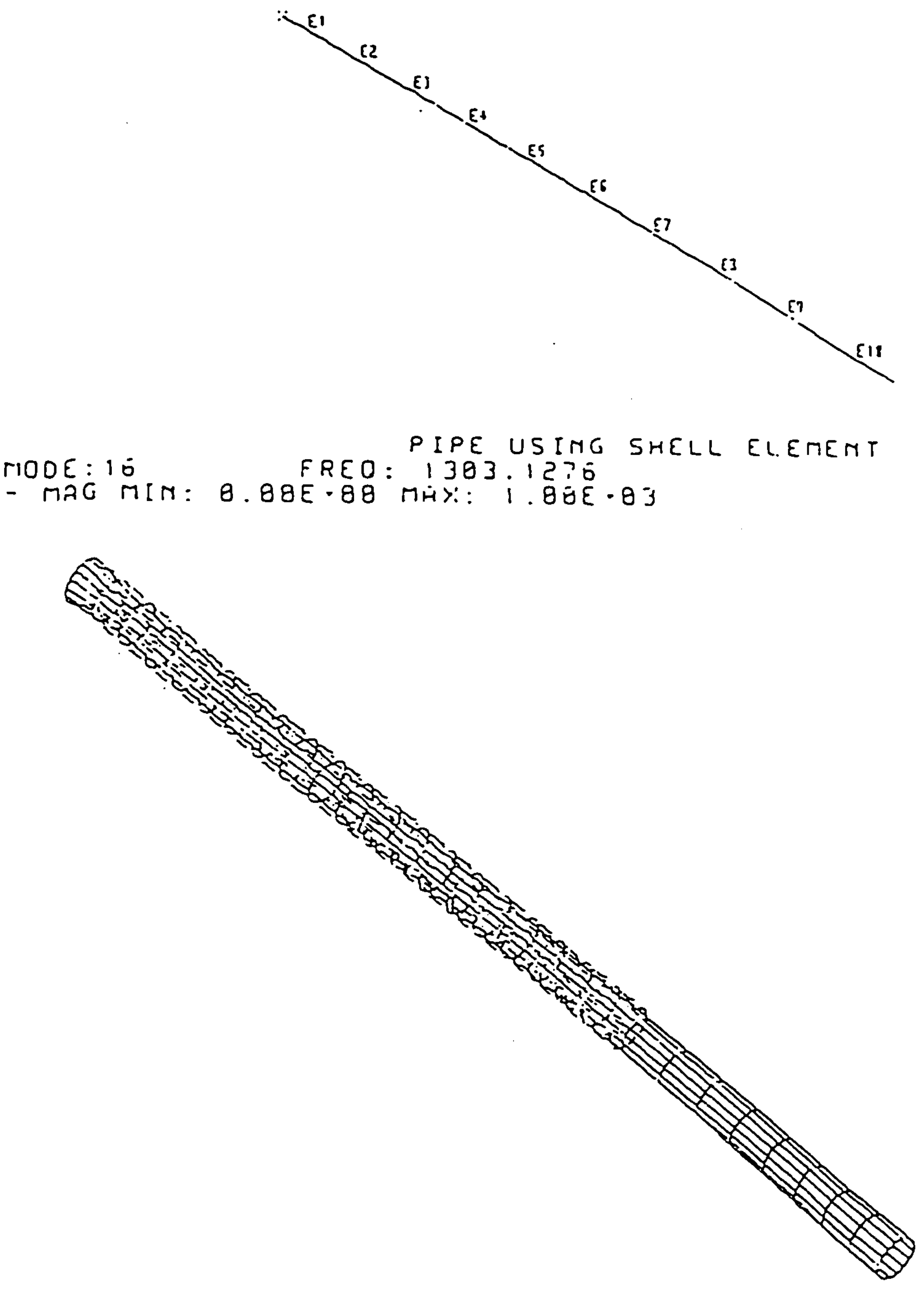

Figure 17. Longitudinal mode.

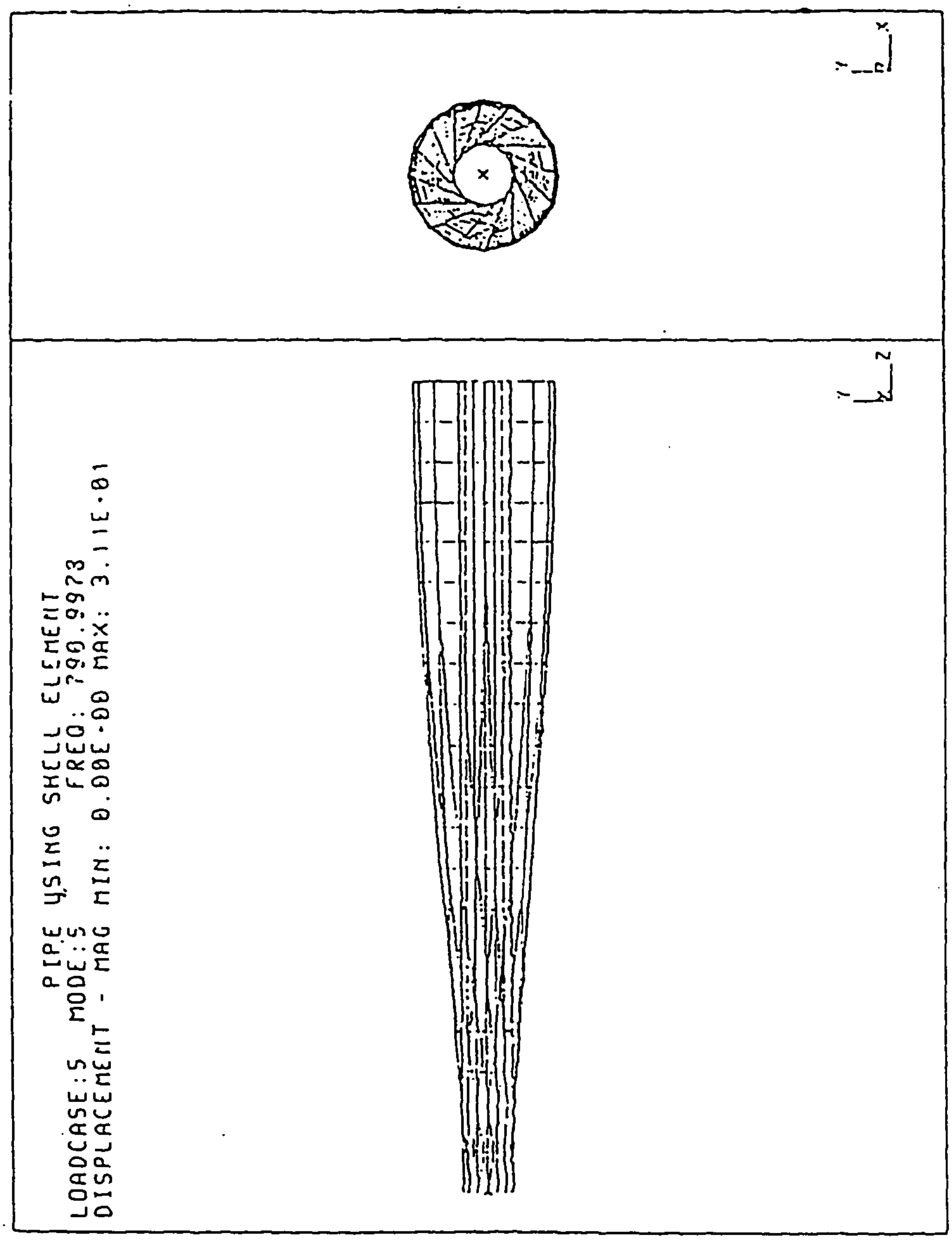

Figure 18. Torsion radial.

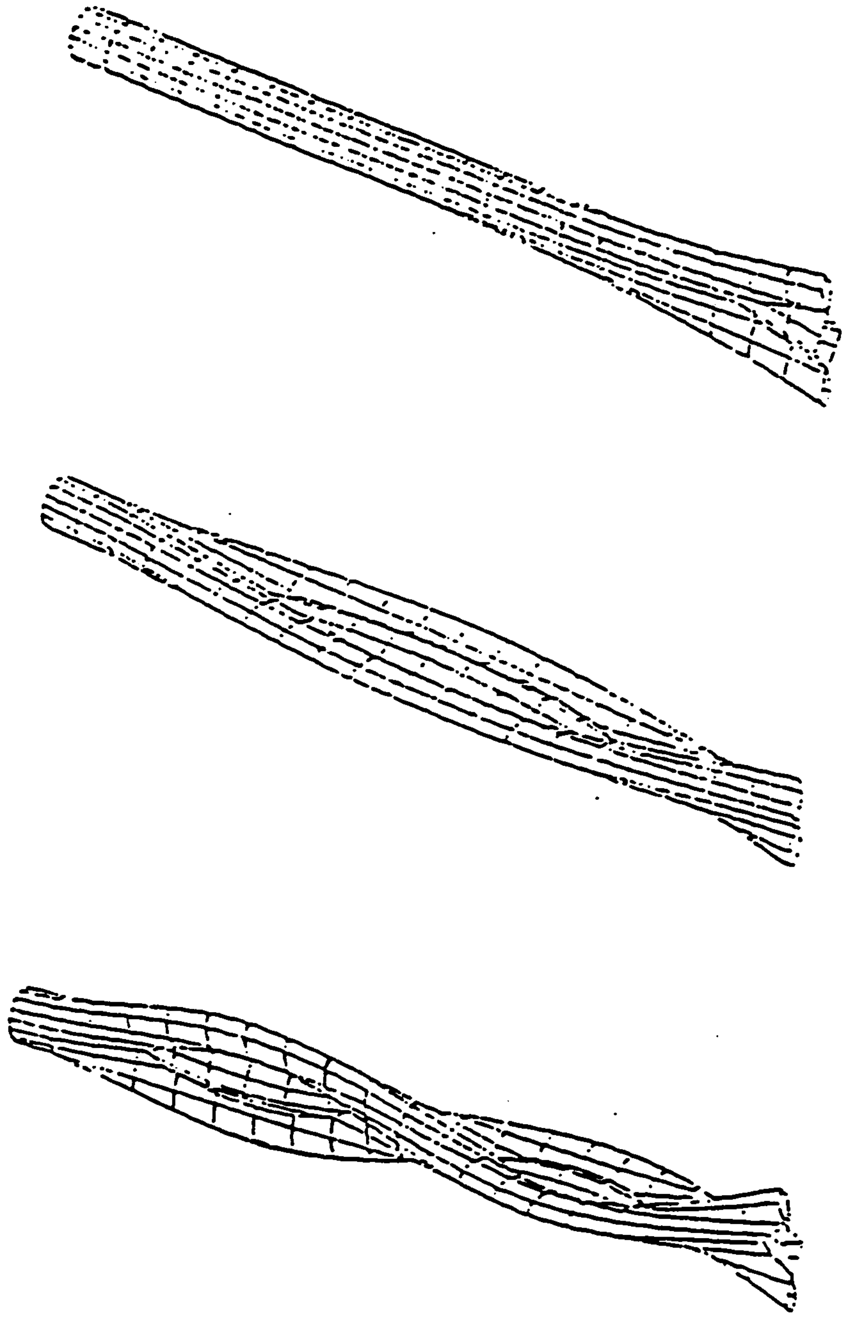

Figure 19. Radial vibration of mast tube.

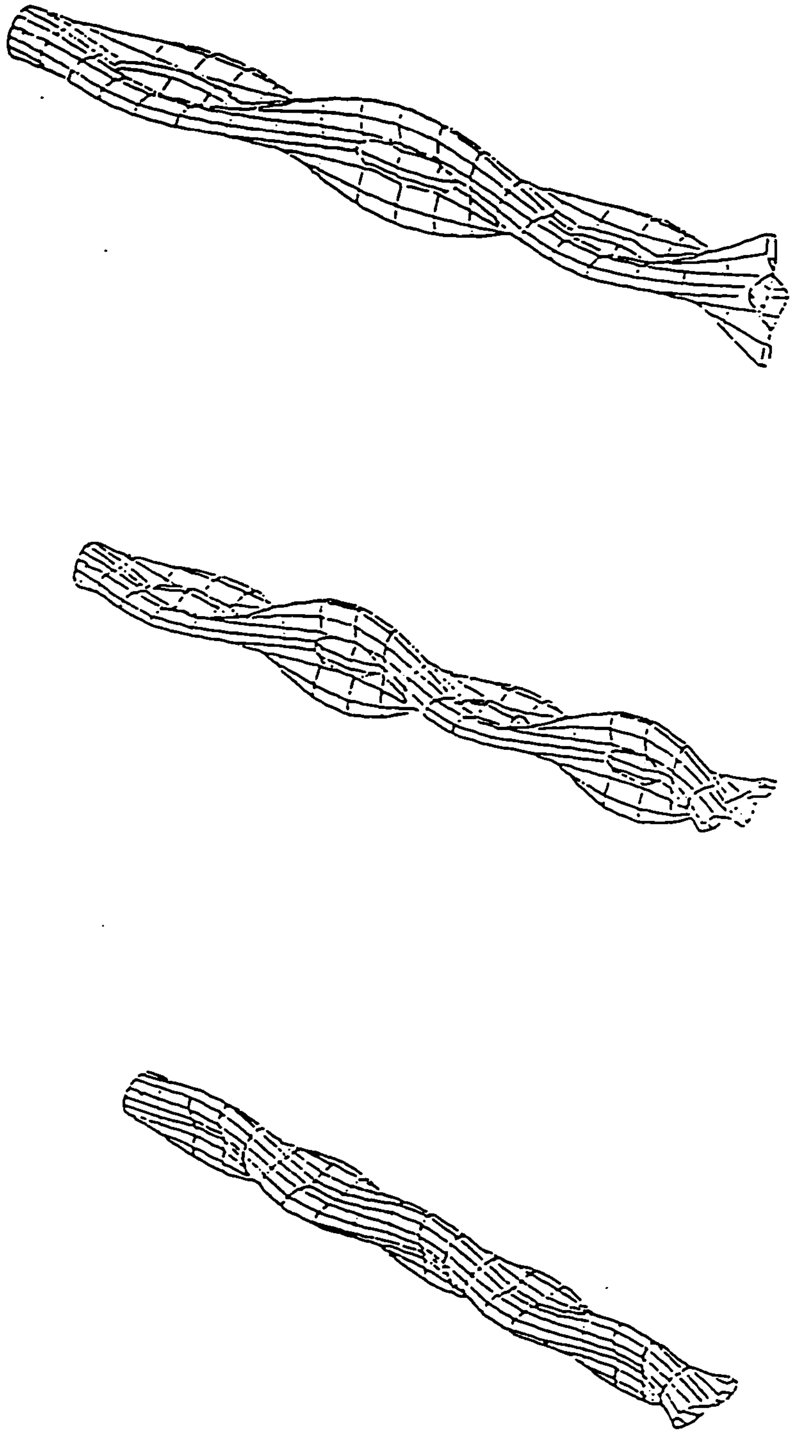

(Figure 19 continues)

Table 4

The Result of Beam Elements Analysis

Type of Oscillation	Natural Frequencies	Model
1.	64.9	1st Bending
2.	391.5	2nd Bending
3.	808.2	Torsion or Radial
4.	1040.2	3rd Bending
5.	1303.1	1st Longitudinal
6.	1915.1	4th Bending

Vibration Analysis of Mast Structure

A finite element analysis model of the mast was used to analyze the natural oscillation frequency and the oscillation state of the mast structure. The illustration in Figure 20 shows the finite element model of the mast structure. The structure model has 40 nodal points and 110 elements, including 110 Linear Space Beam Element and one Circular Plate Element.

Usually any kind of instrument or equipment will experience some oscillation when it is placed on either an airplane or a ship. Serious oscillation can lead to damage to the equipment, and less serious oscillation can affect

Table 5

The Result of Shell Elements Analysis

Type of Oscillation	Natural Frequencies	Model
1.	65.0	1st Bending
2.	391.5	2nd Bending
3.	791.0	Torsion + Radial
4.	918.4	1st Radial
5.	942.4	2nd Radial
6.	1003.0	3rd Radial
7.	1037.7	3rd Bending + Radial
8.	1171.2	4th Radial
9.	1303.1	Longitudinal
10.	1473.9	5th Radial
11.	1900.0	4th Bending
12.	1965.4	4th Bending + Radial

the function of the equipment. Therefore, finding ways to decrease the oscillation of a system has become a very important task in the field of ship engineering.

As mentioned before, SAP6 was used as the oscillation analysis package. In SAP6, there were 460 simultaneous equations in structural analysis. The first frequencies of the oscillation of the mast structure are shown in Table 6.

Table 6

The First Five Frequency Oscillations

Type of Oscillation	Frequencies in rad/sec	Frequencies in cycle/sec
1	113.7	18.09
2	217.9	34.69
3	252.5	40.18
4	259.4	41.28
5	344.7	54.87

Types of oscillation in the finite element analysis are shown in Figure 21 to 25. In these figures, solid lines are used to indicate the original mast structure and dotted lines indicate the mode of oscillation. These figures also present the types of mast structure oscillation, main elements of displacement, displacement directions, and indicate the joint positions of the largest displacement in X, Y, and Z directions which are indicated by symbols.

Regarding oscillation at the lowest frequency, Figure 21 shows that the mast structure oscillation has taken place

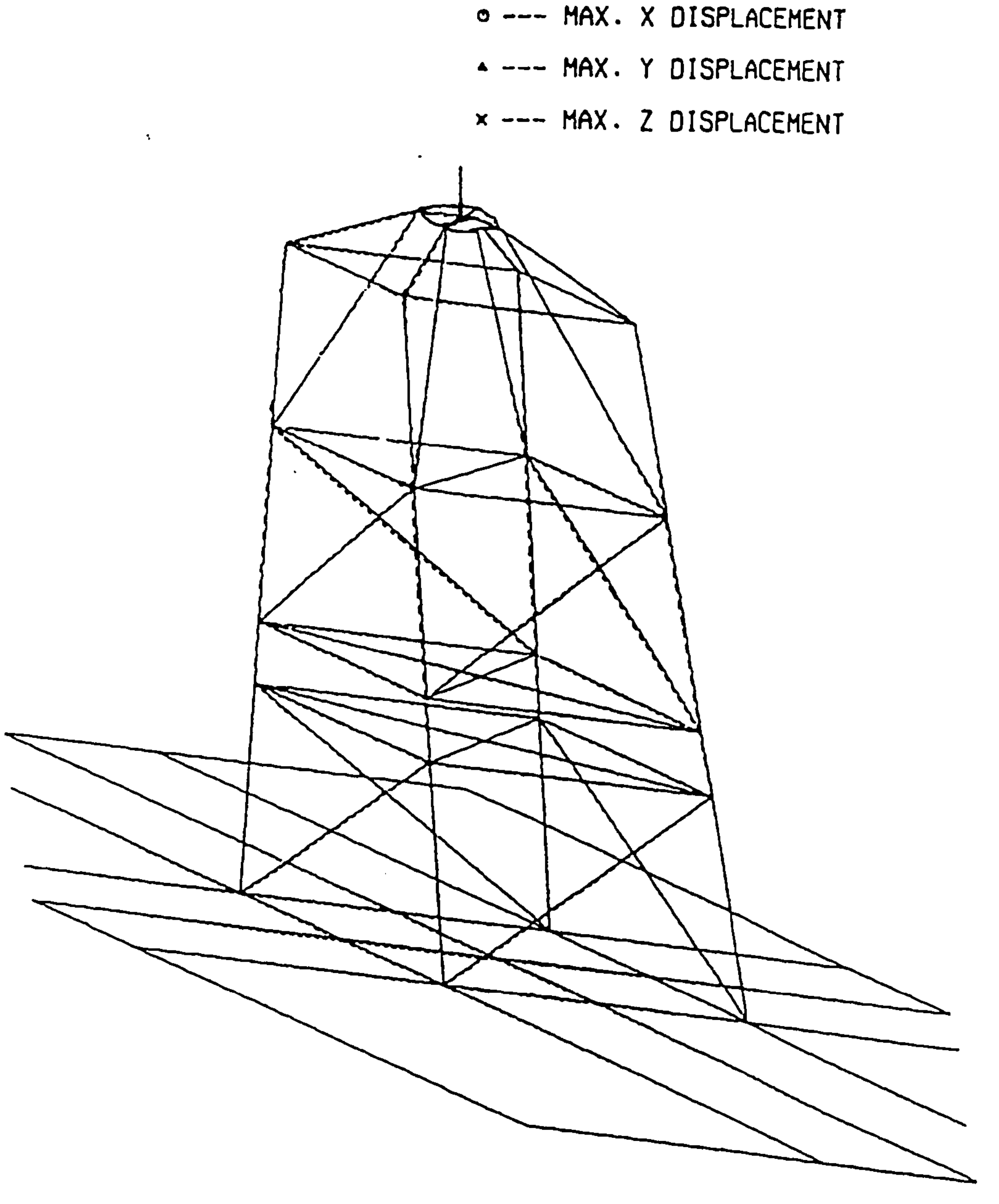

Figure 20. Finite Element Model of Mast Structure.

on the top of the structure. The main oscillation direction was in the X direction. The largest oscillation displacement of the circular radar system was also in the X direction, while the main structure was small.

The illustration in Figure 22 shows the main oscillation of the mast structure in the Z direction (second frequency). The presence of primary damping in the mast significantly affected the optimum damping required for the absorber, when the absorber mass was about half of the mass of the mast. This was shown in the X direction and Z direction.

The illustration in Figure 23 shows the main oscillation of the mast structure in the Y direction (third frequency) of the radar base plate. It was clearly observed that rotation occurred because of damping in the Y direction. This was also shown for the absorbers, however, the effect was mild because their mass is very small compared with main mass.

The illustration in Figure 24 shows the main oscillation in the X direction (fourth frequency). The main displacement of the circular radar base plate was also in the X direction, while the middle part of the main structure had a large displacement.

As shown in Figure 25 (fifth frequency), the main oscillation of the mast structure is in the X and Z directions of the radar base plate, and the Y direction displacement at the bottom of the structure was large. This was also shown in the absorbers, on which this effect was mild because their mass is very small compared with the main mass.

Based on the above observations, one can determine that the aluminum alloy tubes of the mast structure can be considered as space beam elements. This conclusion was the basis for establishing the finite element analysis model.

Research question two: With the addition of a dynamic vibration absorber and isolator, will the vibration amplitude of the radar on the base plate be within the prescribed maximum of 0.2 milli-radians when the ship is subject to stormy waves and wind load?

In this experiment, it was found that an aluminum alloy tube of the mast structure can be considered as an element for the finite element analysis model shown in Figure 26.

The following sea states and wind conditions were used in the finite element analysis:

Front direction wind speed = 70 mile/hr,

Side direction wind speed = 50 mile/hr,

Air density = 0.00238 slug/ft^2,

Sea state number = 7 ,

Constant = 1.28.

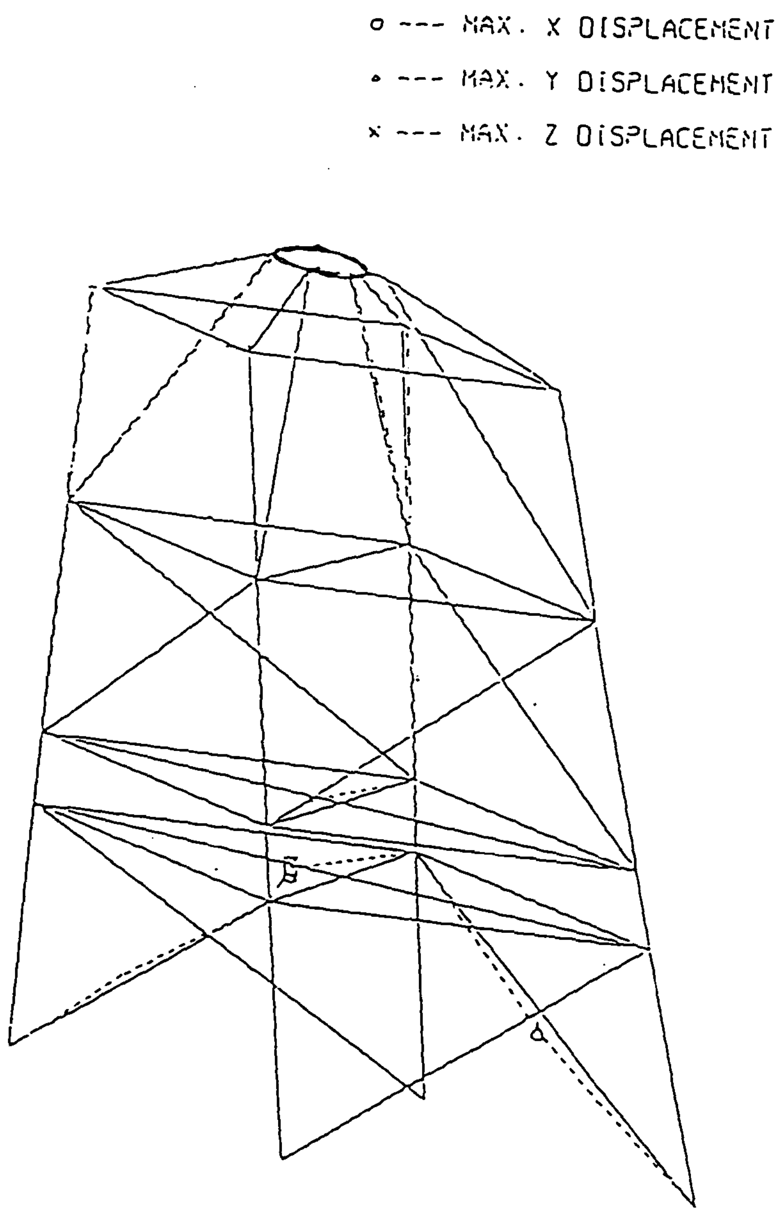

Figure 21. Model of the Finite Element in Mast Structure (Oscillation of the lowest frequency).

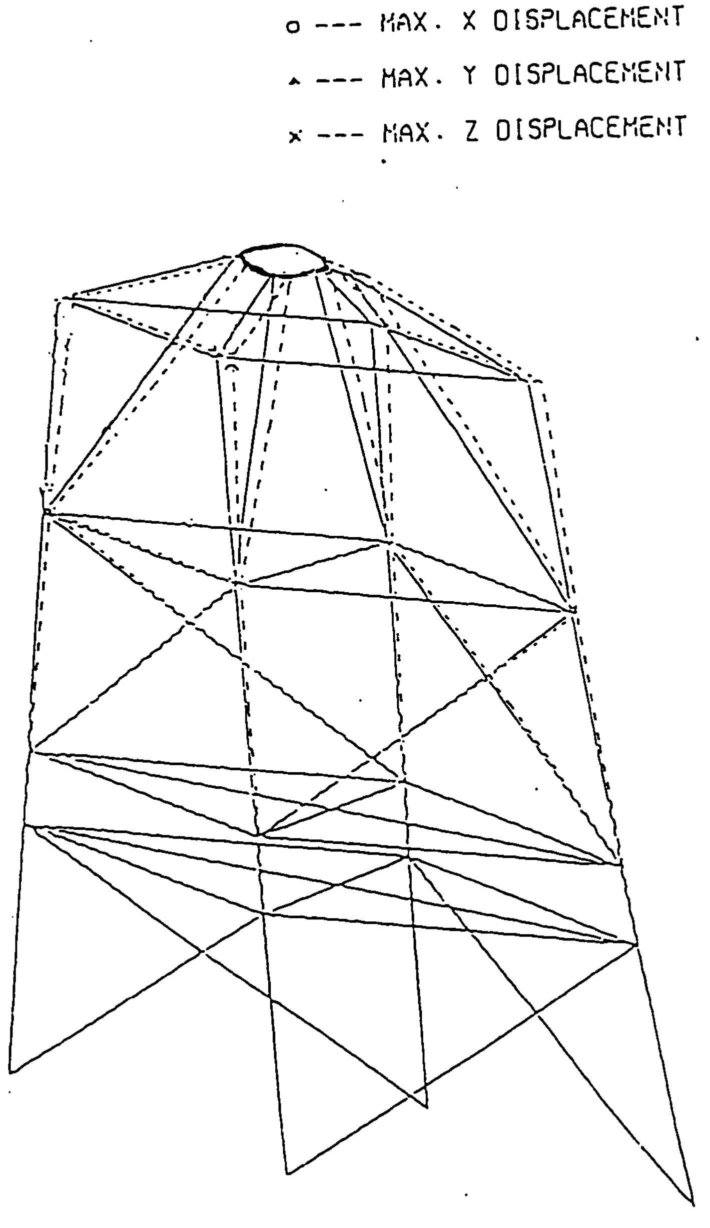

<u>Figure 22</u>. Model of the Finite Element in Mast Structure (Oscillation of the second frequency).

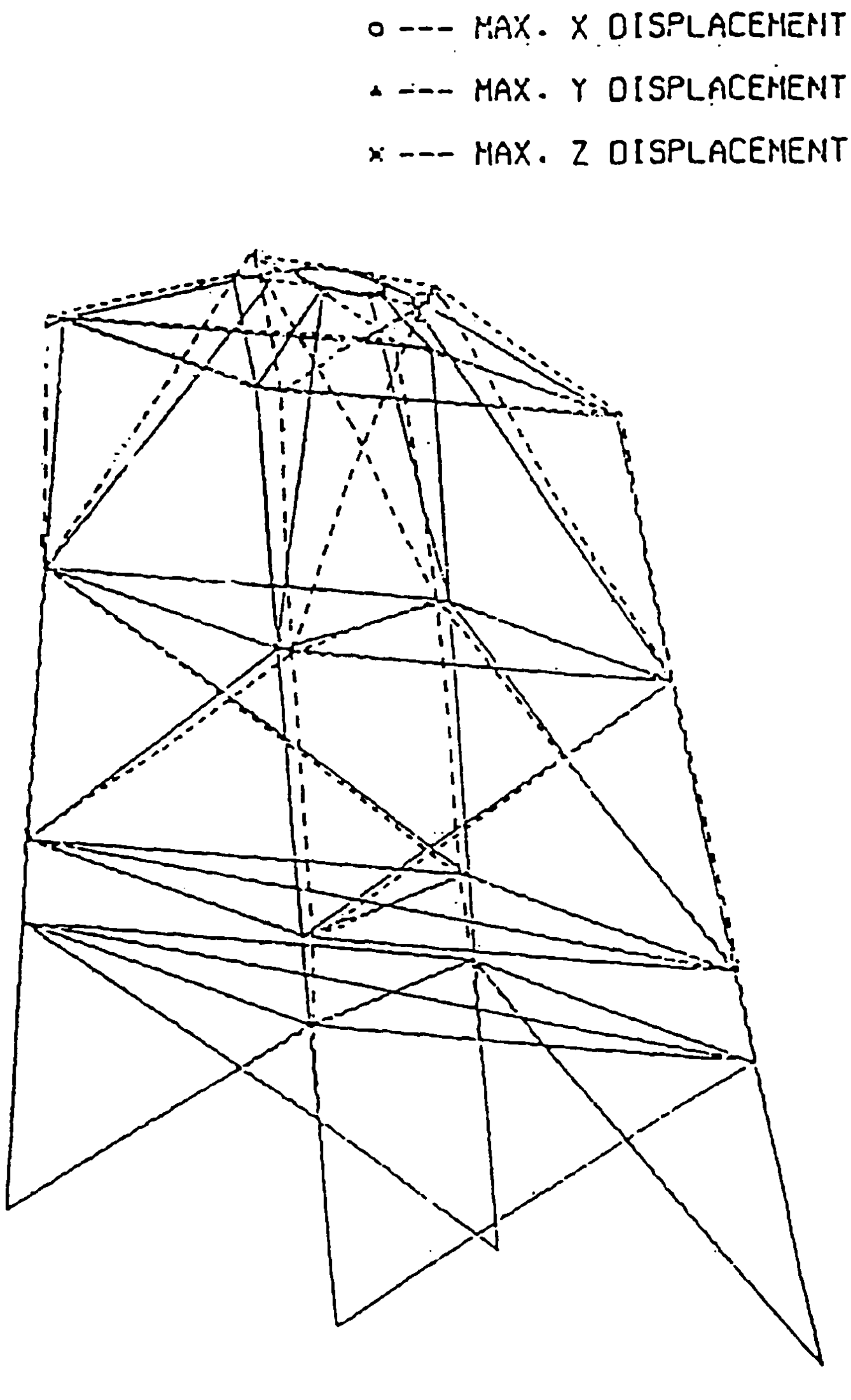

Figure 23. Model of the Finite Element in Mast Structure (Oscillation of the third frequency).

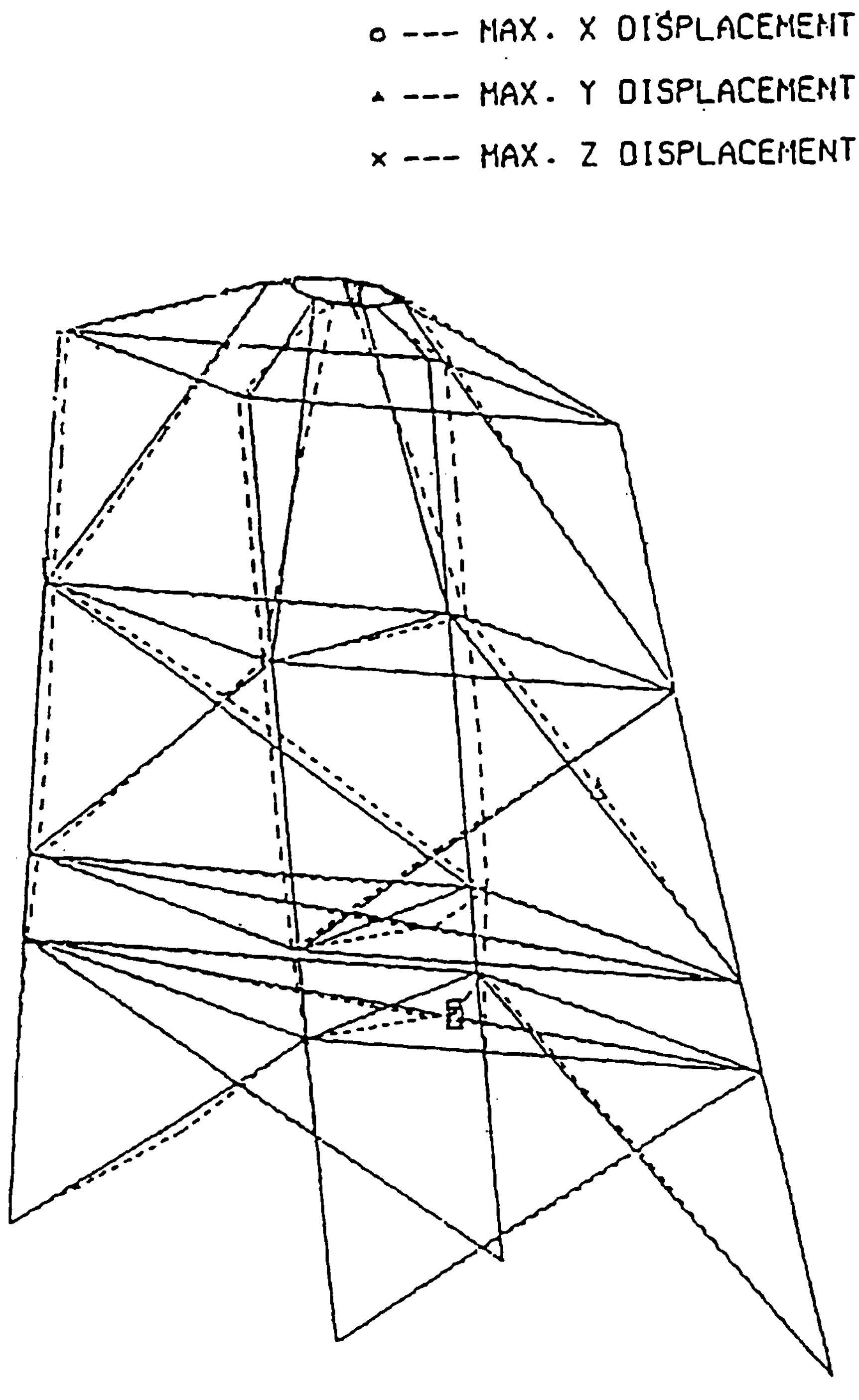

Figure 24. Model of the Finite Element in Mast Structure (Oscillation of the forth frequency).

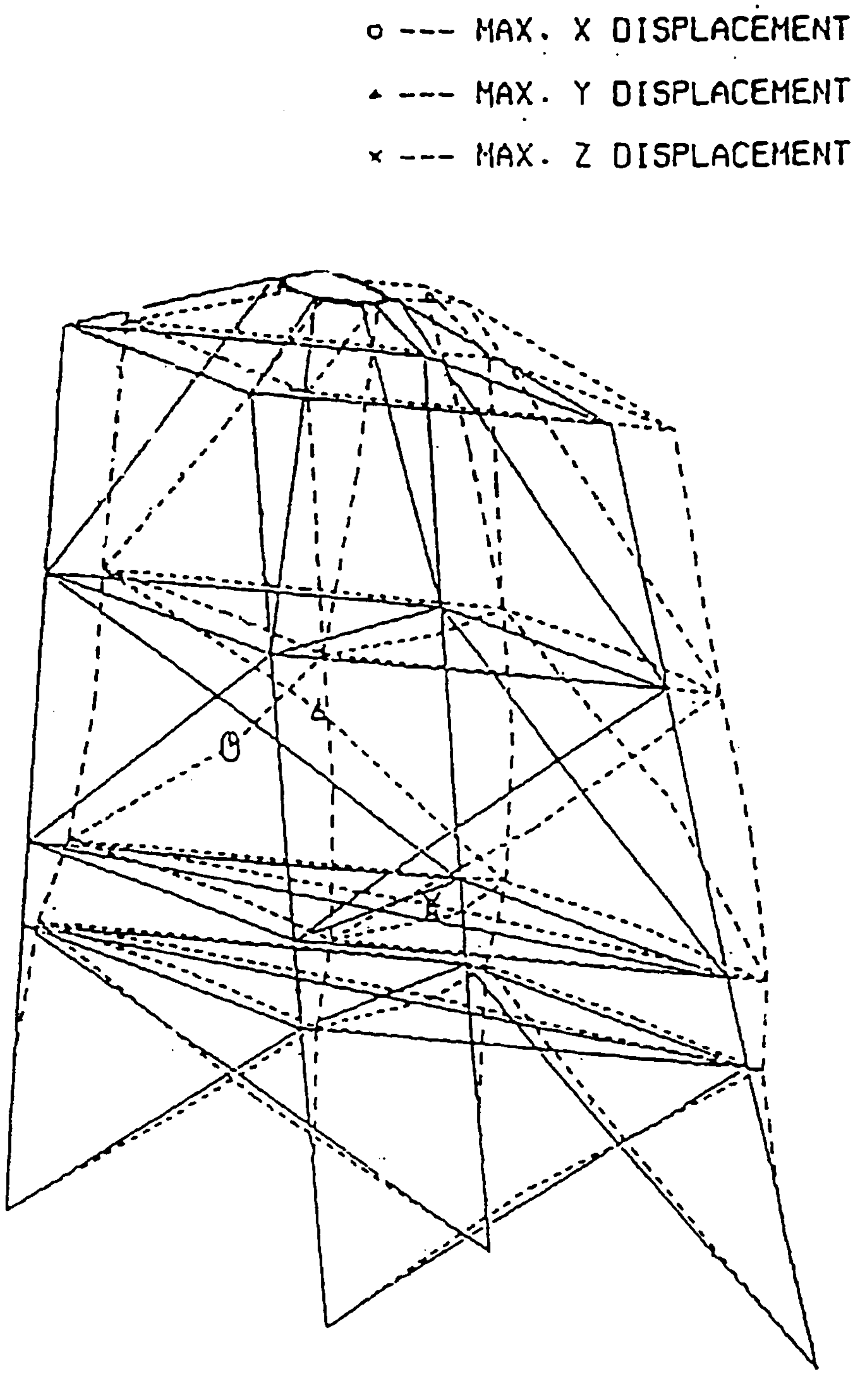

Figure 25. Modal of the Finite Element in Mast Structure (Oscillation of the fifth frequency).

$$A_X = A_s + g * Sin\theta_p + \frac{4\pi^2}{T_p^2}\theta_p^2 X + \frac{4\pi^2}{T_p^2}\theta_p Z$$

$$A_y = g * Sin\theta_p + \frac{1}{2}\frac{4\pi^2}{T_p^2}\theta_p X + \frac{4\pi^2}{T_r^2}\theta_r 2Y + \frac{4\pi^2}{T_r^2}\theta_r Z$$

$$A_z = g \pm\ A_h + \frac{4\pi^2}{T_p^2}\theta_p X + \frac{4\pi^2}{T_r^2}\theta_r Y$$

θ_r = 0.49 radian (Maximum Roll Angle)

θ_p = 0.0873 radian (Maximum Pitch Angle)

T_r = 8.0 seconds (Rolling Period)

T_p = 6.0 seconds (Pitch Period)

A_h = 0.3g (Heave Acceleration)

A_s = 0.15g (Surge)

Ax = Sea state load in X Direction

Ay = Sea state load in Y Direction

Az = Sea state load in Z Direction

g = Gravity Acceleration

X = Distance between the Center of Gravity of the ship and the Longitudinal Axis (fore and aft) of the ship on the deck

Y = Distance between the Center of Gravity of the ship and the Horizontal Axis (port side and starboard side) of the ship on the deck

Z = Distance between the Center of Gravity of the ship and the vertical direction (top and bottom) of the ship on the deck

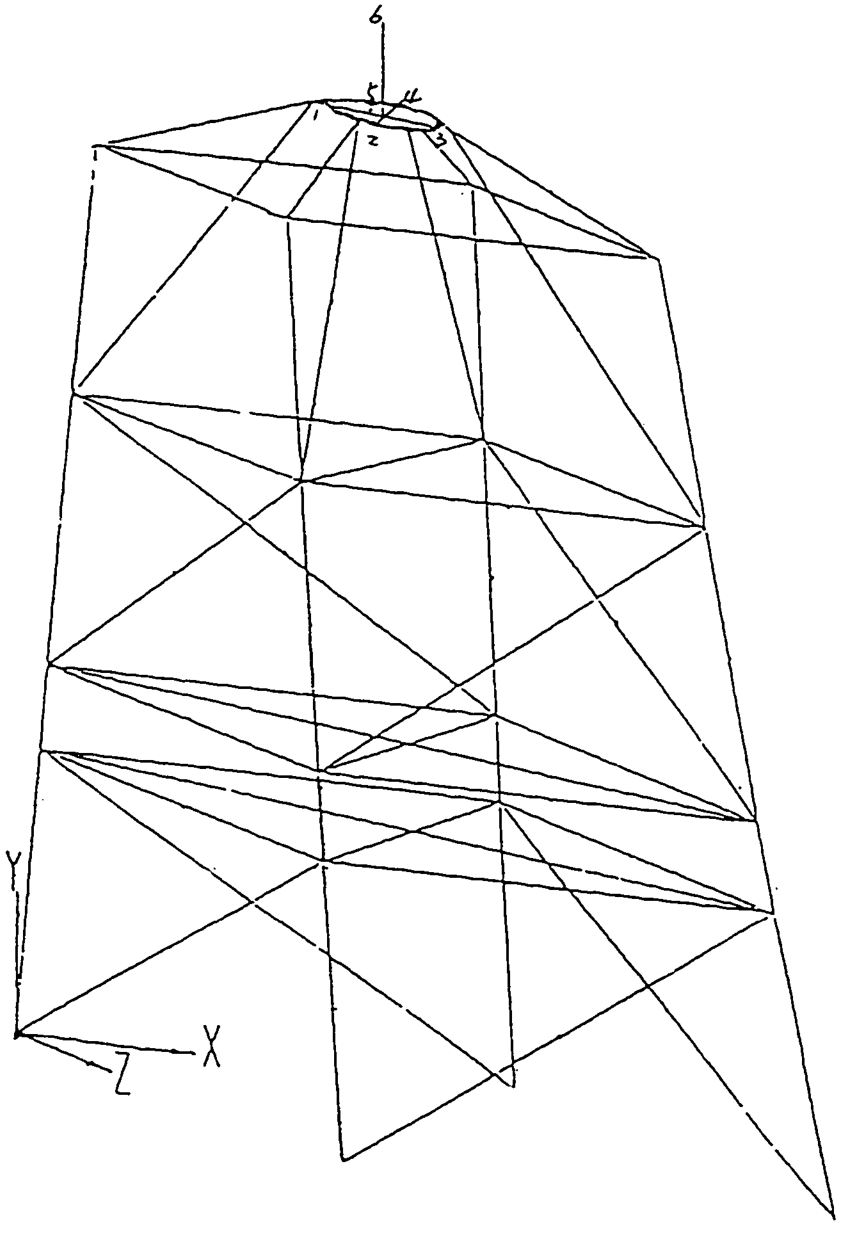

Figure 26. Radar base plate element in finite element analysis model.

Under the above conditions, the displacements(Δx, Δy, Δz) and angular displacements (ΔQ) for four points on the base-plate, are shown in Table 7, while their locations are shown in the circular plate on Figure 27.

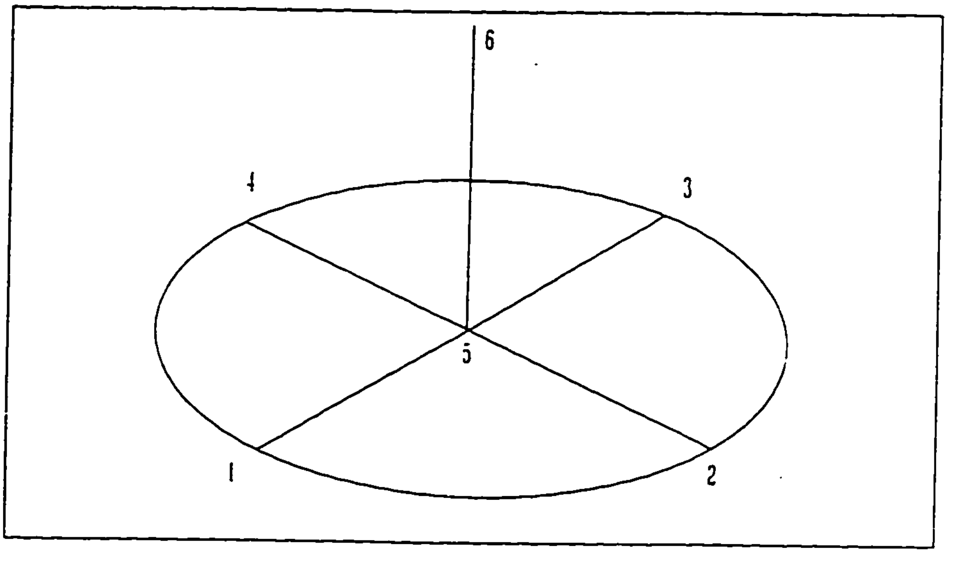

Figure 27. Radar Base Plate.

The most important data to be considered is the angular displacement at the location where the radar is mounted. This location is the middle point of the radar base plate. The angular displacement at this location can be calculated as the average of the angular displacement of the above four points. Under the assumed wind and sea state conditions, the calculated angular displacement at the middle of the

Table 7

The Displacement and Angular Displacement

POSITION	ΔX(in)	ΔY(in)	ΔZ(in)	ΔQ(milliradian)
1	-.0586	.0080	.0028	.1447
2	-.0568	.0081	.0027	.1404
3	-.0566	.0059	.0016	.1390
4	-.0589	.0061	.0018	.1447

Table 8

The Displacement and Angular Displacement (under Super Imposed Loads)

POSITION	ΔX(in)	ΔY(in)	ΔZ(in)	ΔQ(milliradian)
1	-.1124	.1193	.0018	.4008
2	-.1110	.1186	.0059	.3974
3	-.1106	.1209	.0069	.4010
4	-.1126	.1203	.0030	.4030

radar base-plate is less than 0.2 milliradians the acceptable range of angular displacement.

The displacements of these four points under the super imposed loadings (2.5g, wind 70 miles/hr, and sea state 7) are in Table 8.

From the above displacement information, the average of angular displacement at the radar base-plate is .4005 milliradians. This value is higher than the acceptable value which is 0.2 milliradians. Hence, the vibration of the mast needs to be reduced.

Analysis of the Radar Base Plate

The analysis of the radar base plate is described below. Further details may be found in Appendix B.

The data in Figure 28 and Figure 29 show the relationships between the radar displacement alteration μ_2, the mass ratio $\sigma_t{}^2$ between the vibration absorbing instrument and radar μ_2, and the resistance ratio of the vibration separating instrument ζ_1 when the spring constant of the isolator (k) is 25. In Figure 28 the base plate thickness is 1 inch. In Figure 29 the base plate thickness is 1.5 inches. According to the figures, the following conclusions can be made:

1. When μ_2 is less than or equals 0.1, the slope of the radar displacement alteration σ_t^2 rapidly decreases when μ_2 increases.

2. When μ_2 is greater than 0.1, the slope of the radar displacement alteration σ_t^2 changes mildly when μ_2 increases.

3. The σ_t^2 decreases when ζ_1 increases.

4. When comparing Figures 4-18 and 4-19, it was found that the value of σ_t^2 increases when the base plate thickness increases. Based on the above results, one can conclude that the size increase of the base plate does not decrease the angular displacement amplitude at the middle point of the radar base plate when random force is applied to the radar directly.

The data in Figure 30 shows that radar displacement alteration increased when the spring constant K1 of the vibration separating instrument increased and the following two parameters reached their optimal values: (a) resistance ratio/mass ratio of the radar and, (b) frequency modulation ratio/mass ratio of the radar.

The data in Figures 31 and 32 show the relationship between the optimum resistance ratio ζ_{opt} and the ratio of the frequency modulation ratio W_{opt} to mass ratio μ_2, obtained from the optimization analysis for different σ values under the following conditions:

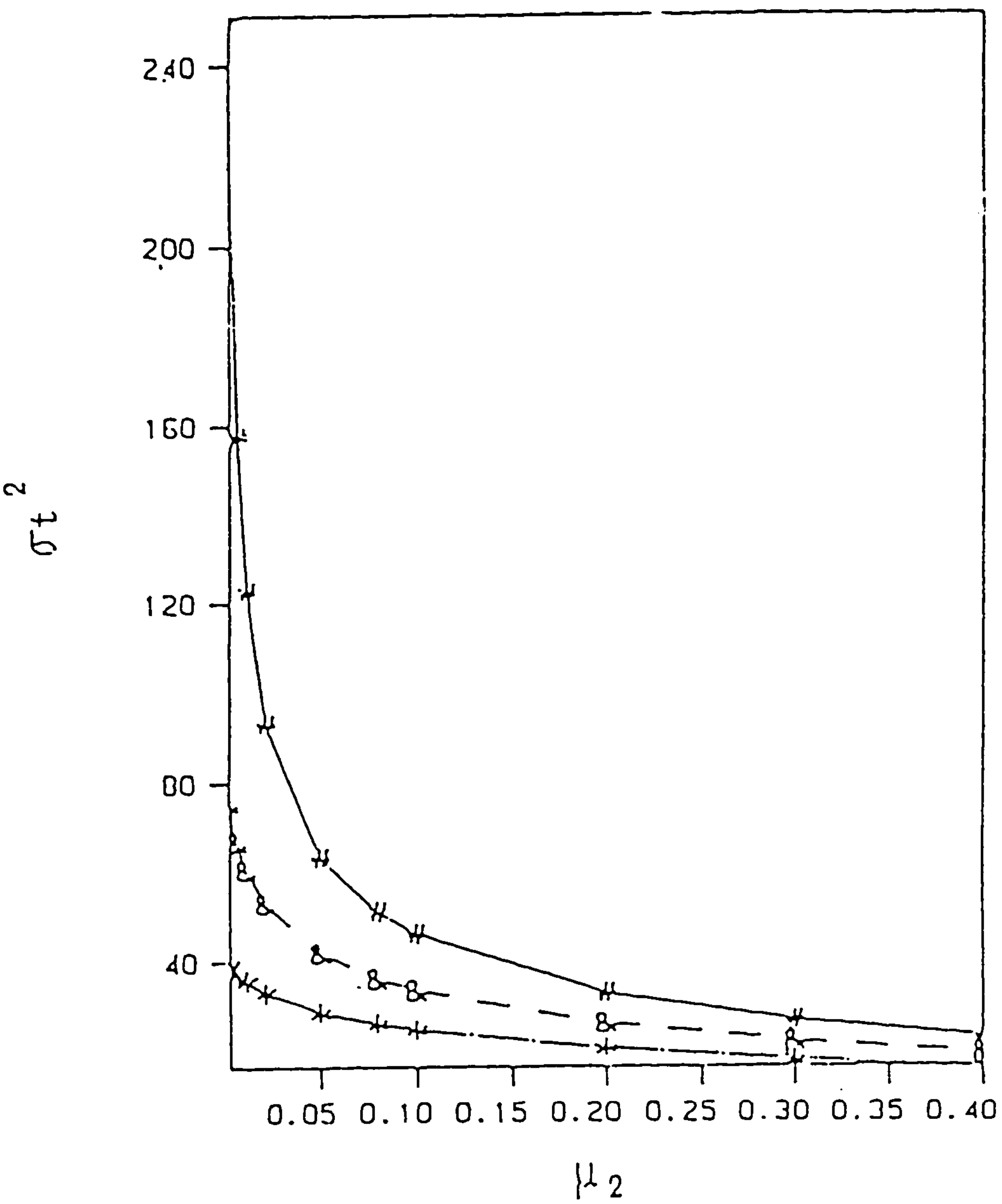

Figure 28. The relationship between the radar displacement alteration, the mass ratio between the vibration absorbing instrument and radar, and the resistance ratio of the vibration separating instrument when the base plate thickness is one inch.

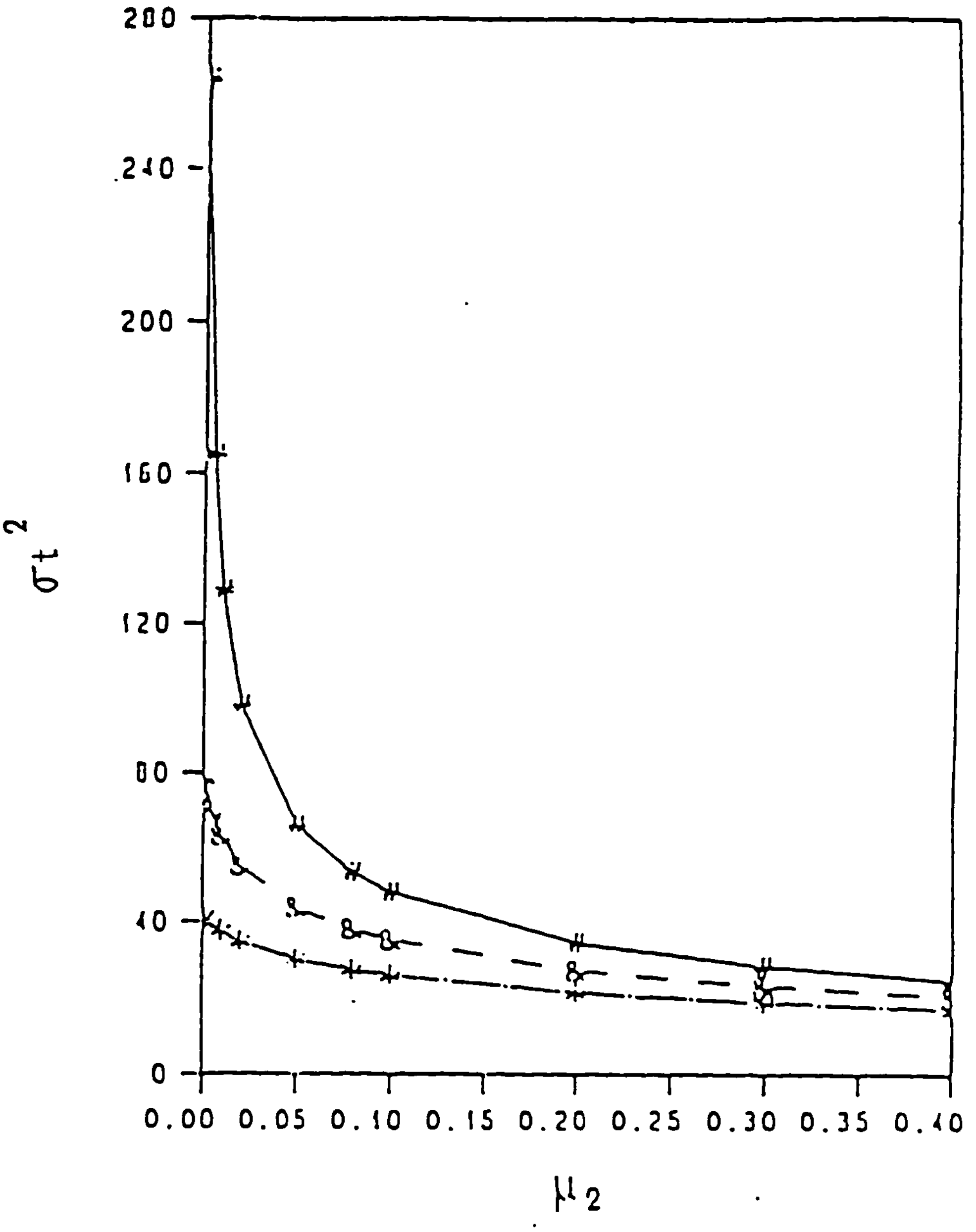

Figure 29. The relationship between the radar displacement alteration, the mass ratio between the vibration absorbing instrument and radar, and the resistance ratio of the vibration separating instrument when the base plate thickness is 1.5 inches.

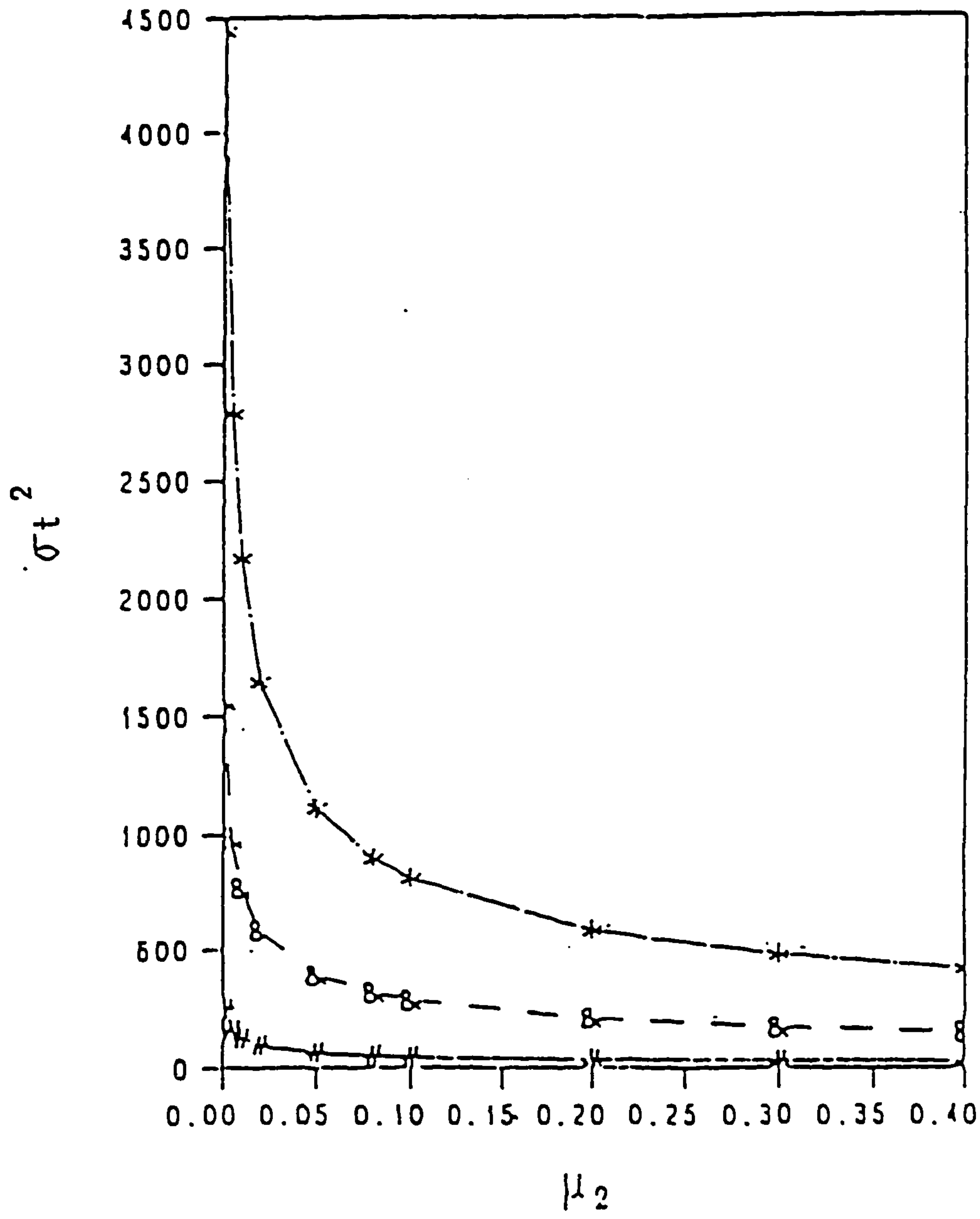

Figure 30. The relationship between the radar displacement alteration, the mass ratio between the vibration absorbing instrument and radar, and the spring constant K1 of the vibration separating instrument when the base plate thickness is one inch.

1. The base plate is 1 inch.

2. The spring constant of vibration absorbing instrument K1 is 25.

The following findings were obtained from the data in Figures 41 and 42:

1. The optimal resistance ratio ζ_{opt} increased when mass ratio μ_2 increased.

2. The optimum resistance ratio ζ_{opt} did not change with the resistance ratio of the vibration absorbing instrument ζ_1.

3. The value of the frequency modulation ratio W_{opt} decreased gradually when the mass ratio μ_2 increased.

4. The optimum frequency modulation ratio W_{opt} decreased slightly when the resistance ratio of the vibration absorbing instrument ζ_1 increased.

5. The frequency modulation ratio W_{opt} was less than 1 consistently. This means that the natural frequency of the optimal dynamic vibration absorbing instrument was always less than the natural frequency of the whole system.

The data in Figures 43 and 44 show the relationship between the optimal resistance ratio ζ_{opt}, the optimal frequency modulation ratio W_{opt}, and the spring constant K1 of the vibration separating instrument when $\zeta_1 = 0.01$. The conclusions made from these figures are as follows:

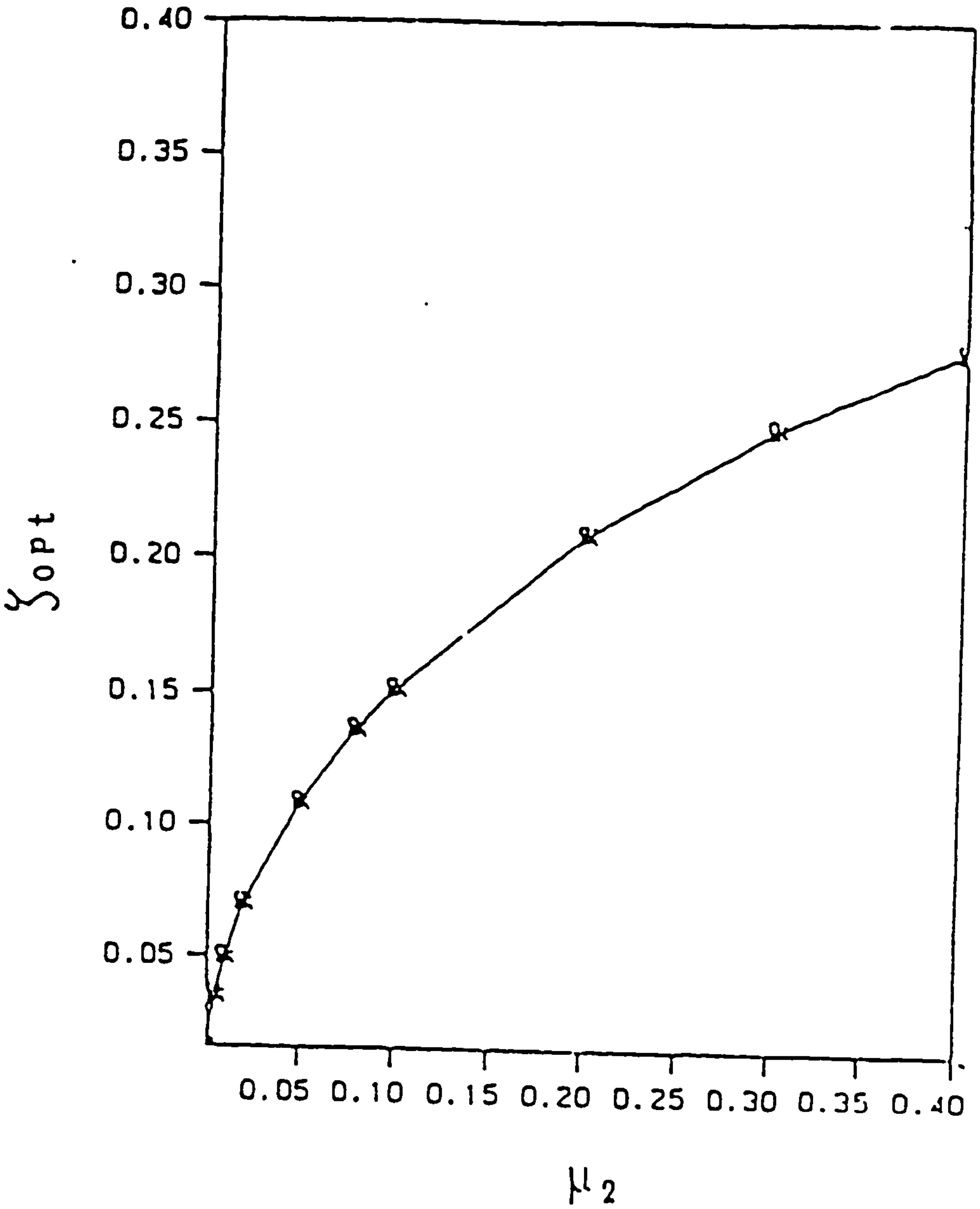

Figure 31. The relationship between the optimum frequency modulation ratio W, the mass ratio between the vibration absorbing instrument and radar, and the resistance ratio of the vibration separating instrument when the base plate thickness is one inch.

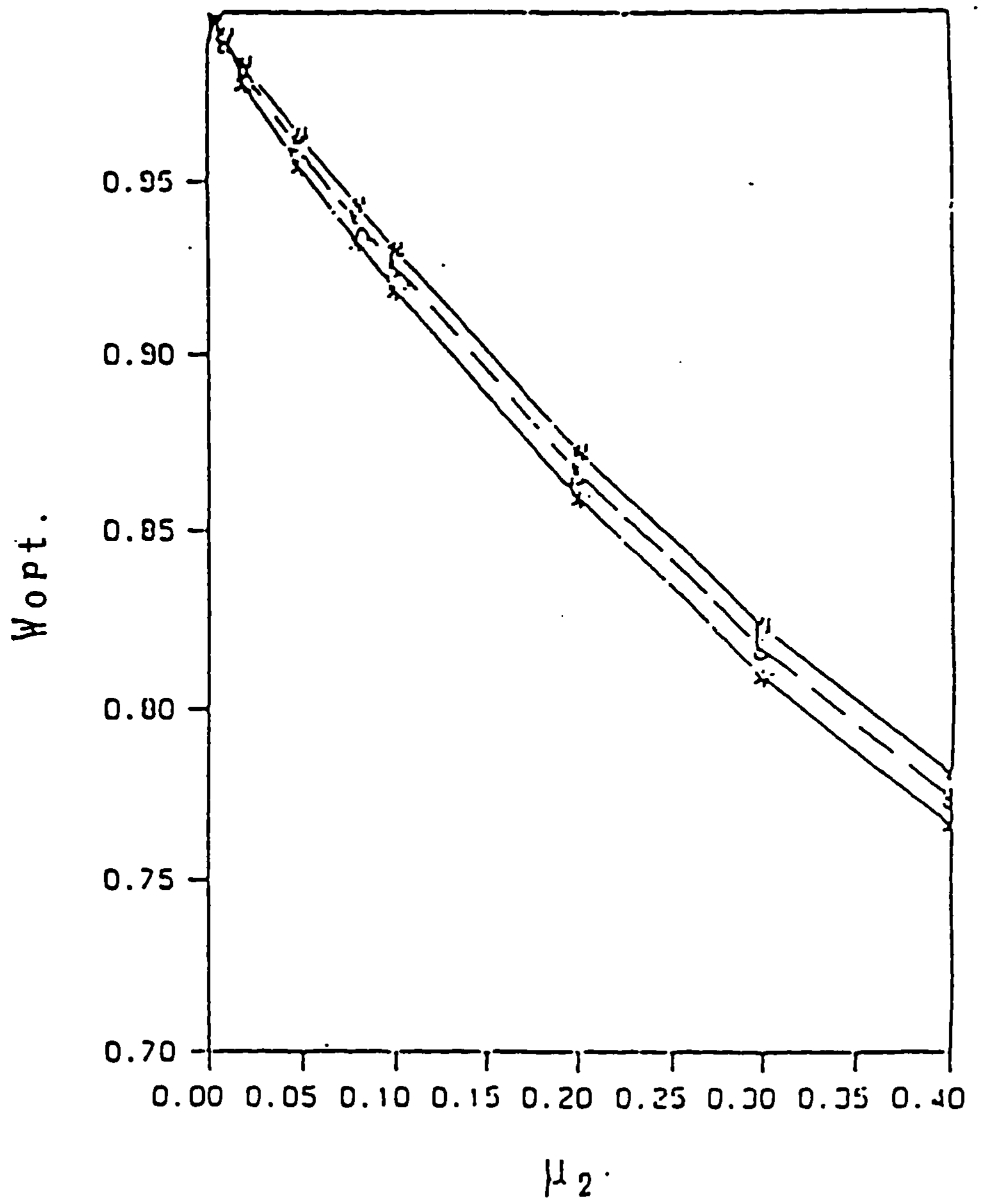

Figure 32. The relationship between the optimum resistance ratio, the mass ratio between the vibration absorbing instrument and radar, and the resistance ratio of the vibration separating instrument when the base plate thickness is one inch.

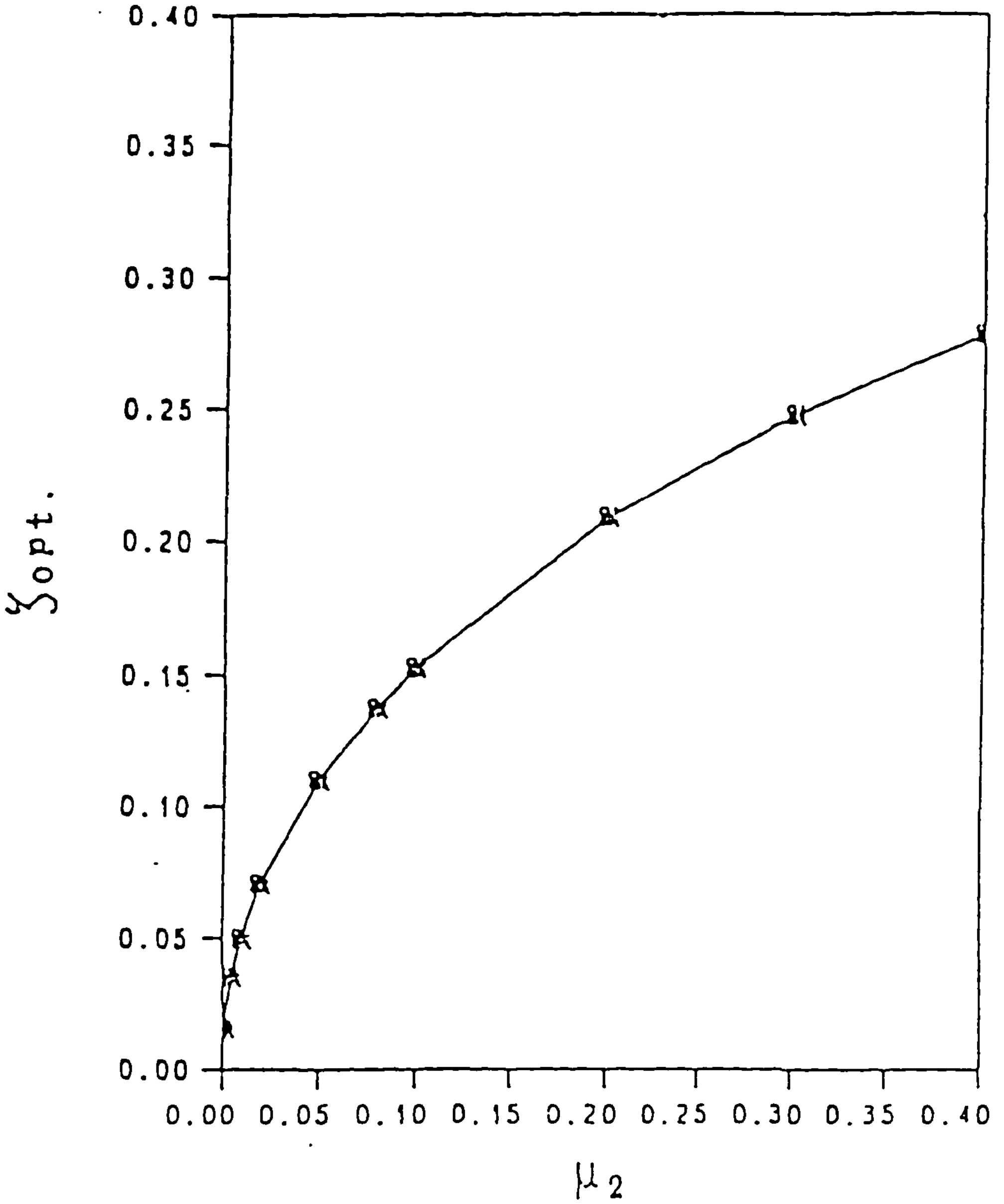

Figure 43. The relationship among the optimum resistance ratio, the mass ratio between the vibration absorbing instrument and radar, and the spring constant K1 of the vibration separating instrument when the base plate thickness is one inch.

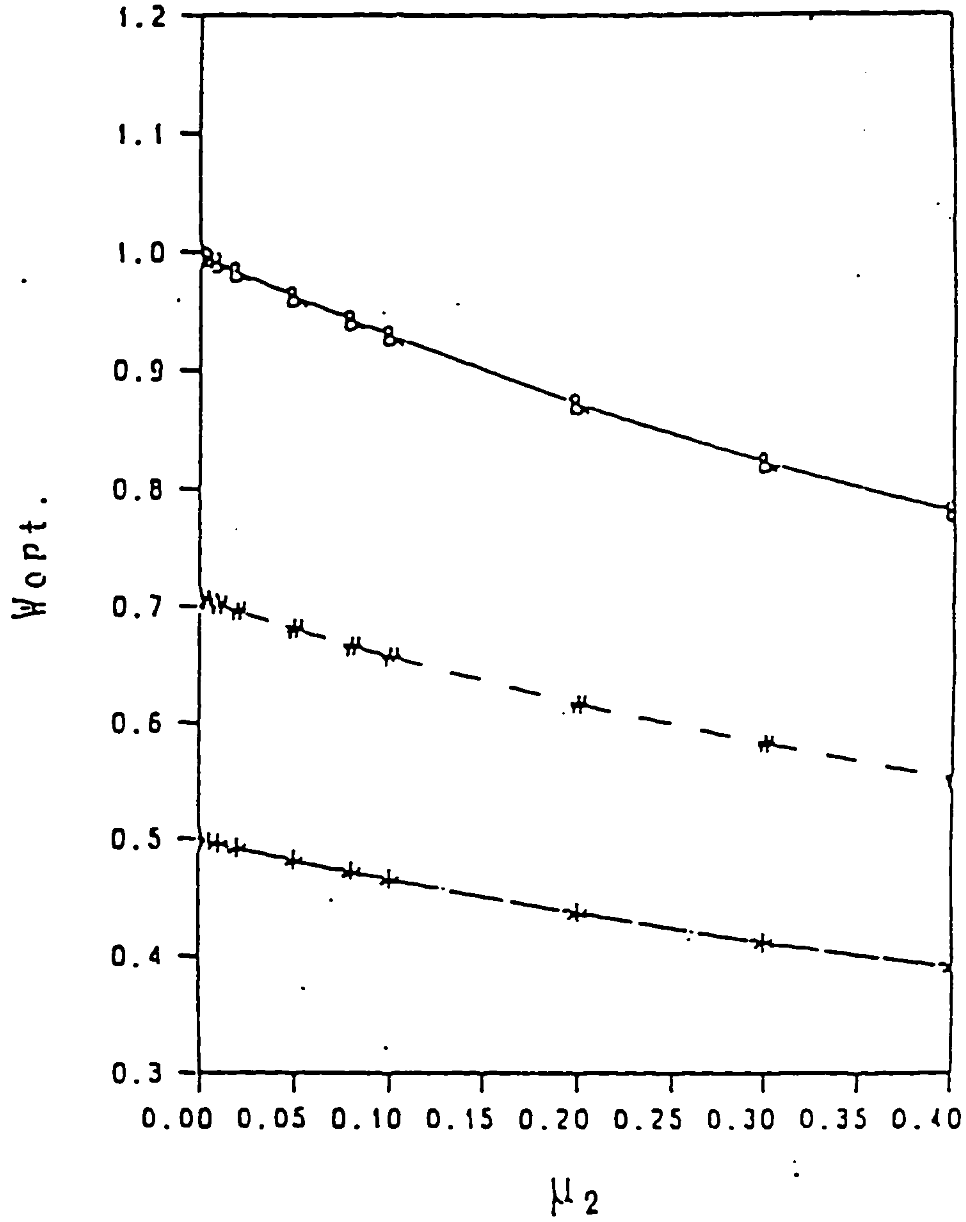

Figure 34. The relationship between the optimum frequency modulation ratio, the mass ratio between the vibration absorbing instrument and radar, and the spring constant K1 of the vibration separating instrument when the base plate thickness is one inch.

1. The value of optimum resistance ratio ζ_{opt} did not change with the spring constant K1 of the vibration separating instrument.

2. The optimal frequency modulation ratio W_{opt} decreased when the spring constant K1 of the vibration separating instrument increased.

The data in Figures 45 and 46 show the relationship between the optimal resistance ratio ζ_{opt} and the optimum frequency modulation ratio W_{opt} when the base plate thickness is 1.5 inches. From data in Figures 41, 42, 45 and 46, it was found that the change in base plate thickness did not influence the optimal value of the resistance ratio ζ_{opt} and the optimal value of frequency modulation ratio W_{opt}.

From the preceding analysis, the following conclusions were obtained:

1. The base plate (h), the resistance ratio of the vibration separating instrument (ζ_1), and the frequency modulation ratio (W1) have no influence on the optimal resistance ratio ζ_{opt}, when the value of the mass ratio between the vibration absorbing instrument and radar (μ_2) is fixed.

2. The value of optimum the frequency modulation ratio W_{opt} will change with the value of ζ_1 and (W_1).

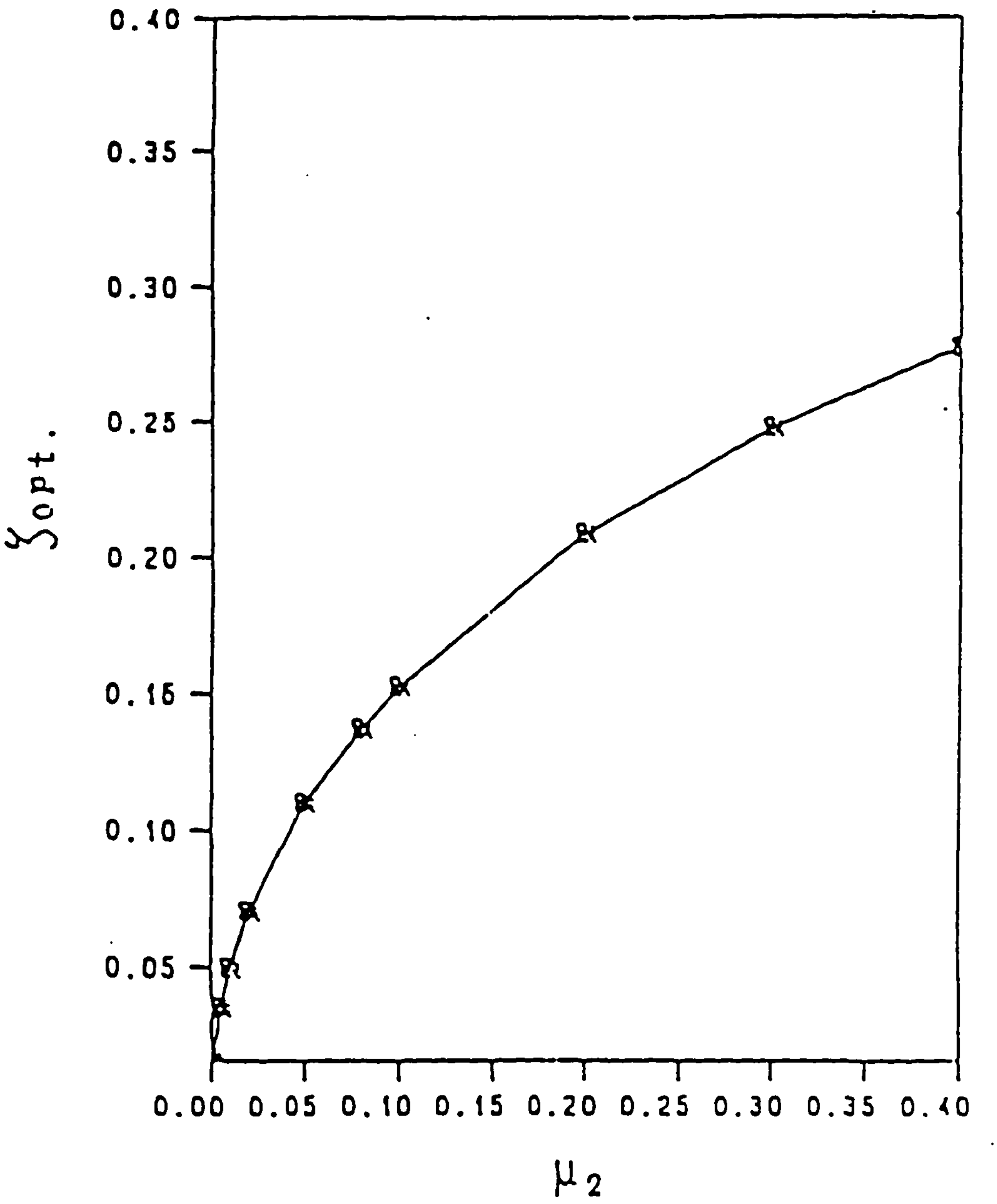

Figure 35. The relationship between the optimum frequency modulation ratio, the mass ratio between the vibration absorbing instrument and radar, and the resistance ratio of the vibration separating instrument when the base plate thickness is 1.5 inches.

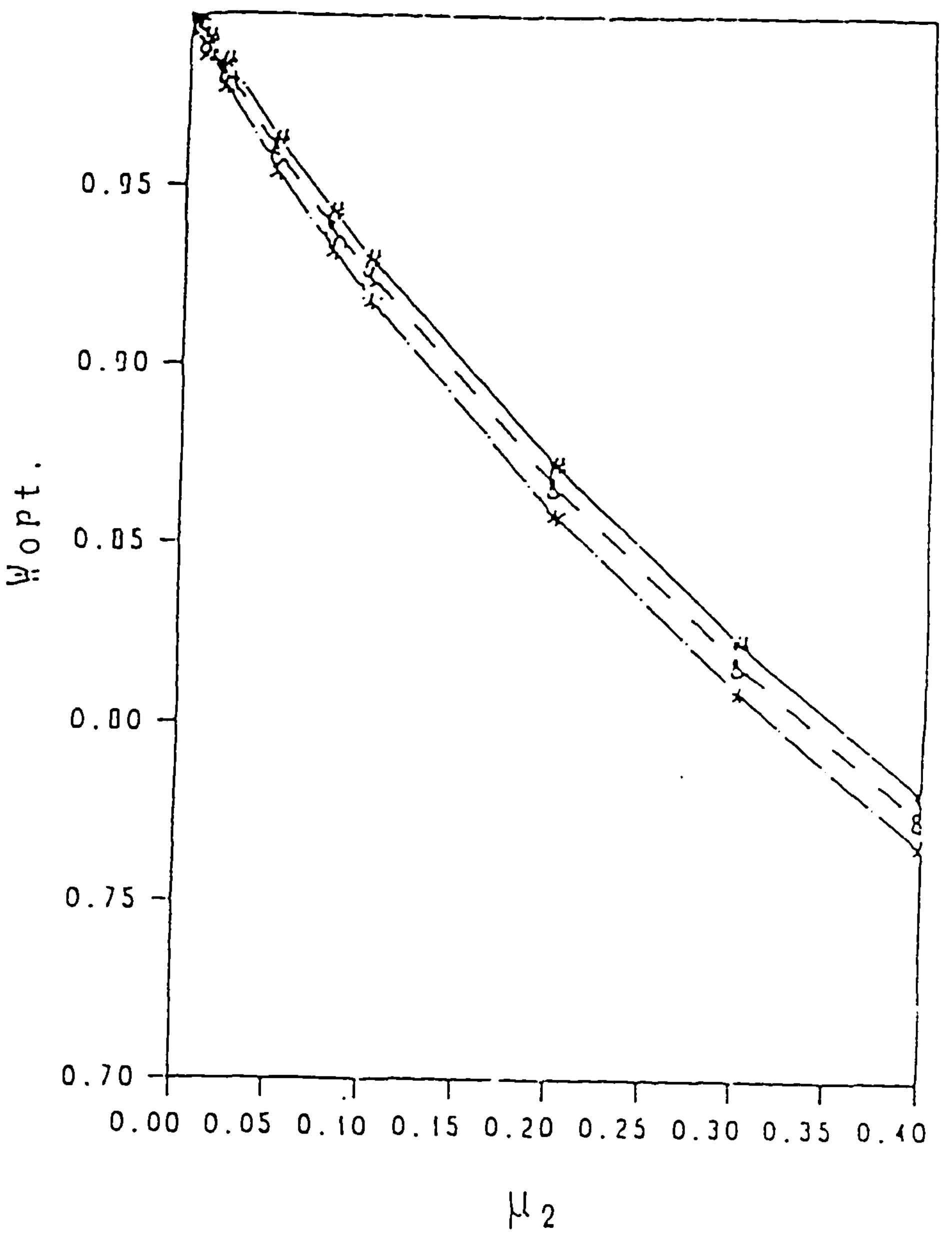

Figure 36. The relationship between the optimum resistance ratio, the mass ratio between the vibration absorbing instrument and radar, and the resistance ratio of the vibration separating instrument when the base plate thickness is 1.5 inches.

3. The value of optimal frequency modulation ratio W_{opt} has no relationship to the base plate.

The Results of the Field Tests

Four field tests were conducted to measure the frequency of the mast vibration at four different speeds: normal speed (15 knots), critical speed (18 knots) economical speed (22 knots), and high speed (30 knots). A knot is about 1.13 miles per hour.

The frequency of mast vibration at normal speed (15 knots) is presented in Figures 37 and 38. The solid lines indicate the frequency of mast vibration when no absorber nor isolator was applied. The dotted lines indicate the frequency when both an absorber and an isolator were applied. The frequency of mast vibration was found to be 50 cycles per second when no absorber or isolators was applied. (Figure 38). On the other hand, the frequency of mast vibration was found to be between 15 and 25 cycles per second when both an absorber and an isolator were applied.

The frequency of mast vibration at critical speed (18 knots) is presented in Figures 39 and 40. Figure 39 shows the frequency of mast vibration when no absorber or isolator was applied. Under this condition the frequency of the mast vibration was found to be over 50 cycles per second.

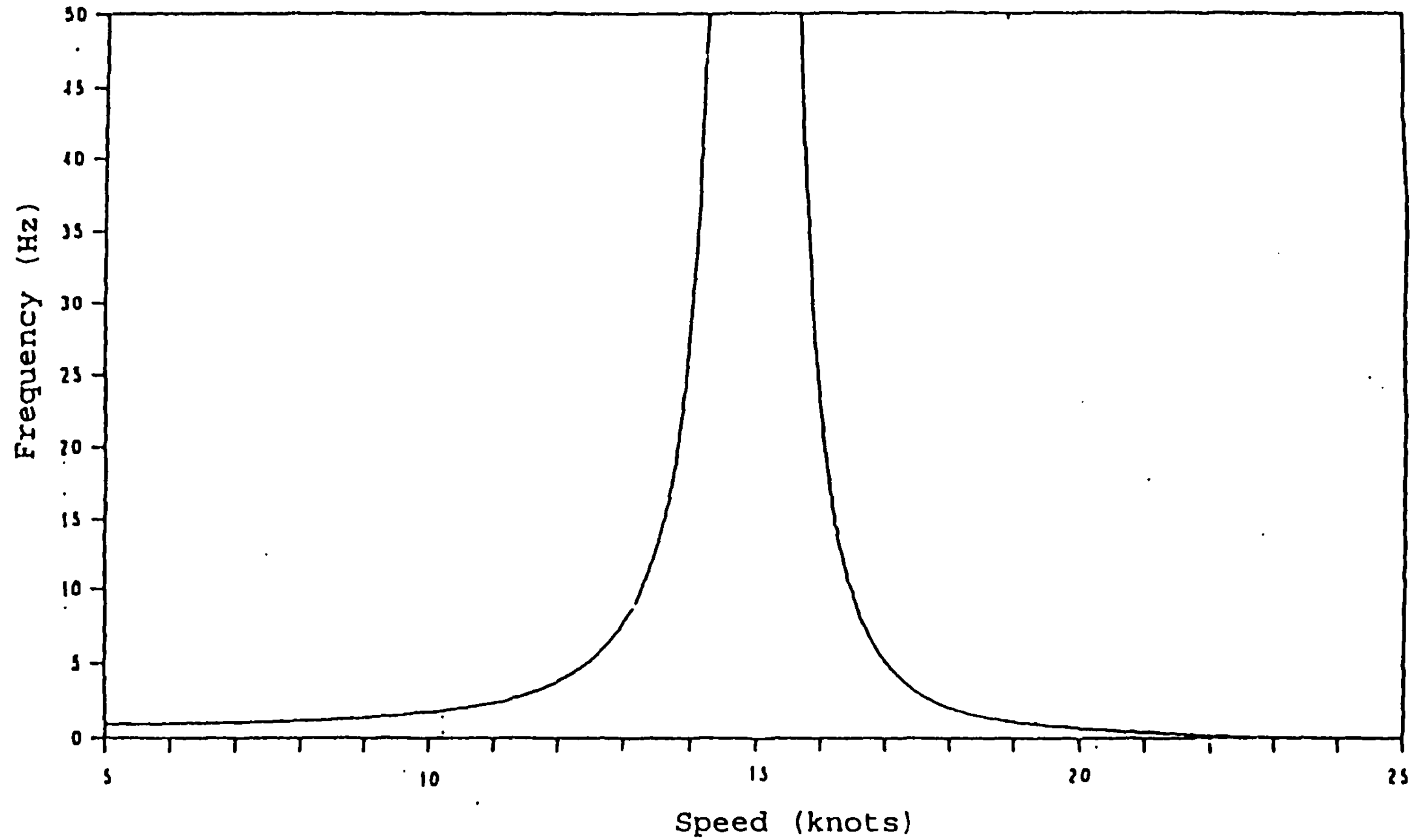

<u>Figure 37</u>. The frequency of mast vibration at general speed (without absorber and isolator).

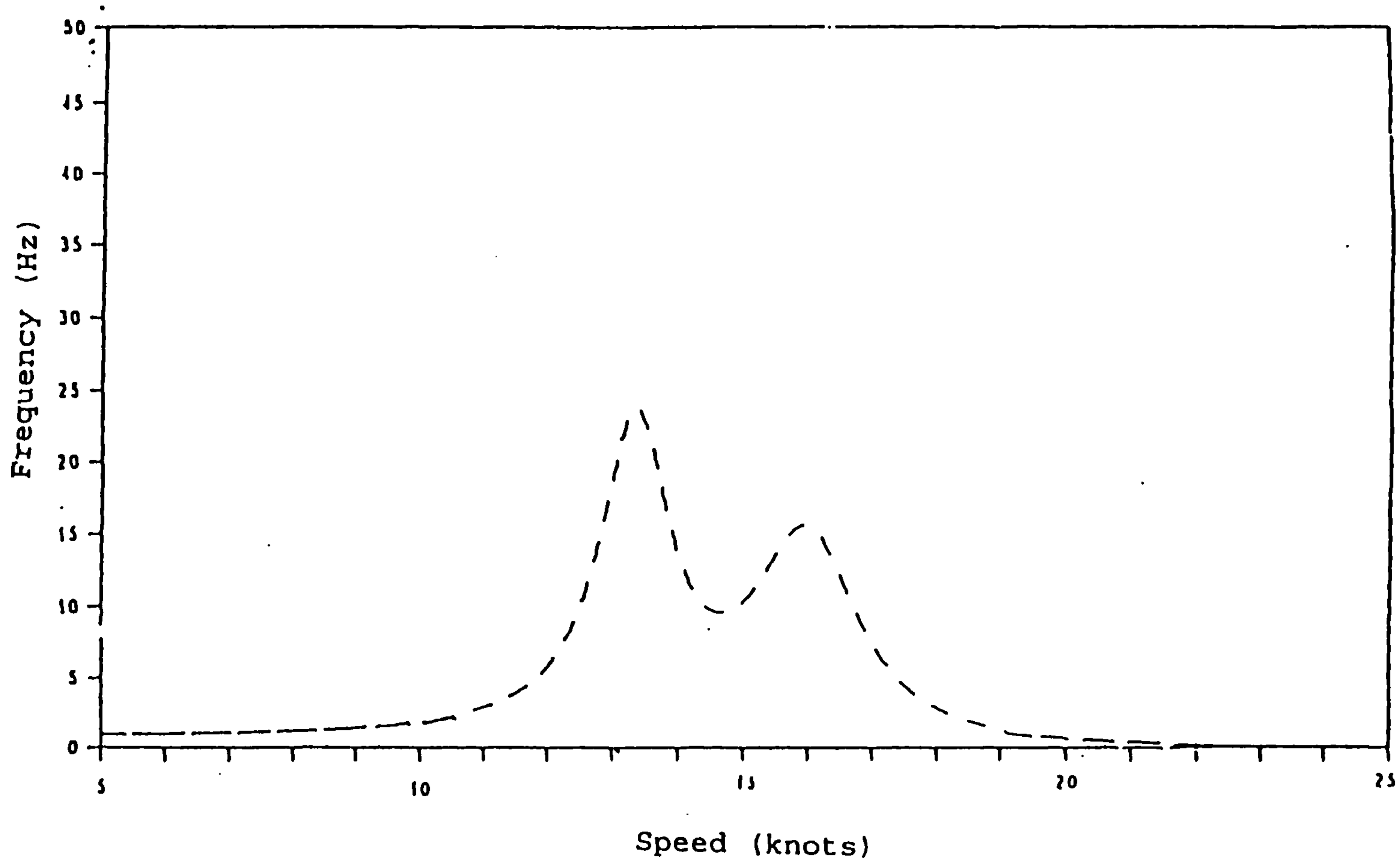

Figure 38. The frequency of mast vibration at general speed (with absorber and isolator).

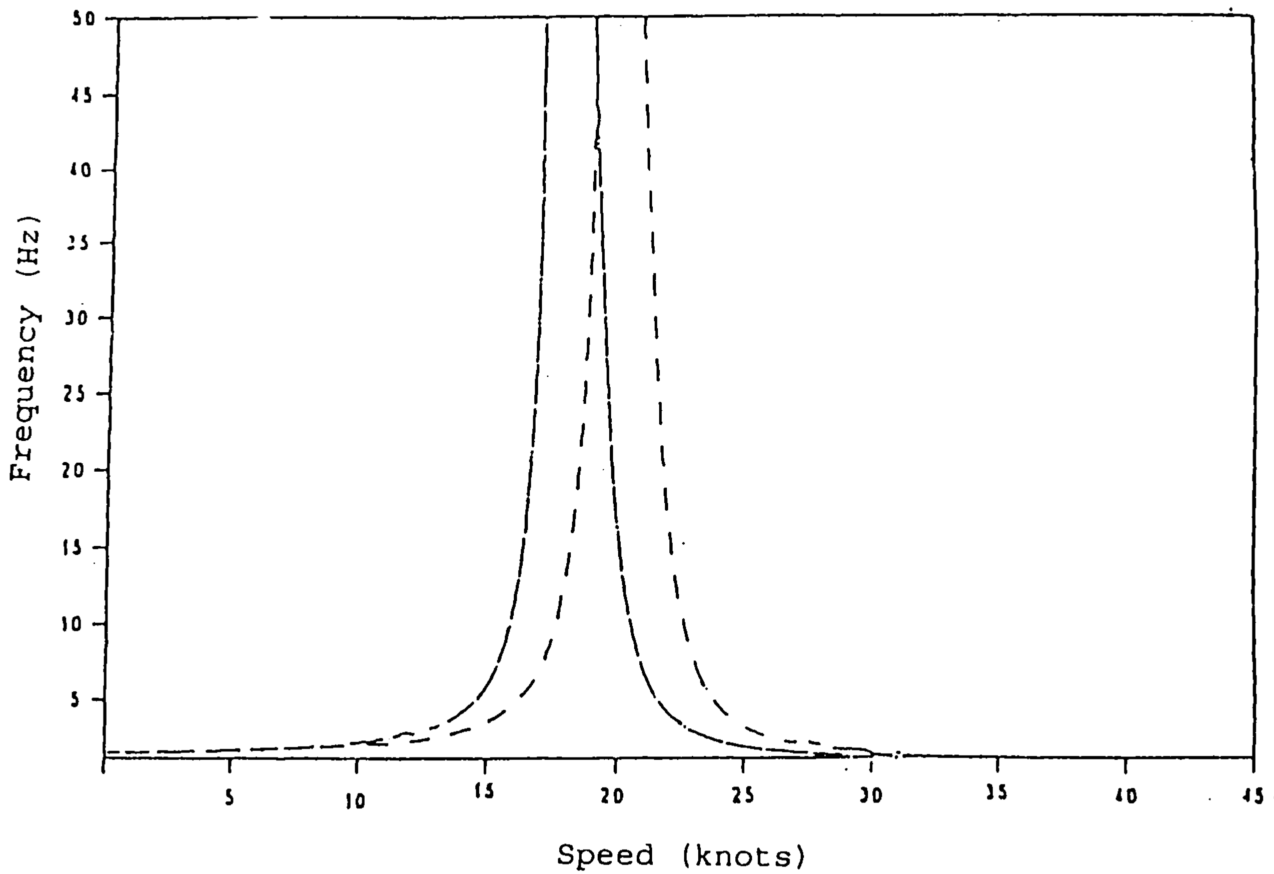

Figure 39. The frequency of mast vibration at critical speed (without absorber and isolator).

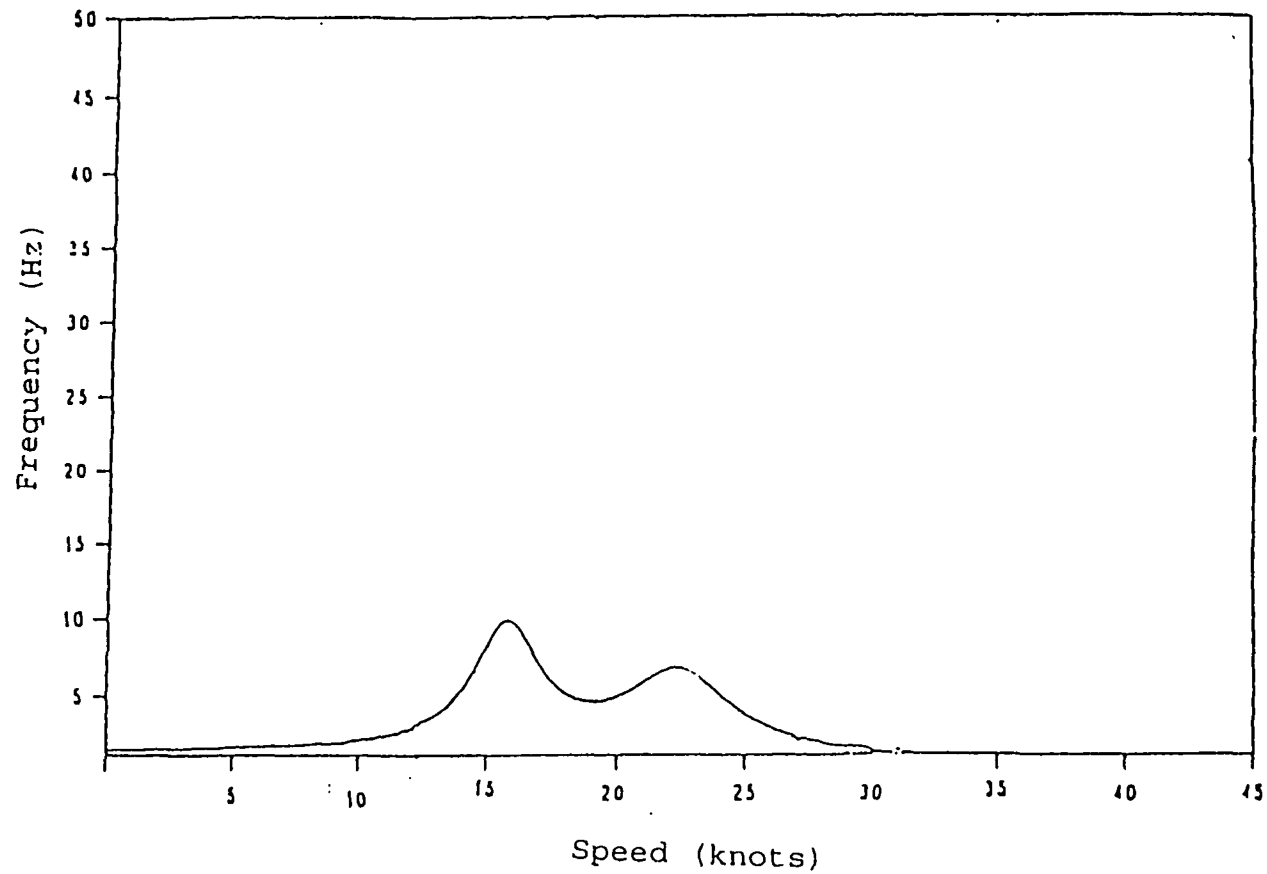

Figure 40. The frequency of mast vibration at critical speed (with absorber and isolator).

Figure 40 presents the frequency of mast vibration when both an absorber and an isolator were applied. Under this condition the frequency of the mast vibration was found to be below 10 cycles per second.

The frequency of mast vibration at economical speed (22 knots) is presented in Figures 41 and 42. Figure 41 shows the frequency of mast vibration when no absorber or isolator was applied. Under this condition, the frequency of mast vibration was found to be between 40 to 50 cycles per second. The data in Figure 42 demonstrated the frequency of mast vibration when both an absorber and an isolator were applied. The frequency of mast vibration was found to be between 15 to 25 cycles per second.

The frequency of mast vibration at high speed (30 knots) is presented in Figures 43 and 44. Figure 43 illustrates the frequency of mast vibration when no absorber or isolator was applied. Under this condition the frequency of mast vibration was found to be over 50 cycles per second. The data in Figure 44 presents the frequency of mast vibration when both an absorber and an isolator were applied. Under this condition the frequency of mast vibration was found to be less than 25 cycles per second.

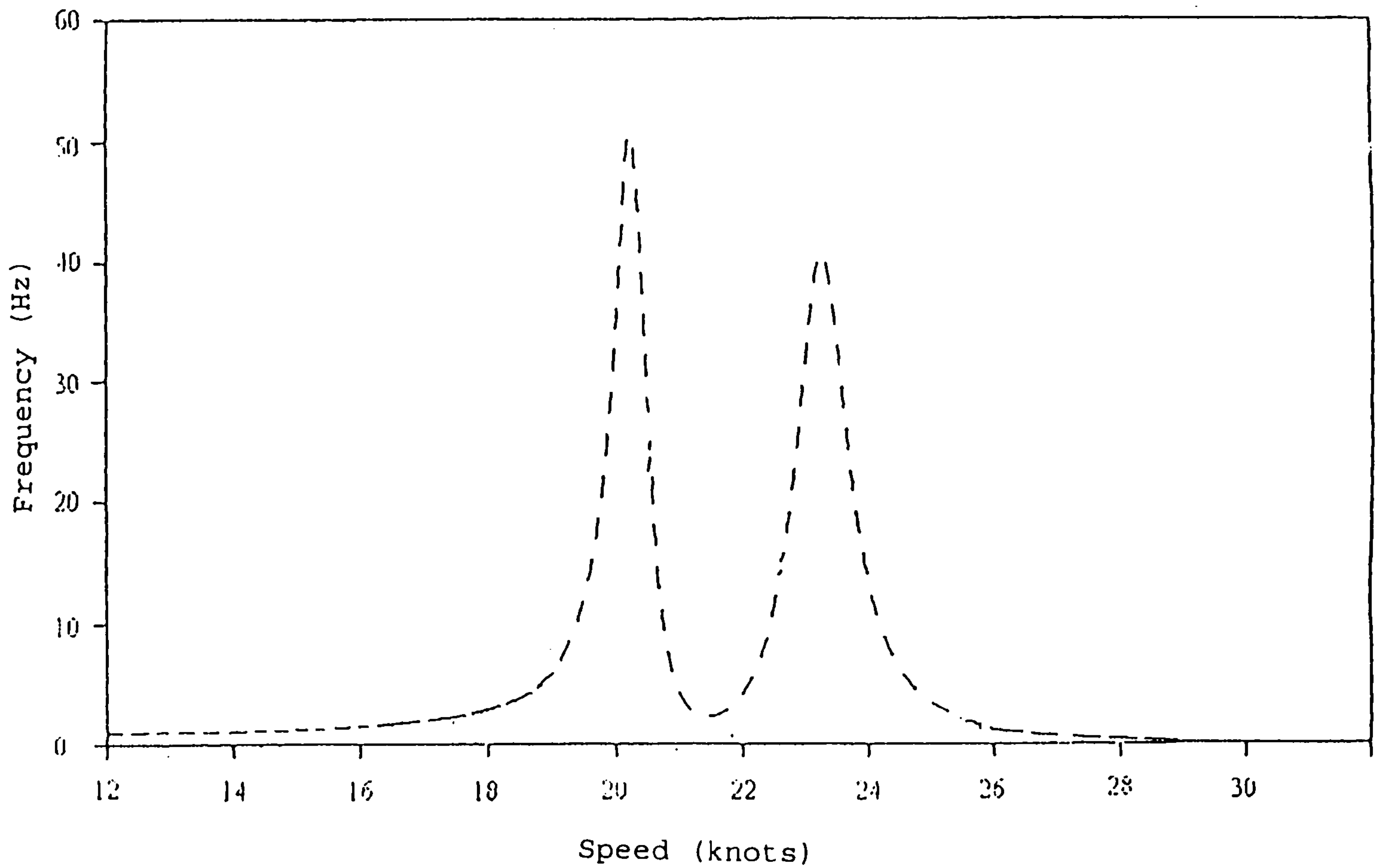

<u>Figure 41</u>. The frequency of mast vibration at economical speed (without absorber and isolator).

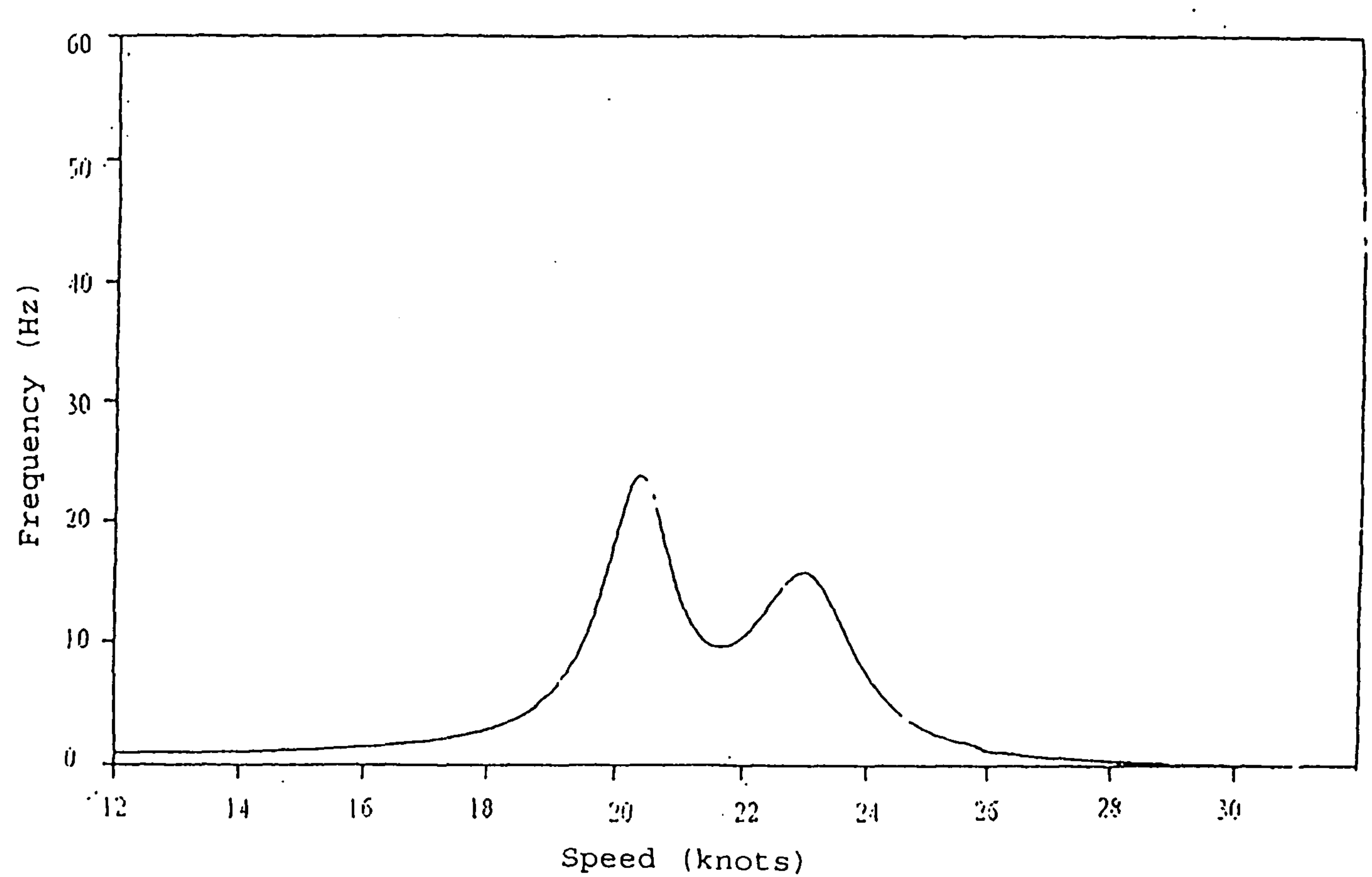

Figure 42. The frequency of mast vibration at economical speed (with absorber and isolator).

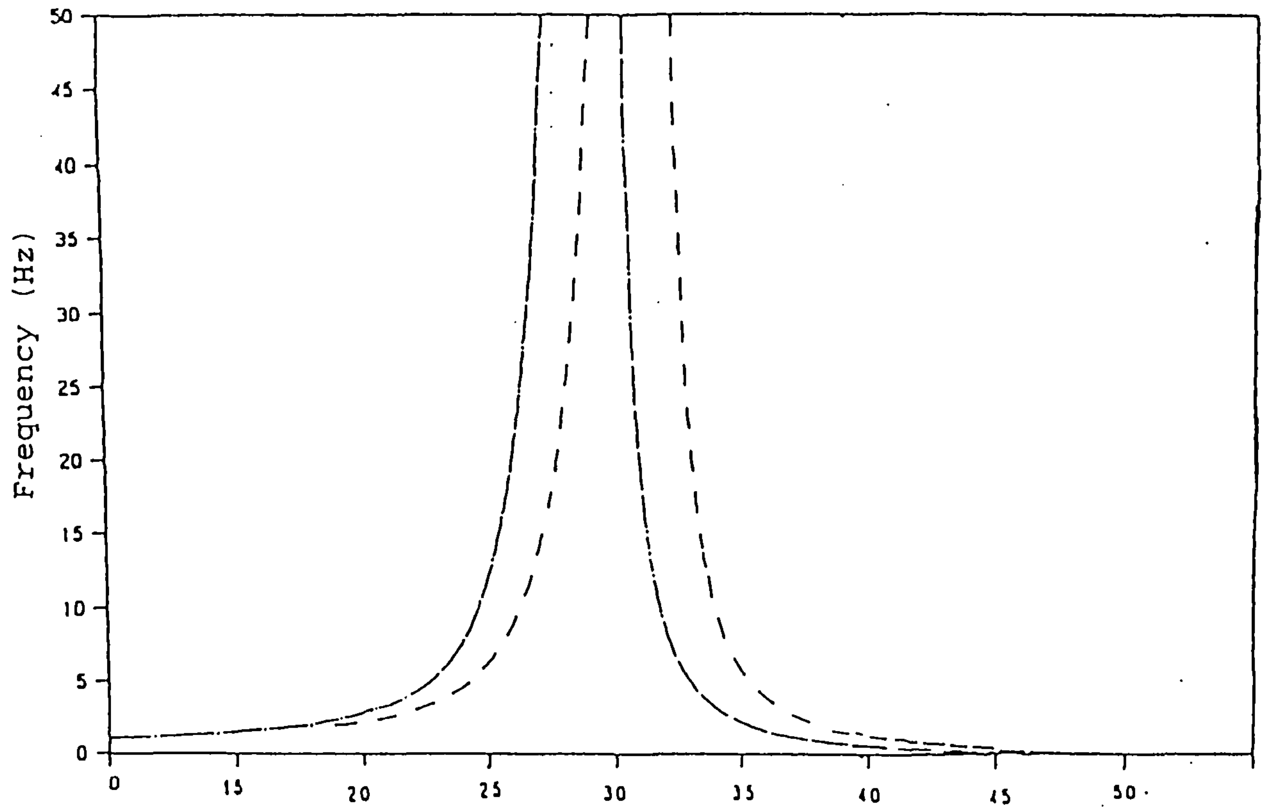

Figure 43. The frequency of mast vibration at high speed (without absorber and isolator).

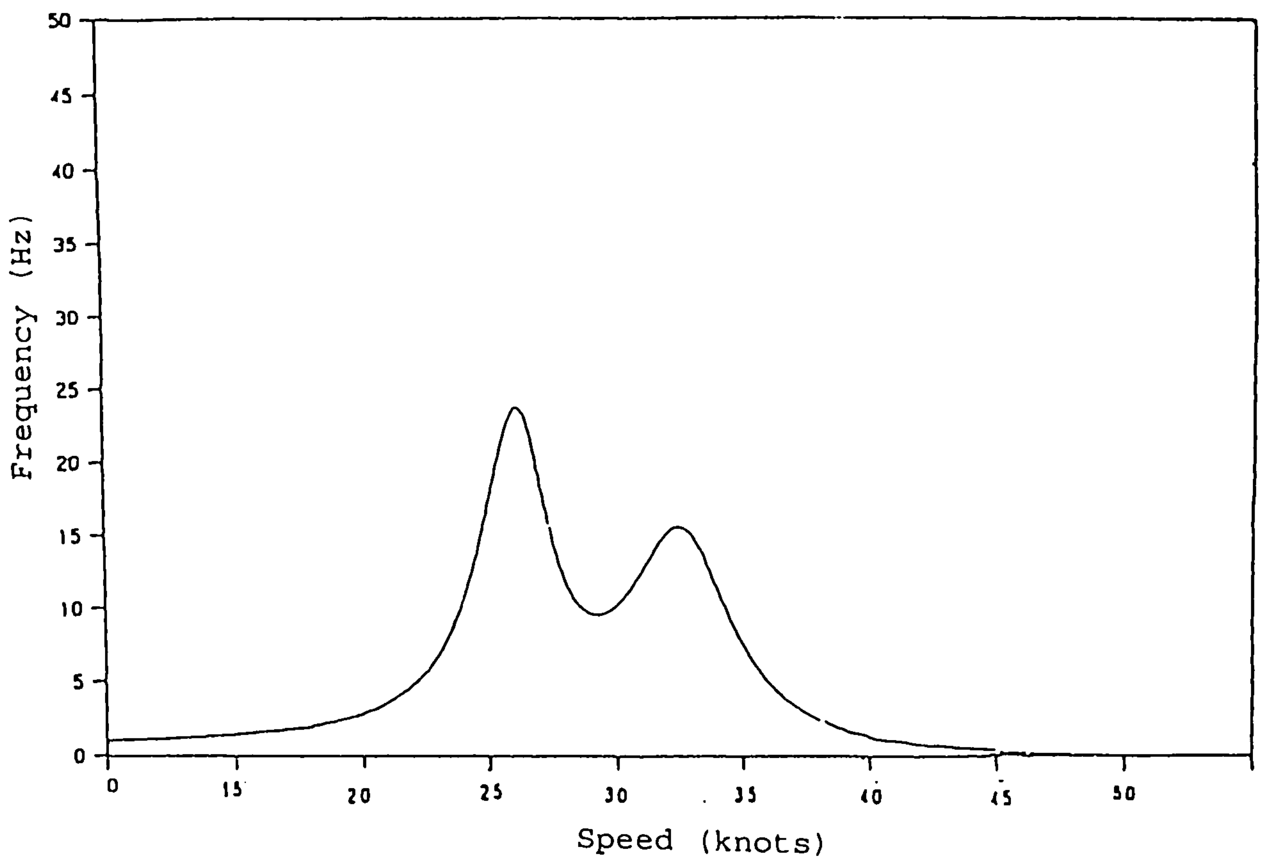

Figure 44. The frequency of mast vibration at high speed (with absorber and isolator).

CHAPTER V

SUMMARY, FINDINGS, CONCLUSIONS, AND RECOMMENDATIONS

In this chapter a summary of the research is presented. Conclusions are based on the findings of this study. Recommendations for further study are also made.

Summary

The purpose of this research was to study methods for reducing the degree of destruction when receiving and analyzing signals from a radar system mounted on a ship's mast. An experiment was designed to imitate the static and dynamic behavior of a ship mast structure to determine the reasonable oscillation modal state, and then optimum vibration absorbers and vibration isolators were designed based on the results of oscillation analysis. The research focused on methods to reduce the vibration amplitude to a certain range. Two research questions were raised and answered:

1. What is the reasonable finite element analysis model to analyze the dynamic behavior of the mast, including the natural oscillation frequencies and the oscillation states of the mast structure?

2. With the addition of a dynamic vibration absorber and isolator, will the vibration amplitude of the radar on

the base plate be within the prescribed maximum of 0.2 milli-radians when the ship is subject to stormy waves and wind load?

Experimentation in this study was composed of two parts: (a) laboratory experiments to simulate the dynamic behavior of the aluminum tubes of a ship's mast and (b) designing the optimum vibration absorber and isolator and comparing the responses of the mast with and without an optimal vibration absorber and isolator in field tests.

The criteria for the experiments of this radar mast system study included: (a) the mast structure needed to be flexible and not vibrate, (b) the radian-displacement at the middle of the radar base plate on top of the mast needed to be less than 0.2 milliradians at normal conditions, and (c) the natural frequency of the radar base plate needed to be less than 50 Hz.

Findings of This Research

1. There were no significant differences in natural frequencies between welded tubes and continuous tubes. Welding had no obvious influence on the mechanical properties of the mast structure. The welded aluminum alloy tubes were considered as rigidly fixed or perfectly connected.

2. The vibration models of aluminum alloy tubes were the same as that of a beam element.

3. From the finite element analysis that was conducted in the laboratory tests to simulate the vibration of the mast system, the angular displacement at the middle of the radar base plate was less than 0.2 milliradians when the wind speed was 70 miles/hour and the sea state was 7.

4. From the laboratory test, the angular displacement at the radar base plate was 0.4005 milliradians when the wind speed was 70 miles/hour and the sea state was 7, and the magnitude of an external force was 2.5 times the ship's weight.

5. When radar displacement alteration μ_2 was less than or equal to 0.1, the slope of the radar displacement alteration $\sigma_t{}^2$ decreased rapidly when μ_2 increased.

6. When μ_2 was greater than 0.1, the change of the slope of the radar displacement alteration $\sigma_t{}^2$ mildly increased when the value of μ_2 increased.

7. The value of $\sigma_t{}^2$ decreased when the resistance ratio of the vibration separating instrument ζ_1 increased.

8. The value of $\sigma_t{}^2$ increased when the thickness of the base plate increased.

9. The value of optimal resistance ratio ζ_{opt} increased when mass ratio μ_2 increased.

10. The value of the optimal resistance ratio ζ_{opt} did not change when the resistance ratio of the vibration absorbing instrument ζ_1 increased or decreased.

11. The value of frequency modulation ratio W_{opt} decreased gradually when mass ratio μ_2 increased.

12. The value of optimal frequency modulation ratio W_{opt} decreased slightly when the resistance ratio of the vibration absorbing instrument ζ_1 increased.

13. The value of optimal resistance ratio ζ_{opt} did not change as the spring constant K1 of the vibration separating instrument $\zeta_1$increased or decreased.

14. The value of optimum frequency modulation ratio W_{opt} decreased when the spring constant K1 of the vibration separating instrument ζ_1 increased.

15. Changing the base plate thickness h, the resistance ratio of the vibration separating instrument ζ_1, and the value of frequency modulation ratio (W1) had no influence on the values of optimal resistance ratio ζ_{opt}, when the value of the mass ratio between the vibration absorbing instrument and radar μ_2 was fixed.

16. The value of optimal frequency modulation ratio W_{opt} was independent of base plate thickness.

17. At general speed (15 knots), the frequency of mast vibration was found to be 50 cycles per second when no absorbers nor isolators were applied. However, it was found

to be between 15 to 25 cycles per second when both an absorber and an isolator were applied.

18. At critical speed (18 knots), the frequency of mast vibration was over 50 cycles per second when no absorbers nor isolators were applied and below 10 cycles per second when both an absorber and an isolator were applied.

19. At economical speed (22 knots), the frequency of mast vibration was found to be between 40 to 50 cycles per second when no absorber or isolator was applied. In addition, the frequency of mast vibration was found to be between 15 to 25 cycles per second when both an absorber and an isolator were applied.

20. At high speed (30 knots), the frequency of mast vibration was over 50 cycles per second when no absorbers and no isolators were applied, and below 25 cycles per second when both an absorber and an isolator were applied.

Conclusions

Based on the results obtained in this study, the following conclusions were made:

1. The aluminum alloy tubes of a mast structure can be considered as space beam elements.

2. The increase of base plate thickness does not decrease the vibration amplitude when random force is applied on the radar directly.

3. The value of frequency modulation ratio W_{opt} is consistently less than 1. This means that the natural frequency of the optimal dynamic vibration absorbing instrument is always less than the natural frequency of the whole mast system.

4. The optimal dynamic vibration absorber is very effective in reducing the resonance of radar in laboratory tests. Hence, it can significantly increase the accuracy of radar signals.

5. When no absorbers and no isolators were applied in the field test, the frequency of mast vibration was found to be between 40 and 50 cycles per second at economical speed. Moreover, the frequency of mast vibration was found to be greater then or equal to 50 cycles per second at normal speed, critical speed, and high speed. However, when both an absorber and an isolator were applied, the frequency of mast vibration was found to be between 10 and 25 cycles per second at any of the above four speeds. In short, the use of the absorber and the isolator is an effective approach to optimize the design of the radar base plate.

Recommendation for Further Research

1. A study should be conducted to assess the effects of isolators and absorbers made of various materials to reduce the vibration of the mast systems.

2. The laboratory test should be replicated using aluminum alloy tubes and tubes of other materials in order to compare the effect of these materials.

3. A study should be conducted to determine the optimum design of the radar base plate of the masts of merchant ships that weigh more than 3000 tons.

4. A study should be conducted to assess the effects of isolators and absorbers on vibration reduction of the radar mast systems of offshore barges, offshore petroleum rigs, and port equipment.

5. A replication of this study should be conducted to verify the procedure and compare the results.

REFERENCES

Abrupt, S. (1996). Maximizing the fundamental natural frequency of triangular composite plates. Journal of Vibration and Acoustics, 118(2), 141-146.

Adorned, E. O., & Warburton, G. B. (1980). Minimizing structure vibrations with absorber. Earthquake Engineering and Structural Dynamics, 8, 219-236.

Around, J. L. (1971). Minimum-mass design of a plate-like structure for specified fundamental frequency. AIAA Journal, 9(9), 1739-1945.

Bathe, K. J., Wilson, E. L., & Peterson, F. E. (1974). SAP IV-A structural analysis program for static and dynamic response of linear systems (Earthquake Engineering Research Center Report No. EERC 73-11). Los Angeles: University of California, College of Engineering.

Bellagamba, L., & Yang, T. Y. (1981). Minimum-mass truss structures with constraints on fundamental natural frequency. AIAA Journal, 19(11), 1452-1458.

Bernitsas, M. M. (1982). Three dimensional, nonlinear large deflection model of dynamic response of risers, pipelines and cables. Journal of Ship Research, 26(1), 59-64.

Bernitsas, M. M. (1984). NA-550 Informal class notes. Ann Arbor: The University of Michigan, Department of Naval Architecture and Marine Engineering.

Bernitsas, M. M., Hoff, C. J., & Kokarakis, J. E. (1984). Nonlinear inverse perturbation in structural redesign of risers. ASME Transactions Journal of Energy Resources Technology, 107(2), 06-12.

Bhat, R. B., Singh, J., & Mundkur, G. (1993). Plate characteristic functions and natural frequencies of vibration of plates by iterative reduction of partial differential equation. Journal of Vibration and Acoustics, 115(2), 177-181.

Borgman, L. E. (1958). Computation of the ocean-wave forces on inclined cylinders. American Geophysical Union, Transactions, 39,(5), 10-16.

Canfield, R. A., & Meirovitch, L. (1994). Integrated structural design and vibration suppression using independent modal space control. AIAA Journal, 32(10), 2053-2060.

Clough, R. W., & Peuzien, J. (1975). Dynamics of structure. New York: McGraw-Hill, Inc.

Den Hartog, J. P. (1956). Mechanical vibrations (4th ed.) New York: McGraw-Hill.

Fallick, J. C., Szumachowski, E. R., & Snyder, R. (1978). Welding handbook (7th ed.). Miami, FL: American Welding Society.

Fiacco, A. V., & McCormick, G. P. (1968). Nonlinear programming: Sequentially unconstrained minimization techniques. New York: John Wiley and Sons, Inc.

Fletcher, R., & Reeves, C. M. (1964). Function minimization by conjugate gradients. The Computer Journal, 7, 149-160.

Fox, R. L. (1965). Constraint surface normal for structural synthesis techniques. AIAA Journal, 3(8), 1517-1518.

Gallagher, R. H. (1973). Full stressed design. Optimal structural design. New York: John Wiley and Sons, Inc.

Haug, E. J., & Arora, J. S. (1979). Applied optimal design. New York: John Wiley and Sons, Inc.

Hoff, C. J. (1983). Linear dynamic redesign-University of Michigan: Theoretical and user's manual, version 1.0 (Report SM-83/5.1). Ann Arbor: The University of Michigan, Department of Aerospace Engineering.

Hoff, C. J., & Bernitsas, M. M. (1984). Nonlinear inverse perturbation methods in structural dynamics redesign of offshore structures. Proceedings of the 3rd International Congress on Marine Technology, Athens, Greece.

Jacquot, R. G. (1978). Optimal dynamic vibration absorbers for general beam systems. Journal of Sound and Vibration, 60, 535-542.

Jacquot, R. G., & Hoppe, D. L. (1973). Optimal random vibration absorbers. Journal of Engineering Mechanics Division, ASCE 99, 612-616.

Kim, K. O., Anderson, W. J., & Sandstrom, R. E. (1983). Nonlinear inverse perturbation method in dynamic analysis. AIAA Journal, 21(9), 1310-1316.

Kirsch, U. (1981). Optimal structural design. New York: McGraw-Hill Book Company.

Knot, N. S., & Berke, L. (1984). Structural optimization using optimality criteria methods. In E. Atrek, R. H. Gallagher, K. M. Ragsdell, & O. C. Zienkiewicz (Eds.), New directions in optimum structural design (pp. 309-330) New York: John Wiley and Sons, Ltd.

Koo, K. N., & Lee, I. (1994). Effects of in-plane displacements on frequency and damping of composite laminates. AIAA Journal, 32(1), 221-223.

Kvaternik, R. G. (1992). DAMVIBS looks at rotorcraft vibration (Design analysis method for vibrations program; Focus 1992: Structures, Materials & Structural Dynamics). Aerospace America, 30(9), 22-24.

Lee-Glauser, G., Juang, J. N., & Sulla, J. L. (1995). Optimal active vibration absorber: Design and experimental results. Journal of Vibration and Acoustics, 117(2), 165-171.

Lewis, F. M. (1980). The extended theory of viscous vibration damper. Journal of Sound and Vibration, 70, 481-486.

Liu, M., & Gorman, D. G. (1993). Improved method for evaluating damping ratios of a vibrating system. AIAA Journal, 31(7), 1357-1360.

Mayne, R. W. (1980). Optimization techniques for shock and vibration isolator development. Shock Vibration Digest, 25-33

McCart, B. R., Haug, E. J., & Streeter, T. D. (1970). Optimal design of structures with constraints on natural frequency. AIAA Journal, 8(6), 1010-1019.

McCormick, C. W., Ed. (1982). MSC/NASTRAN Version 62 user's manual. San Francisco: MacNeal-Schendler Corporation.

Nosier, A., Kapania, R. K., & Reddy, J. N. (1993). Free vibration analysis of laminated plates using a layer wise theory. AIAA Journal, 31(12), 2335-2346.

Palle, T. C., & Yoshisada, M. (1986). Application of structural systems reliability theory. Berlin: Springer-Verlag.

Pannossian, H. V. (1992). Structural damping enhancement via non-obstructive particle damping technique. Journal of Vibration and Acoustics, 114(1), 101-105.

Park, S., Park, I., & Ma, F. (1992). Decoupling approximation of unclassically damped structures (Structural Mechanics and Materials). AIAA Journal, 30(9), 2348-2351.

Pegg, N. G. (1985). Destroyer mast vibration analysis using finite elements. Tenth Canadian Congress of Applied Mechanics, London, Canada.

Pierson, B. L. (1972). A survey of optimal structural design under dynamic constraints. International Journal Numerical Methods in Engineering, 4, 491-499.

Qin, J. N., Gray, C. E., & Mei, C. (1993). Vector unsymmetric eigen equation solve for nonlinear flutter analysis on high-performance computers. Journal of Aircraft, 30(5), 744-750.

Racca, R. (1982). How to select isolators for a long service life. Design News, 38, 43-47.

Rao, B. N. (1992). Nonlinear free vibration characteristics of laminated anisotropy thin plates (Structural Mechanics and Materials). AIAA Journal, 30(12), 2991-2993.

Rosen, J. B. (1961). The gradient projection method for nonlinear programming part I - Linear constraints, SIAM Journal of Applied Mathematics, 8(1), 181-217.

Roy, R., & Craig, Jr. (1981). Structural dynamics: An introduction to computer methods. Austin, TX: The University of Texas.

Rubin, C. P. (1970). Minimum weight design of complex structures subject to a frequency constraint. AIAA Journal, 8(5), 923-927.

Sandstrom, R. E. (1979). Component mode synthesis in compact form and its application to ship vibration. Unpublished doctoral dissertation, University of Michigan, Ann Arbor.

Schmit, L. A. (1984). Structural optimization - Some key ideas and insights. In E. Atrek, R. H. Gallagher, K. M. Ragsdell, & O. C. Zienkiewicz (Eds.), New directions in optimum structural design (pp. 270-308). New York: John Wiley and Sons Ltd.

Schmit, L. A., & Miura, H. (1976). A new structural analysis/synthesis capability - ACCESS 1. AIAA Journal, 14(5), 661-671.

Schwartz, R. J. (1954). The dictionary of business and industry. New York: B. C. Forbes and Sons Pub. Co.

Segalman, D. J., Dohrmann, C. R., & Slavin, A. M. (1996). Example calculations (A method for calculating the dynamics of rotating flexible structures, part 2). Journal of Vibration and Acoustics, 118(3), 318-322.

Sepulveda, A. E., & Thomas, H. L. (1995). New approximation for steady-state response of general damped systems. AIAA Journal, 33(6), 1127-1133.

Sheu, C. Y. (1968). Elastic minimum-weight design for specified fundamental frequency. International Journal Solid Structures, 4, 953-958.

Shi, Y., Lee, R. Y., & Mei, C. (1997). Finite element method for non-linear free vibrations of composite plates. AIAA Journal, 35(1), 159-166.

Shiau, L. C. (1992). Flutter of composite laminated beam plates with delimitation (Structural mechanics and materials). AIAA Journal, 30(10), 2504-2511.

Sippel, D. L., & Warner, W. H. (1973). Minimum-mass design of multi-element structures under a frequency constraint. AIAA Journal, 1(4), 483-489.

Spillers, W. R., & Funaro, J. (1975). Iterative design with deflection constraints. International Journal of Solids and Structures, 11, 793-802.

Stetson, K. A. (1975). Perturbation method of structural design relevant to holographic vibration analysis. AIAA Journal, 13(4), 457-459.

Sundaresan, M. K., Radhakrishnan, G., & Rao, B. N. (1996). Vibration and stability of simply supported elliptical plates. AIAA Journal, 34(12), 2637-2639.

Taylor, J. E. (1968). Optimum design of a vibration bar with specified minimum cross section. AIAA Journal, 6, 1379-1381.

Taylor, J. E. (1977). Scaling a discrete structural model to match measured modal frequencies. AIAA Journal, 15(11), 1647-1649.

U.S. Navy. (1985). Interface standards for shipboard systems. Ship Motion and Attitude. Military Standard Section 301A, DOD-STD-1399, Navy Ship Systems Command, USA.

Venkayya, V. B. (1971). Design of optimum structures. Computers and Structures, 1, 265-309.

Walker, P. M. (1988). Chambers science and technology dictionary. Cambridge, U.K.: Chambers Co.

Wang, S. C., & Shao, C. T. (1992). Dynamic analysis of warship structure to explosion loading. Journal of China Ship Building, 12(4), 166-215.

Wang, Y. J., Haung, I. M., & Hu, S. Y. (1991). An adaptive design of ship's masts. Unpublished report, Metal Industries Research & Development Center, Kaohsiung, Taiwan.

Warburton, G. B. (1981). Optimum absorber parameters for minimizing vibration response. Earthquake Engineering and Structural Dynamics, 9, 251-262.

White, G. J., & Ayyab, B. M. (1985). Reliability methods for ship structure. Naval Engineer Journal, 5, 86-96.

Yoshio, A. (1988). Reliability and damage of ship structure. Marine Structure, 1, 89-114.

Zhou, Y. H., Zheng, X. J., & Harik, I. E. (1995). Free-vibration analysis of compressed clamped circular plates. Journal of Engineering Mechanics, 121(12), 1372-1376.

APPENDIX A

THE MATHEMATICAL MODEL OF WIND LOADING AND SEA STATE LOADING EFFECTS ON RADAR SYSTEM BASE PLATE DISPLACEMENT

The Mathematical Model of Wind Loading and Sea State Loading Effects on Radar System Base Plate Displacemnet

The mathematical analysis of the radar system base plate displacement (Wang & Shao, 1992), is as follows:

(1) Wind loading formula:

$Fw = Pw \times A = 1/2 c\rho V^2$

Fw = wind loading

Pw = wind pressure (lbs/ft)

A = wind application area (ft^2)

ρ = air density ($slug/ft^3$)

V = wind speed (ft/sec)

C = Constant

In this experiment, the following data were used:

Front (longitudinal) wind speed = 70 mile/hr,

Side (transverse) wind speed = 50 mile/hr,

Air density = 0.00238 $slug/ft^2$,

Constant = 1.28.

(2)Sea state loading formula:

$$A_x = A_s + g*Sin\theta_p + \frac{4\pi^2}{T_p^2}\theta_p^2 X + \frac{4\pi^2}{T_p^2}\theta_p Z$$

$$A_y = g*Sin\theta_p + \frac{1}{2}\frac{4\pi^2}{T_p^2}\theta_p X + \frac{4\pi^2}{T_r^2}\theta_r 2Y + \frac{4\pi^2}{T_r^2}\theta_r Z$$

$$A_z = g \pm (A_h + \frac{4\pi^2}{T_p^2}\theta_p X + \frac{4\pi^2}{T_r^2}\theta_r Y)$$

g = Gravity Acceleration

θ_r = Maximum Roll Angle

θp = Maximum Pitch Angle

T_r = Rolling Period

Tp = Pitch Period

A_h = Heave Acceleration

A_s = Surge Acceleration

X = Distance between the Center of Gravity of the ship and the Longitudinal Axis (fore and aft) of the ship on the deck

Y = Distance between the Center of Gravity of the ship and the Horizontal Axis (port side and starboard side) of the ship on the deck

Z = Distance between the Center of Gravity of the ship and the vertical direction (top and bottom) of the ship on the deck

Ax = Sea state load in X Direction

Ay = Sea state load in Y Direction

Az = Sea state load in Z Direction

The folllowing parameter values for sea state load calculation were recorded on the ship under stage 7 and were used in this experiment:

$\theta p = 0.0873$ radian,	$Tp = 6.0$ sec
$\theta_r = 0.49$ radian,	$T_r = 8.0$ sec
$A_h = 0.3g$,	$A_s = 0.15g$

(3) The mathematical model of radar system base plate displacement:

$$\Delta\theta = \frac{\sqrt{(\Delta x)^2 + (\Delta y)^2 + (\Delta z)^2}}{\sqrt{x^2 + y^2 + z^2}}$$

(4) The results of displacement analysis for wind loading:

NODE NO.	X-TRANS	Y-TRANS	Z-TRANS	X-ROTAT	Y-ROTAT	Z-ROTAT
1	-.13637E-01	-.34469E-01	-.17292E-02	.31591E-04	-.13302E-04	-.42007E-05
2	-.13588E-01	-.34288E-01	-.27934E-02	.28184E-04	-.85253E-05	.74858E-05
3	-.13553E-01	-.34489E-01	-.27301E-02	.27741E-04	-.91224E-05	-.19769E-05
4	-.13621E-01	-.34347E-01	-.17260E-02	.32005E-04	-.28713E-05	-.11155E-04
5	-.13685E-01	-.34406E-01	-.23072E-02	.23172E-04	.10210E-05	.27184E-05
6	-.13672E-01	-.35038E-01	-.22813E-02	.14411E-04	.46620E-05	.20829E-05

(5) The results of displacement analysis of sea state loading:

NODE NO.	X-TRANS	Y-TRANS	Z-TRANS	X-ROTAT	Y-ROTAT	Z-ROTAT
1	-.15828E-01	-.72134E-02	.24457E-03	.78139E-05	-.11403E-04	.16119E-05
2	-.15381E-01	-.71302E-02	-.77697E-04	.60909E-05	-.10959E-04	.12675E-04
3	-.15312E-01	-.77084E-02	-.28024E-03	.77671E-05	-.13382E-04	.10832E-04
4	-.15888E-01	-.76353E-02	.30673E-04	.52591E-05	-.10640E-04	.28092E-06
5	-.15651E-01	-.73952E-02	-.16477E-04	.76484E-05	-.49881E-05	.13475E-04
6	-.15786E-01	-.75892E-02	-.16611E-04	.39347E-05	.19260E-05	.12538E-04

(6) The results of displacement analysis of wind loading and sea state loading:

NODE NO.	X-TRANS	Y-TRANS	Z-TRANS	X-ROTAT	Y-ROTAT	Z-ROTAT
1	-.29465E-01	-.41682E-01	-.14846E-02	.39505E-04	-.24704E-04	-.25888E-05
2	-.28968E-01	-.41418E-01	-.28711E-02	.34275E-04	-.19484E-04	.20161E-04
3	-.28865E-01	-.42198E-01	-.30103E-02	.35508E-04	-.22504E-04	.88550E-05
4	-.29509E-01	-.41982E-01	-.16954E-02	.37264E-04	-.13511E-04	-.10875E-04
5	-.29335E-01	-.41801E-01	-.23236E-02	.30820E-04	-.39671E-05	.16194E-04
6	-.29458E-01	-.42628E-01	-.22979E-02	.18346E-04	.65880E-05	.14621E-04

(7) The results of displacement analysis of wind loading, sea state 7 stage loading and 2.5g accelerate loading:

NODE NO.	X-TRANS	Y-TRANS	Z-TRANS	X-ROTAT	Y-ROTAT	Z-ROTAT
1	-.11246E+00	-.11938E+00	-.17642E-02	.11113E-03	-.85027E-04	-.20777E-05
2	-.11104E+00	-.11869E+00	-.58871E-02	.95347E-04	-.70141E-04	.53601E-04
3	-.11068E+00	-.12097E+00	-.69376E-02	.10292E-03	-.82816E-04	.34477E-04
4	-.11268E+00	-.12037E+00	-.30084E-02	.10034E-03	-.58435E-04	-.17104E-04
5	-.11207E+00	-.11975E+00	-.45071E-02	.90977E-04	-.23941E-04	.46294E-04
6	-.11281E+00	-.12220E+00	-.44577E-02	.62841E-04	.27647E-05	.42488E-04

APPENDIX B

A MATHEMATICAL MODEL FOR AN ISOLATOR AND ABSORBER OF A RADAR SYSTEM BASE PLATE

A Mathematical Model for an Isolator and Absorber of a Radar System Base Plate

Method of Truncated Modal Expansion (Wang, Haung, & Hu, 1990):

$$\{S(t)\}=\sum_{R=1}^{m}\{u\}_r q_r(t)$$

Method of the mast structure and radar System without added absorbers:

$$K.E.=\frac{1}{2}M_1\dot{T}_1^2+\frac{1}{2}\sum_{R=1}^{m}\{u\}_r^t(m)\{u\}_r\dot{q}_r^2$$

$$\dot{T}_1=\sum_{r=1}^{m}(u_{n+1})_r\dot{q}_r$$

Method of the mast structure and radar System with added absorbers:

$$u_r^T[m]u_r=Ms, \qquad r=1,2\cdots m$$

$$K.E.=\frac{1}{2}M_1\dot{T}_1^2+\frac{1}{2}Ms\sum_{r=1}^{m}\dot{q}_r^2$$

Dissipation Function:

$$P.E. = \frac{1}{2}K_1[T_1 - \sum_{R=1}^{m}(u_1)_r q_r]^2 + \frac{1}{2}Ms\sum_{r=1}^{m}(\Omega_r^{\bullet})^2 q_r^2$$

Lagrange's Methods:

$$K.E. = \frac{1}{2}M_1\dot{T}_1^2 + \frac{1}{2}Ms\sum_{r=1}^{m}\dot{q}_r^2 + \frac{1}{2}M_2\dot{T}_2^2$$

$$P.E. = \frac{1}{2}K_1[T_1 - \sum_{r=1}^{m}(u_1)_r q_r]^2 + \frac{1}{2}Ms\sum_{r=1}^{m}(\Omega_r^{\bullet})^2 q_r^2 + \frac{1}{2}K_2(T_2 - T_1)^2$$

$$D.F. = \frac{1}{2}C_1[\dot{T}_1 - \sum_{r=1}^{m}(u_1)_r q_r]^2 + \frac{1}{2}C_2(\dot{T}_2 - \dot{T}_1)^2$$

$$Ms\ddot{q}_j + Ms(\Omega^{\bullet})^2 q_j + C_1(u_1)_j[\sum_{r=1}^{m}(u_1)_r\dot{q}_r - \dot{T}_1] + K_1(u_m)_j[\sum_{r=1}^{m}(u_1)_r q_r - T_1] = 0, \qquad j = 1, 2, \cdots n+1$$

Mast Structure:

$$M_1\ddot{T}_1 + C_1[\dot{T}_1 - \sum_{r=1}^{m}(u_1)_r\dot{q}_r] + K_1[T_1 - \sum_{r=1}^{m}(u_1)_r q_r] + C_2(\dot{T}_1 - \dot{T}_2) + K_2(T_1 - T_2) = F(t)$$

Radar System:

$$F(t)=F_0 e^{i\Omega t}$$

Dynamic Absorbers:

$$M_2\ddot{T}_1+C_2(\dot{T}_2-\dot{T}_1)+K_2(T_2-T_1)=0$$

System Transfer Function:

$$\begin{aligned}&(T_1,T_2,q_r)=(T_{10},T_{20},q_{r0})e^{i\Omega t};\Omega_1=\sqrt{K_1/M};\\&2\Omega_1\zeta_1=C_1/M_1;\Omega_2=\sqrt{K_2/M_2};2\Omega_2\zeta_2=C_2/M_2;\\&(W_1,W_2,W_r^*,W)=(\Omega_1,\Omega_2,\Omega_r^*,\Omega)/\Omega_1^*;M_1/M_3;\\&\mu_2=M_2/M_1;F_0=F_0/M_1(\Omega_1^*)^2\end{aligned}$$

and

$$(W_j^{*2}-W^2)q_{j0}+(2W\zeta_1+W_1)(\mu_1 W_1)(u_1)_j[\sum_{r=1}^{m}(u_1)_r q_{r0}-T_{10}]=0,\qquad j=1,2,\cdots m$$

Result:

$$\begin{aligned}&[(W_1^2-W^2+i2W_1W\zeta_1)+\mu_2(W_2^2+i2W_2W\zeta_2)]T_{10}-\\&\mu_2(W_2^2+i2W_2W\zeta_2)T_{20}-(W_1^2+i2W_1W\zeta_1)[\sum_{r=1}^{m}(u_1)_r q_{r0}]=F_0\end{aligned}$$

$$(W_2^2-W_2+i2W_2W\zeta_2)T_{20}-(W_2^2+i2W_2W\zeta_2)T_{10}=0$$

Transfer Function:

$$(W_1^2+i2W_1W\zeta_1)\,[\sum_{r=1}^{m}(u_1)_r q_{ro}] = [(W_1^2-W^2+i2W_1W\zeta_1)-\mu_2\frac{(W_2^2W^2+i2W_2W^3\zeta_2)}{(W_2^2-W^2+i2W_2W\zeta_2)}]\,T_1$$

$$q_{jo}=\frac{\mu_1(u_1)_j}{(W_j^{*2}-W^2)}\,[\frac{(1+\mu)(W_2^2W^2+i2W_2W^3\zeta_2)-W^4}{(W_2^2-W^2+i2W_2W\zeta_2)}T_{10}-F_0],\qquad j=1,2\cdots m$$

$$\begin{aligned}&\{1-(W_1^2+i2W_1W\zeta_1)\,[\sum_{r=1}^{m}\frac{\mu_1(u_1)^2}{(W_r^{*2}-W^2)}]\}F_0=\{(W_1^2-W^2+i2W_1W\zeta_1)\\&-\mu_2\frac{(W_2^2W^2+i2W_2W^3\zeta_2)}{(W_2^2-W^2+i2W_2W\zeta_2)}(W_1^2+i2W_1W\zeta_1)\,[\sum_{r=1}^{m}\frac{\mu_1(u_1)_r^2}{(W_r^2-W^2)}\\&\frac{(1+\mu_2)(W_2^2W^2+i2W_2W^3\zeta_2)-w^4}{(W_2^2-W^2+i2W_2W\zeta_2)}]\}T_{10}\end{aligned}$$

Optimum Design of Dynamic Absobers:

$$H(W)=\frac{THE\ SHIFT\ OF\ RADAR}{EXTENER\ FORCE\ ACT\ FOR\ RADAR}=\frac{T_{10}}{F_0}=\frac{H_1(W)}{H_2(W)}$$

$$H_1(W)=PR1+i\ PI1$$

Band-Limited White Noise Function:

$$PI1=-2W_1W\zeta_1\,[\sum_{r=1}^{m}\frac{\mu_1(u_1)_r^2}{(W_R^{*2}-W^2)}]$$

$$H_2(W) = (PRA-PRB) + i(PIA-PIB)$$

$$PRA = [(W_1^2 - W_2^2) - \mu_2 \frac{W_2^4 W^2 - W_2^2 W^4 + 4 W_2^2 W^4 \zeta_2^2}{(W_2^2 - W^2)^2 + 4 W_2^2 W^2 \zeta_2^2)}]$$

$$PRB = \{\frac{[(1+\mu_2)(W_2^2 W^2) - W^4](W_1^2 W_2^2 - W_1^2 W^2 + 4 W_1 W_2 W^2 \zeta_1 \zeta_2)}{(W_2^2 - W^2)^2 + 4 W_2^2 W^2 \zeta_2^2}$$

$$\frac{-(1+\mu_2)(4 W_1 W_2 W^4 \zeta_2)(\zeta_1 W_2^2 - \zeta_2 W_1 W_2 - \zeta_1 W_2)}{}\}[\sum_{r=1}^{m} \frac{\mu_1 (u_1)_r^2}{(W_2^{*2} - W_2)}]$$

$$PIA = 2 W W_1 \zeta_1 + \mu_2 \frac{2 W_2 W^5 \zeta_2}{(W_2^2 - W^2)^2 + 4 W_2^2 W^2 \zeta_2^2)}$$

$$PIB = \{\frac{(1+\mu_2)(2 W_1 W^3)(W_2^2 - W^2)(\zeta_1 W_2^2 - \zeta_2 W_1 W_2 W^2) +}{(W_2^2 - W^2)^2 + 4 W_2^2 W^2 \zeta_2^2)}$$

$$\frac{(1+\mu_2)(2 W_1 W_2 W^3 \zeta_2)(W_1 W_2^2 - W_1 W^2 + 4 W_2 W^2 \zeta_1 \zeta_2)}{}\}[\sum_{r=1}^{m} \frac{\mu_1^2 (u_1)_r}{(W_r^{*2} - W^2)}]$$

Band-Limited White Noise Function:

$$H(W) = \frac{PR1 + iPI1}{(PRA-PRB) + i(PIA-PIB)}$$

$$|H(W)|^2 = \frac{(PR1)^2 + (PI1)^2}{(PRA-PRB)^2 + (PIA-PIB)^2}$$

$$S_t(W)=S_f(W)\,|H(W)|^2$$

$$\sigma_t^2=\int_{-\infty}^{\infty} S_t(W)\,dW$$

$$S_f(W)=\begin{cases} S_0, & W_1\leq W\leq W_u \\ 0, & \end{cases}$$

$$\sigma_t^2=\int_{W_1}^{W_u} S_0\,|H(W)|^2\,dW$$

$$\frac{\partial\sigma_t^2}{\partial W_2}=0$$

$$\frac{\partial\sigma_t^2}{\partial\zeta_2}=0$$